PREFACE

We would like to introduce the report of the scientific activity of the Frank Laboratory of Neutron Physics for 1995. The first part is a brief review of the experimental and theoretical results of investigations in condensed matter physics, nuclear physics and applied research. The second part presents the investigations which characterize the main directions of research in greater detail. The reader can receive a more complete picture of the research carried out in the Laboratory from the list of publications for 1995 following Part 2.

In 1995, the Laboratory Directorate paid special attention to the Laboratory's basic facilities. On 27 March 1995, the IBR-2 reactor resumed regular operations with a new movable reflector, PO-2R, the third movable reflector since the IBR-2 startup. The concept for modernization of IBR-2 for the period from 1996 to 2005 was elaborated.

Considerable advance has been made in the realization of the project for a new source of resonance neutrons - IREN - which is to replace the IBR-30 booster, currently in operation. Solution of the problems associated with the fulfilment of obligations for constructing the main parts of the accelerator by the Institute of Nuclear Physics, Siberian Branch, Russian Academy of Sciences, and the transferrence of the nuclear fuel needed the multiplying target by the Ministry of Atomic Energy of the Russian Federation created the necessary conditions for a successful execution of the Project in 1998.

Further development of the User Policy continued, aimed at attracting a larger number of physicists, chemists, biologists, and specialists in materials science to carry out experiments at the IBR-2 reactor. User Committees were formed for the four research directions: diffraction, small-angle scattering, inelastic scattering, and polarized neutrons (reflectometry and depolarization). The first call for proposals resulted in 76 applications requesting 406 experimental days on 7 of the 12 IBR-2 spectrometers.

The financial situation in the Laboratory did not change noticeably in 1995. The basic facilities and technical infrastructure were financed from the JINR budget as in previous years. Instrument upgrades and the scientific program were provided for mainly from financial contributions in the frame of JINR-FRG and JINR-Hungary agreements for cooperation, as well as from other programs and funds.

The Frank Laboratory of Neutron Physics is one of the leading neutron centers of Europe and continues to develop in spite of the difficulties its host country is currently experiencing.

V.L.Aksenov
Director

21 February 1996

1.1. CONDENSED MATTER PHYSICS

1.1.1. EXPERIMENTAL

After the movable reflector at IBR-2 was successfully replaced by a new one in March 1995, physicists of the Department of Condensed Matter Physics (SDCMP) resumed investigations in condensed matter physics by neutron scattering methods with all of the IBR-2 spectrometers. At present, experiments are being carried out with 10 spectrometers: HRFD, DN-2, NSVR, DN-12, SNIM-2, YUMO, NERA-PR, KDSOG-M, DIN-2, and SPN-1. At the REFLEX spectrometer, the adjustment stage is nearing its completion, test experiments have started, and the first physical experiments have been conducted.

As previously, the program in condensed matter physics was divided into four main directions of research: diffraction investigations of ordered structures, investigations of large-scale inhomogeneities by small-angle scattering, neutron-optical investigations of surfaces and magnetic phenomena, and investigations of atomic dynamics in solids by the method of inelastic neutron scattering.

Neutron diffraction. The program initiated in 1994 for investigating novel mercury-containing superconductors continued. The work involved: precision investigations of *Hg*-compounds and accompanying structures with HRFD, *in situ* experiments to reveal the influence of oxygen stoichiometry on structure with DN-2, and the influence of high pressure (up to 50 kbar) on the structure of *Hg-1201* and *Hg-1212* compounds with DN-12. The investigations were carried out in cooperation with MSU, Moscow (E. V. Antipov's group) and RRC KI, Moscow (V. A. Somenkov's group). From the results of the HRFD measurements of $HgBa_2CuO_{4+y}$ compounds with different oxygen contents in the base plane (z=0), namely, y=0.05, 0.11, 0.12, and 0.18, precision structure data (including measurements at T=8 K) were obtained and the influence of oxygen stoichiometry on the value of T_c was refined. The experiment using a sample with y=0.05 was repeated on the 3T2 diffractometer in LLB (Saclay) and yielded practically coinciding results. Figure 1 shows the dependence of T on oxygen content for *Hg-1201*. The oxygen at site (1/2,1/2,0) is actually a doping atom and by changing its concentration, one can obtain any level of doping.

A monocrystal of $La_2CuO_{4.04}$ was used on HRFD to investigate the phenomenon of macroscopic phase separation in the Bmab and Fmmm phases arising at a low temperature. This is connected with the diffusion of non-stoichiometric oxygen through the volume of the crystal. The high resolution of HRFD allowed not only the splitting of the diffraction peaks to be observed (Fig.2), but also the dimensions of the coherent Fmmm phase areas to be estimated. These dimensions appeared to be different in the directions of the *b*- and *c*-axes and were: L_b=1490 +/- 60 Å, L_c=1020 +/- 20 Å.

On HRFD, the first experiments to measure internal stresses in composite materials were conducted together with IFzP, Germany.

On DN-2, investigations in the real-time mode (diffraction and small-angle scattering) of metallic copper oxidation revealed new peculiarities of the process. Decomposition of the *CuO* oxide film (initially covering the copper granules) occurred at 210°C, while copper oxide in a massive state decomposes only at T>1050°C. Simultaneously with the decomposition of the oxide film, an anomalous extension of the metallic copper lattice was observed. At 210°C, a sharp increase in the small angle scattering over the momentum transfer area, corresponding to

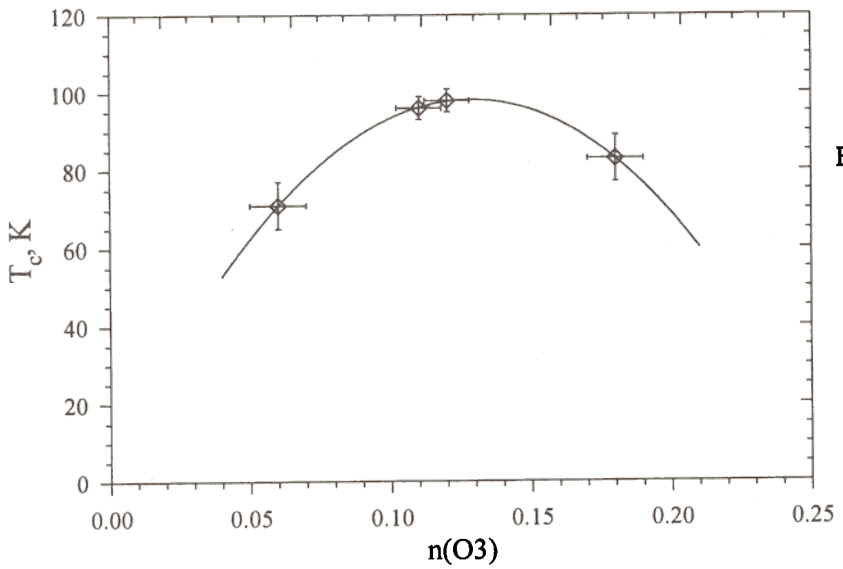

Fig.1 The dependence of the superconducting transition temperature on the value of y for $HgBa_2CuO_{4+y}$ compounds. Experimental points are approximated to the conditional parabolic dependence.

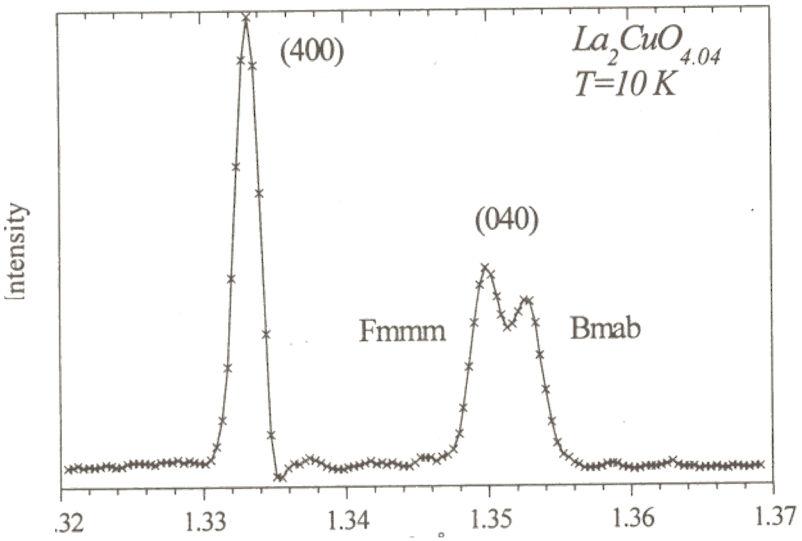

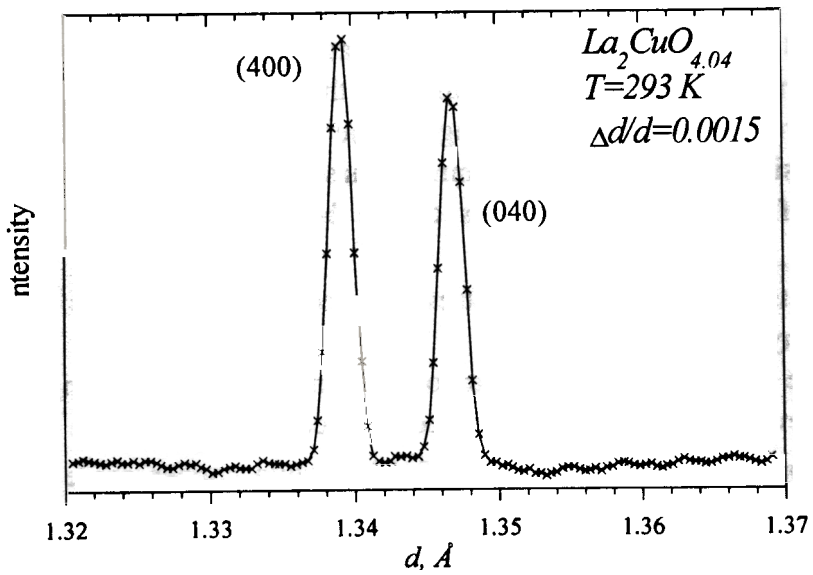

Fig.2 Diffraction spectra (in the vicinity of the (400) peak) from the $La_2CuO_{4.04}$ monocrystal with T_c=38 K as measured with the HRFD diffractometer. At room tempera-ture, two reflexes corresponding to two orientations of 90°-domains in the sample can be observed. At low temperatures, the (040) peak splits into two components corresponding to two structural phases.

the dimensions of 100–200 Å, was observed and the diffraction lines from Cu_2O, and later from CuO appeared. The sequence of these events allows one to assume that the oxidation mechanism of finely dispersed metallic copper covered with a CuO film is an explosive type.

Small-angle neutron scattering. In the reported year, a large number of proposals for experiments with the YUMO small-angle scattering spectrometer were received. In addition, investigations in the frame of long-term joint programs continued with the participation of Germany, France, Slovakia, Czechia and Hungary.

In the experiments conducted together with Germany, glass with CdS_xSe_{1-x}–type admixtures, which radically change the properties of the glass, was investigated. The dimensions of defects arising in the glass, whose radii of inertia appeared to be equal to 27 Å, were determined.

Investigations to study the structure of particles formed in the process of thermotropic micelle-lamellar transitions were begun. This direction of research is connected with the fundamental problem of the mechanism of self-assembly in membranes, as well as with the applied problem of studying the influence of bile salts on biological membranes.

Measurements of *DMPC*–Sodium Cholate *(NaCh)* and *DPPC–NaCh* were performed with small-angle spectrometers in Dubna and Budapest. Structures of particles in the initial and final stages of the thermotropic transition were determined. Figure 3 shows small angle scattering spectra from micelle, created from high *NaCh* concentrations at room temperature. Division of the lipid-detergene system into two phases under the action of temperature was discovered. In this case, the upper phase in *DMPC–NaCh* mixtures has a scattering anisotropy which is evidence of self-orientation of the formed particles.

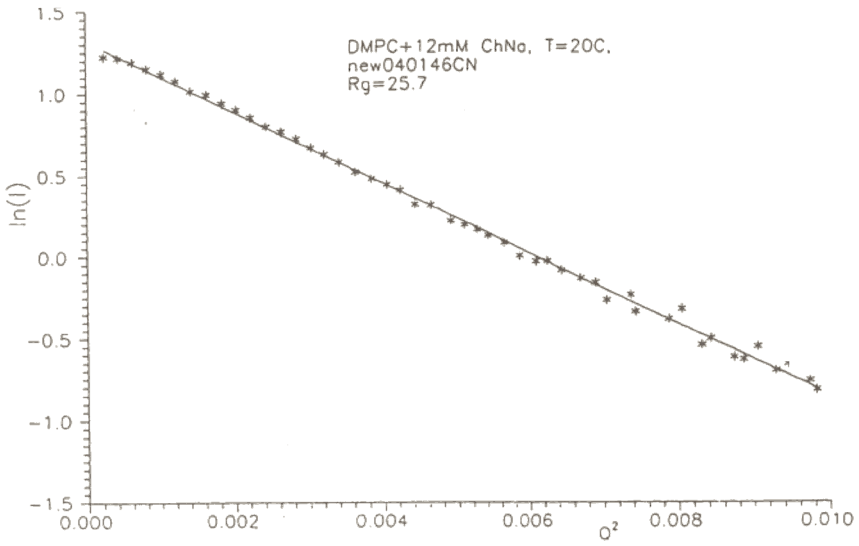

Fig.3 The Guinier plot of DMPC in a *NaCh* mixture at room temperature. The slope of the curve corresponds to the radius of inertia of 25.7 Å.

Experiments to investigate the influence of external pressure on the properties of $C_{14}DMAO/C_{14}TMABr$-based self-organizing micelle systems were continued in cooperation with the University in Bayreyth, Germany. Phase transitions were observed at T=28°C and T=52°C

for pressures of 1.5 and 2.3 kbar, and the first phase diagram of this system was constructed. On the basis of general principles, it was demonstrated that the change in entropy connected with phase transitions is negative, i.e., the entropy of high pressure phases is lower than the initial phase entropy and, thus, they are better ordered.

Polarized neutron investigations in neutron optics. Experiments to investigate the reflecting properties of periodic multi-structures built of ^{56}Fe and ^{57}Fe layers were started on SPN-1. It is expected that such layers will be an effective neutron monochromator.

Reflectrometric measurements of a new type composite material, polymeric lamellar structures with inclusions of $-Fe_2O_3$ particles with sizes of about 40 Å, were conducted. The purpose of the measurements was to obtain data about the distribution of inclusions over structure and the possibility of lamellarity violations.

The stage of neutron reflectometry studies (together with the University in Meinz, Germany) of the formation process of multilayer polyionic films obtained by precipitation from electrolytic salt solutions, was completed. The obtained data convincingly proved the periodic nature of the polymeric structures produced by this technique.

Inelastic neutron scattering. Vibrational spectra of two modifications of highly disperse SiO_2: hydroxylated (saturated with surface OH-groups) and siliconized (OH-groups partly replaced by CH_3-groups), were measured with the KDSOG spectrometer. The measurements demonstrated a strong difference between the vibrational spectra of these two modifications, in contrast to the IR-spectroscopy data. This difference was explained by the presence of torsion vibrations of the CH_3-groups that was seen clearly by neutron scattering.

Measurements of inelastic scattering spectra of different ice phases obtained by a combination of the cooling mode and the external field application mode were conducted with the KDSOG and NERA inverted geometry spectrometers. Figure 4 shows the phonon density for several types of crystal and amorphous states of ice in comparison with usual hexagonal ice.

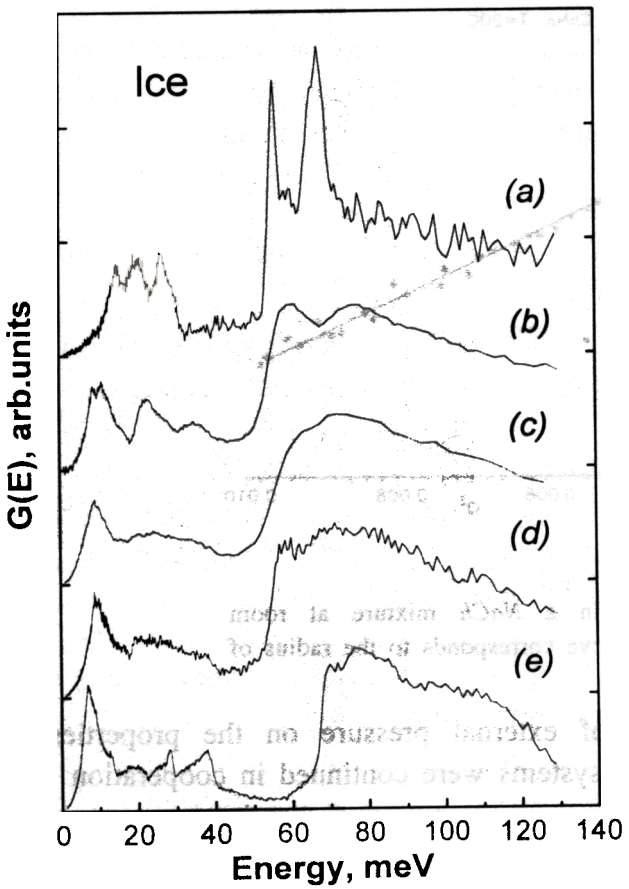

Fig.4 Generalized densities of states for different H_2O ice modifications: (a) crystalline ice-VIII cooled from 340 to 110 K during 20 sec. at 40 kbar; (b) ice-VII obtained by slow cooling to 77 K at 15 kbar; (c) a mixture of hexagonal ice, Ih, and high density amorphous phase ice, hda, compressed to 15 kbar at 77 K; (d) "defect" ice VI' obtained from Ih ice by compressing to 33 kbar at 77 K; (e) ice Ih under normal conditions. The applied pressure was removed from the samples at 77 K and further manipulations were carried out at nitrogen temperatures.

In the experiment conducted together with RRC KI, the dynamic interaction of structural components of the La_2CaCuO_6 compound, the basic compound for lanthanum-containing high temperature superconductors, was investigated. The phonon density of states of the basic compound and the La_2CuO_4 and $CaCuO_2$ compounds forming its layered structure were measured. The phonon spectrum of the basic compound appeared, with good accuracy, to be the sum of the spectra of the structural components. This was evidence of the weakness of the interaction between the layers.

Investigations of the temperature dependence of the structure of the spectra of excited quantum liquids continued on the DIN-2K spectrometer. Simultaneously, calculations to choose a model for approximating the structural dynamic factor of liquid helium were conducted. As the model considerably influences the determined parameters of one-phonon scattering, the choice is of principal importance. The obtained data speaks in favor of the damping harmonic oscillator model.

Development activities. During the reported year, work on upgrading many of the operating spectrometers was conducted.

Complex adjustment of all the elements of the REFLEX-P reflectomer (including the electronics) was performed and the main physical parameters of the reflectometer were measured. On the basis of the obtained data, mutual positionings of collimators and the neutron-optical polarizing system of the reflectometer were corrected during the summer shut-down of the IBR-2 reactor. After additional test experiments, the REFLEX-P will be commissioned and resume regular operations.

On the SPN-1 spectrometer, tests of the new optical elements, the straight and curved soller polarizers, as well as a supermirror, were conducted. All the elements were found to be suitable for further operation, and allow the working wavelength interval to be increased by 2-3 times. In addition, the new optical elements were used to check the inelastic neutron scattering measurement mode over the energy interval from 3 to 50 MeV.

On the DN-12 high pressure diffractometer, experiments to test the second detector ring, installed to analyze inelastically scattered neutron energies and designed for operations with a cooled Be-filter and graphite monochromators, were carried out. Manufacturing of a mirror neutron-guide for this diffractometer was begun and its assembly on the beam is planned for the middle of 1996.

On the high resolution Fourier diffractometer (HRFD), the 20-element detector at a scattering angle of 90° and d-spacing resolution of about 0.003 started operations. This detector will allow the d_{hkl} working interval to be increased considerably in investigations of complex structures. However, that detector is mainly dedicated to investigations of internal stresses in bulk materials.

On the SNIM-2 spectrometer, experiments to measure inelastic neutron scattering from monocrystals (dispersion curves) to reveal additional capabilities of the instrument, which has not been used as a diffractometer before, were performed. The result of the experiment is that SNIM-2 can be successfully used to measure dispersion relationships of magnetic excitations in phase states induced by pulsed magnetic fields up to 200 kOe. In this respect, the SNIM-2 will be without competition until pulsed magnetic instruments are created at other neutron sources.

A large volume of methodological work was conducted to update the NSVR spectrometer. New possibilities of conducting experiments with this spectrometer have appeared and the process of data collection and preliminary processing was radically improved. The new possibilities for conducting experiments include the EPSILON setup, which allows one to

conduct analysis of internal stresses in bulk products. The specialized goniometer which was put into operation allows a sample to be rotated around the vertical axis (the rotation accuracy is better than 0.0025°) and *XYZ*-movement of the sample can be accomplished with an accuracy not worse than 0.0025 mm. In 1995, the NSVR electronics to control experiments and data storage was transferred to VME standard and is currently operating under the control of the OS-9/XWINDOW system. This now allows one to use all the advantages of the multi-task mode and network operations. The SKAT project, foreseeing the complete replacement of the NSVR detector system with the new one, better adapted for measurements of pole figures from textured samples, is nearing its completion.

1.1.2. THEORETICAL

1. The Landau phenomenological theory of phase transition to a polymeric-like phase in AC_{60} *(A=K,Rb)* crystals was developed. The theory correctly describes spontaneous crystal cell strains following the phase transition and also, predicts partial ordering of alkali metal atoms over positions allowed in the octahedral environment of C_{60} molecules. For decreasing temperature, the appearance of another structural phase transition leading to complete ordering of the metal atoms is also possible. The increase in the phase transition temperature in AC_{60} fullerides in comparison with C_{60} is explained.

2. The temperature dependence of mid-infrared (MIR) spectra, the Hall coefficient and the thermoelectric power have been calculated on the basis of a two-fluid model consisting of localized polarons and delocalized carriers. It is shown that in the case of intermediate polarons, the inplane temperature dependence of the optical conductivity is determined by the thermal activation energy and can both increase and decrease with temperature in agreement with the observed results. The same charge carriers were used to calculate the Hall coefficient and the thermoelectric power. The temperature dependence of the Hall coefficient and the thermoelectric power is determined by the same thermal activation energy and the agreement with experiments is good.

3. The PES data were analysed using exact diagonalization with respect to the coupling of the electron with the $A_g(2)$ mode and the truncated Hilbert space for the H_g modes. PES experimental data fitting, just as good as in the papers of other authors for low binding energies, and better than in these papers - for the higher energy region, was obtained. Coupling with high frequency phonons dominates in the electron-phonon interaction. Consequently, the nonadiabatic small polaron theory rather than the adiabatic Migdal-Eliashberg approach should be applied to M_xC_{60}.

4. The behavior of the asymmetric D-SQUID in superimposed RF and DC magnetic fields was rigorously described. Criteria for the determination of the operation regime type were found. A new interesting aspect of RF-pumped SQUIDs which might find applications in future was discovered: following the variation of the magnetic flux of the input signal the behavior of the system radically changes from a nonlinear to a linear one with respect to the RF perturbation.

5. The following well-known paradox was investigated. On one hand, for each quantum system with a time-periodic Hamiltonian, the solutions of the Schrodinger equation, which are the time-periodic functions modulated by the factor $e^{iEt/\hbar}$, exist. On the other hand, the amplitude of the harmonic oscillator, under the action of a time-periodic force with a resonant frequency, increases with time for any initial condition. The paradox is resolved with the help of

the exact solution of the corresponding Schrodinger equation. It is shown, the paradox arises, if one does not take into account the transmutation of the quasienergy spectrum and the steady state (quasienergy state) basis at the resonant point.

6. The high energy asymptotic of the coefficient of the neutron reflection from laminated periodic substances is considered. It is shown that the reflection coefficient depends power-like on the energy and the exponent is defined by the smoothness of the substance potential.

7. It is shown that the magnetic moment of the neutron moving in antiferromagnetics with a spiral-ordered magnetic field, experiences slow precession. The precession pitch strongly depends on the value and the direction of the neutron velocity.

1.2. NEUTRON NUCLEAR PHYSICS

In the course of 1995, experiments to investigate fundamental interaction symmetry violations and electromagnetic properties of the neutron were conducted. A number of investigations in the fields of fission physics, the study of highly excited states of nuclei as well as reactions with the emission of charged particles (related, in particular, to astrophysical problems), were carried out. Work to modernize the existing and create new experimental facilities was also conducted in the reported year. Measurements were performed on beams of the IBR-30 and IBR-2 reactors and other neutron sources of various research centers in Russia, Germany, the USA, China, and France.

1.2.1. EXPERIMENTAL

Parity Violation in Interactions of Neutrons with Resonance Nuclei

Measurement of the P-odd effect following transmission of unpolarized neutrons through a longitudinally polarized ^{139}La target

The experiment was performed on the POLYANA setup of FLNP JINR. A 2 kg ^{139}La sample was polarized by the "rude force" method in the ^{3}He-^{4}He dilution cryostat with an external magnetic field of 1 T. A nuclear polarization $f_N = 0.0065$ was achieved at a temperature of 0.07 K. The transmission effect ε_N is illustrated in Fig 5. From the experimental data, the value of the matrix element of the weak interaction leading to a parity violation $w_{sp} \approx 3.6 \pm 1.2$ meV was estimated.

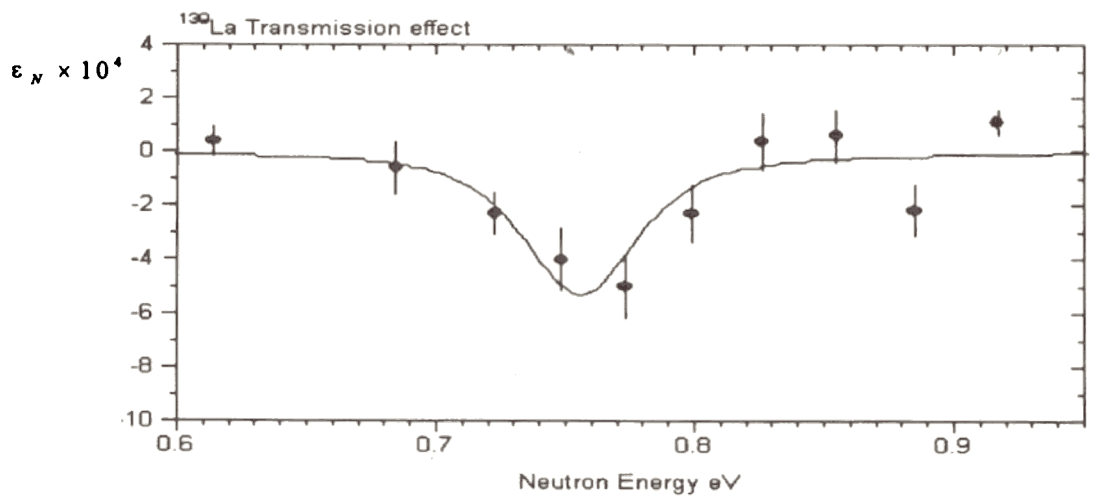

Fig. 5 The transmission effect of unpolarized neutrons through the longitudinally polarized ^{139}La target.

Study of neutron depolarization following transmission through ^{165}Ho

The investigation was performed in the frame of planning an experiment to search for time invariance violation in the P-even, T-odd interaction, which results in the appearance of the

$\vec{s}\cdot(\vec{k}\cdot\vec{I})\left[\vec{k}\times\vec{I}\right]$ correlation, where $\vec{s},\vec{k},\vec{I}$ are neutron spin, neutron moment, and the nucleus spin, respectively. Time violations will be sought in the total interaction cross section of polarized neutrons with an aligned target.

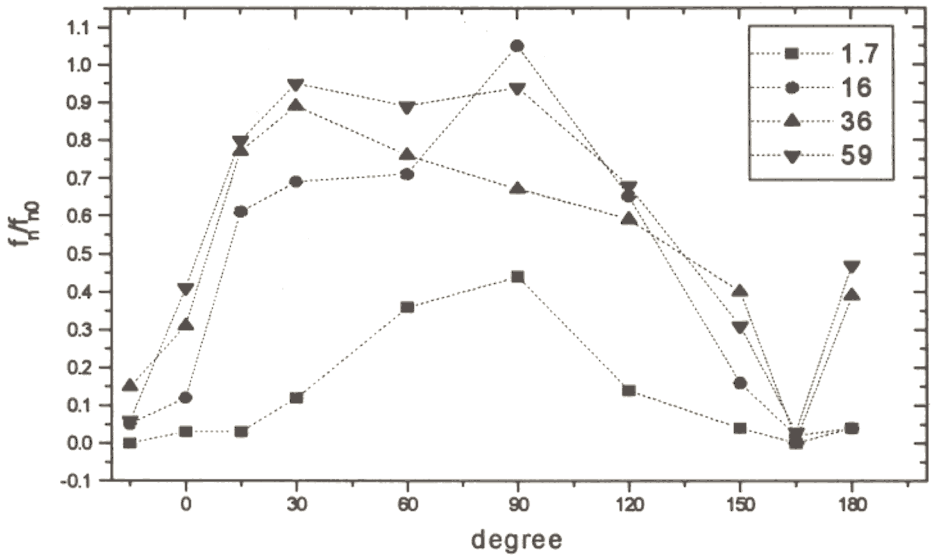

Fig.6 Neutron depolarization in ^{165}Ho.

In the conducted experiment, the transversely polarized neutron beam was transmitted through a cylindrical ^{165}Ho monocrystal. The polarized *Dy* target was used as an analyzer of the neutron polarization at the exit from the sample. The energy dependence of the polarization was measured in *Dy* resonances at 1.7, 2.7, 14, 16, 18, 36, 59 eV. In addition, the dependence of the depolarization on the angle between the neutron and the crystallographic axis *C* was measured. The measurements were conducted at room, nitrogen, and helium temperatures of the sample.

Analogous measurements were carried out using the longitudinally polarized neutron beam. Measurements with different external magnetic fields on the sample, *i.e.*, of 100, 200, and 400 Gauss, were also conducted.

The angular dependence of the depolarization effect expressed as f_n/f_{n0} for the energies of the transversely polarized neutron beam (1.7, 16, 36, 59 eV) is shown in Fig. 6. The obtained results allowed us to estimate the domain dimensions along the *C* axis at a level of 114 μm.

Parity violation: the TRIPLE collaboration experiments

The TRIPLE collaboration, including LANL (Los Alamos), JINR (Dubna), the KYOTO University (Kyoto), TUNL (Durham), TRIUMF (Vancouver), and the DELFT Technology University (Delft), continued measurements of parity violation effects in resonance nuclei with *A~100* to investigate the mass dependence of the matrix element of the weak interaction. The experiments were conducted on the longitudinally polarized beam of resonance neutrons at the LANSCE pulsed source up to the energies of 2000 eV. For the ^{106}Pd, ^{108}Pd, *Sb*, *Cs*, and *I* targets, the helical asymmetry of the resonance cross section was measured by the methods of

transmission and registration of radiative capture gamma-rays. Parity violation effects were observed in many resonances of all of the designated nuclei.

Analysis of the obtained data has begun. Analysis of the effects in 34 *p*-resonances of ^{115}In with energies up to 300 eV, previously measured, yielded the matrix element of weak neutron-nucleus interaction: $M(^{115}I) = 0.59^{+0.25}_{-0.15} meV$. This result, together with the data for *A~110* and *A~230*, point to the permanency of the matrix element *M* for nuclei with the same level density. The statistical method for extracting the matrix element from resonance data containing incomplete spectroscopic information about spins and channel mixing parameters was developed and realized.

Electromagnetic Properties of the Neutron

Precision measurements of the ^{208}Pb total neutron cross section

To estimate the neutron polarizability α_n, measurements of the total neutron cross section σ_t for ^{208}Pb were carried out on the 70 m flight path of the IBR-30 reactor. The classical time-of-flight method with "black" resonance filters was used up to the energies of ~100 eV. The σ_t values were obtained for nine energy intervals within an error of 3-5 mb. To perform energy selection of the keV neutrons, a combination of the time-of-flight method and ^{60}Ni and ^{56}Fe interference filters was used. The experimental points for σ_t at 4.0, 5.1, 6.5 and 24 keV were obtained within an error of 13-18 mb. These new data, though not a record in accuracy, played an important role in promoting further advances towards an exact determination of α_n.

In the analysis of the obtained σ_t, to account for far *s*-resonances, an additional parameter *h*, giving the scattering radius an energy dependence in the form of $R=R_0-hE$ and represented by the sum over all the resonances not accounted for directly was introduced:

$$h = 2276\frac{A+1}{A}\sum\frac{gG_n^{(0)}}{E_0^2} \quad fm/eV. \tag{1}$$

The obtained value was unexpectedly large, $h\rangle 10^{-6}$ fm/eV, which made us return to the detailed analysis of σ_t for ^{208}Pb previously measured in Oak Ridge that gave $\alpha_n = (1.20\pm0.15)10^{-3}\ fm^3$ for the *a* expansion coefficient only:

$$\sigma(k)=\sigma(0)+ak+bk^2+ck^4 \tag{2}$$

Comparing the "mathematical" formula (2) with the physical formula

$$\sigma(E)=\frac{4p}{k^2}\sin^2\left[-k(R_0' - hE + a_pQ)\right]+\frac{12p}{k^2}\sin^2\delta_1 \tag{3}$$

adds two other drawbacks of the corresponding work to these already mentioned, namely, the absence of the *p*-wave contribution (deficit of the coefficient *c* in (2)) and neglect of the term with k^3, which depends only on α_n and is ~12% of the *ak* term for *E*=40 keV.

As far as the parameter *h* is concerned, processing the Oak Ridge data using expression (3) yields $h=(20.4\pm0.3)^{-7}$ fm/eV (in this case $\alpha_n=(1.70\pm0.17)\cdot10^{-3}$ fm^3). For comparison: the strongest (also the nearest) resonance of ^{208}Pb, with E_0=507 keV and $\Gamma_n^{(0)}$=74 eV, would give only $h=6.6\cdot10^{-7}$ fm/eV. Thus, one has to ascertain the presence of at least one previously

unknown strong resonance. Testing of this role for the only $1/2^+$ level below the neutron binding energy in the ^{209}Pb nucleus (the negative resonance with E_0=—1.9 MeV) for $h=0$, leads to α_n =(2.08±0.19)·10^{-3} fm^3 and a resonance width $\Gamma_n^{(0)}$=(2640±30) eV. For comparison: the Wigner width limit is ~2300 eV for a nucleus radius of 8 fm.

In conclusion, it should be said that for the precision determination of α_n, one must either simultaneously look for the k- and k^3-components of $\sigma_t(k)$, or get additional information on unknown s-resonances of ^{208}Pb.

Highly Excited States of Nuclei

Studying the (n,2γ) reaction

Experiments to study the cascade decay of nuclei with the thermal neutron beam of the IBR-30 reactor continued. De-excitation of γ-cascades for the compound states of ^{198}Au, ^{192}Ir, and ^{125}Te nuclei were studied. Under the auspices of an international collaboration (Munich, Grenoble, Darmstadt, Riga), the most complete and reliable decay schemes up to the excitation energy of 2-3 MeV have been constructed for these nuclei.

Analysis of the energy distributions of cascade intensities, aimed at investigating the properties of levels over the nuclear excitation energy range from zero to the neutron binding energy, was also continued. Indications of the possibility that the equidistant bands previously observed for intense cascades can be linearly related to the number of boson pairs in unfilled nucleon shells were obtained, allowing the interpretation of this experimental fact as an exhibition of phonon excitations of nuclei within the the model of interacting bosons.

Experimental determination of the neutron resonance parameters of nuclei with A=100-200

Investigations with the ^{113}In and ^{115}In isotopes continued via the (n,γ)-reaction at ROMASHKA setup and new investigations were started with ^{116}Sn, ^{117}Sn, ^{127}I, ^{175}Lu. In addition to determining the parameters of s-wave resonances, identification of p-wave resonances (^{116}Sn, ^{117}Sn) and their spin determinations were conducted. In the ^{177}Hf + n reaction, spins of 180 previously unknown resonances of ^{177}Hf were measured by the γ-ray multiplicity spectrometry method over the neutron energy interval from 300 to 700 eV.

Nuclear Fission

Angular anisotropy of fission fragments from aligned ^{235}U nuclei

The first stage of measurements of the energy dependence of fission fragments from the resonance neutron induced fission of aligned ^{235}U nuclei was completed. The dependence for the interval of neutron energies from 1.5 to 15 eV, containing over ten s-levels of the ^{236}U compound nuclei, was obtained for the first time. Comparison of the experimental data with a simplified version of the theory illustrated in Fig.7, points to the necessity of including s-levels of different spins in the interference analysis.

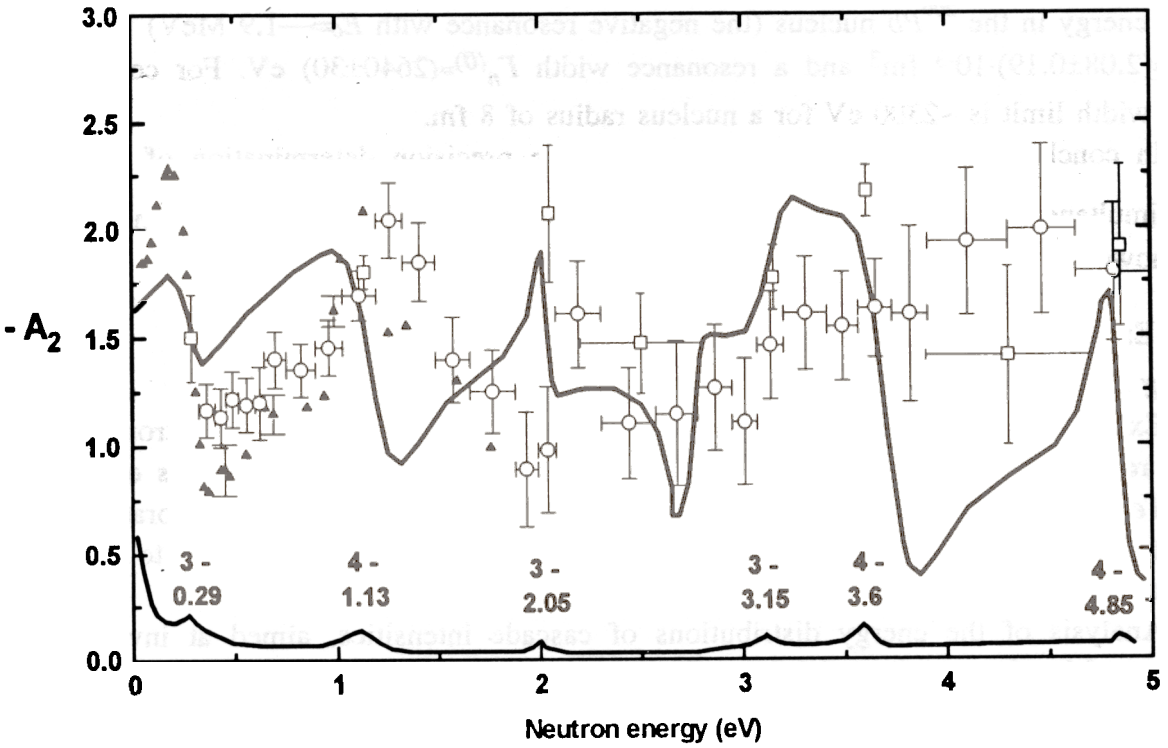

Fig.7 Energy dependence of the angular anisotropy coefficient A_2. Symbols □, Δ display the data by Postma, Pattenden, 1971, 1974; and o display the data obtained in FLNP JINR, 1995. The solid curve presents the theoretical calculations by Moore, 1995.

Fission cross sections and resonance parameters of ^{237}Np in the subthreshold energy region

Time-of-flight experiments to measure the fission cross sections and resonance parameters of ^{237}Np over the subthreshold energy region (3-500 eV) were carried out at the IBR-30 reactor.

Measurements were conducted using fission chambers containing 1.5 g of highly purified plutonium (10^{-6} g/g, of the isotopes ^{235}U, ^{239}Pu) with large fission cross sections. In these experiments fission γ-quanta from ^{237}Np were simultaneously measured by a six-section liquid scintillation detector. The registration of fission events in coincidence with three or more γ-quanta allowed the γ-quanta yield multiplicity to be investigated in separate resonances of ^{237}Np, and as well as in resonance clusters at the neutron energies of 40 eV, 119 eV, and 200 eV related to the levels in the second potential well.

The measurements pointed to the existence of a correlation between γ-yields and the inverse values of the fission widths of the levels. This, in turn, allows the probability of the $(n,\gamma f)$ process to be estimated, including participation of the levels of the second well in the potential deformation energy.

This was the first time that such measurements were conducted for the subthreshold fission region.

Investigating of delay neutrons

In the course of 1995, investigations of delayed neutrons continued on the ISOMER setup in the frame of the collaboration with the 6th subgroup of the Nuclear Data Committee of IAEA. An *Am(Li)* neutron source with a spectrum close to the delayed neutron spectrum was constructed, and a neutron detector was calibrated using the *Am(Li)* and *Cf* sources. The mirror neutron guide on neutron beam 11 of the IBR-2 reactor was reconstructed allowing the thermal neutron output rate at the exit to be increased up to 8×10^5 n/cm^{2}s. New samples from ^{233}U and ^{239}Pu on nickel substrates were prepared to reduce the neutron background from the (α,n)-reaction. As a result, the background in the ^{233}U measurements decreased by 4 times. Measurements of delayed neutron yields using the ^{235}U (50 mg), ^{233}U (67 mg), and ^{239}Pu (170 mg) samples were conducted for cold and thermal neutrons. The energy of the neutrons to induce fission was selected by means of a change of the chopper rotation phase with respect to the starting pulse of the reactor. In the ^{239}Pu measurements, the background amounted to 95% of the total counting rate over the delayed neutron range. The measurements were performed, nevertheless, with a statistical accuracy on the order of 1% and allowed the preliminary value for β_{eff} for ^{239}Pu to be obtained.

To continue the measurements, a new 40 g sample from superpure ^{237}Np purchased. Another new sample (in metallic form) of ^{239}Pu to reduce the background from the (α,n)-reaction will be manufactured.

Studies of the peculiarities of mass and charge distributions of fission fragments from resonance compound states

Under the auspices of the DELRENE program, work to investigate the peculiarities of the fission of actinide nuclei from compound states was carried out. Investigations used the method of gamma-spectroscopy of fission fragments with the aim of identifying the fragments and determining their mass and charge distributions with absolute resolution in *A* and *Z*. Experiments on the precision measurement of prompt gamma-spectra of fragments from the thermal and resonance neutrons fission of ^{239}Pu by at the IBR-30 reactor were completed.

On the basis of the measured intensities of 41 γ-transitions, independent yields of 20 even-even fragments, as well as data on the life-times of four long-lived isotopes were obtained. Comparing the obtained data for the thermal point with known data collected by other methods gives evidence of the adeq uacy of the applied method. Within experimental errors, no variations in relative yields of the fission fragments in the neutron resonances with $J^{\pi}=1^+$ were observed, confirming the theoretical prediction previously made at FLNP for the ^{240}Pu compound nucleus: it undergoes fission only through the $J^{\pi}K=1^+0$ channel.

Further development of the method is connected with increasing the number of fragments identified and the accuracy of the measurements. The high efficiency of anti-Compton spectrometers for such measurements was proved by the results of the methodological experiments on neutron beams.

Investigations of Fast Neutron Induced Reactions with the Emission of Charged Particles

Measurements of the cross sections and angular distributions for the $^{40}Ca(n,a)^{37}Ar$ and $^{64}Zn(n,a)^{61}Ni$ reactions

Investigations of (n,α) reactions induced by fast neutrons are of interest for the purposes of both power engineering and the verification of nuclear models. At present, for the neutron energy range from 3 to 10 MeV which contains the thresholds of many *(n,α)* reactions, the existing experimental data are scarce and significant differences between the results of different authors exist.

The measurements were performed with neutrons from the $D(d,n)^3He$ reaction at the Van-de-Graaf accelerator of the Institute of Heavy Ion Physics, Beijing University, China. The α-particles from the *(n,α)* reaction were registered using the double flat ionization chamber with grids designed at FLNP JINR.

Angular distributions of α-particles for the neutron energies of 4 and 5 MeV were obtained for the $^{40}Ca(n,\alpha_0)^{37}Ar$ reaction and are presented in Fig.8. As can be seen, at E_n=4 MeV the angular distribution is practically symmetrical with respect to 90° and has a small forward rise at E_n=5 MeV. This result does not coincide with known data from the literature. For the reaction $^{64}Zn(n,\alpha)^{61}Ni$ at E_n=5 MeV, this symmetrical angular distribution was also obtained.

The integral cross section σ=234±23 mb for the $^{40}Ca(n,\alpha)^{37}Ar$ reaction at E_n=5 MeV obtained in the given experiment is illustrated in Fig.9 with a comparison of the data from other authors and calculated results.

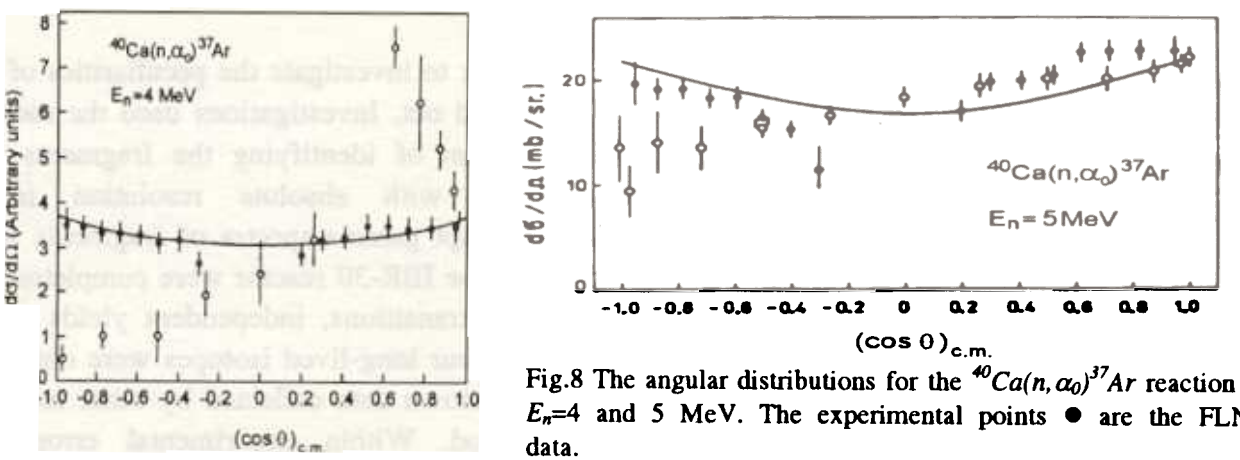

Fig.8 The angular distributions for the $^{40}Ca(n,\alpha_0)^{37}Ar$ reaction at E_n=4 and 5 MeV. The experimental points ● are the FLNP data.

Cross section systematics for fast neutron induced (n,α) reactions

Previously at FLNP, an analysis of the isotopic dependence of *(n,p)* reaction cross sections over the neutron energy interval from 6 to 16 MeV was conducted. Recently, the known cross sections of *(n,α)* reactions for the neutron energies of 8, 10, 14.5, and 16 MeV were systematized. To approximate the cross sections, the following formula, analogous to that previously used for *(n,p)*-reaction cross sections, was obtained:

$$\sigma_{n\alpha} = C\pi(R + \lambda)^2 \exp\left[-\frac{K(N - Z)}{A}\right]$$

where $R = r_0 A^{1/3}$ is the radius of the target nucleus, λ is the wavelength of incident neutrons, A, N, and Z are the mass number, number of neutrons, and the charge of the target nucleus, respectively. The parameters K and C are determined by experimental data fitting. The formula was demonstrated to describe the (n,α) reaction cross sections satisfactorily over the range from 8 to 16 MeV.

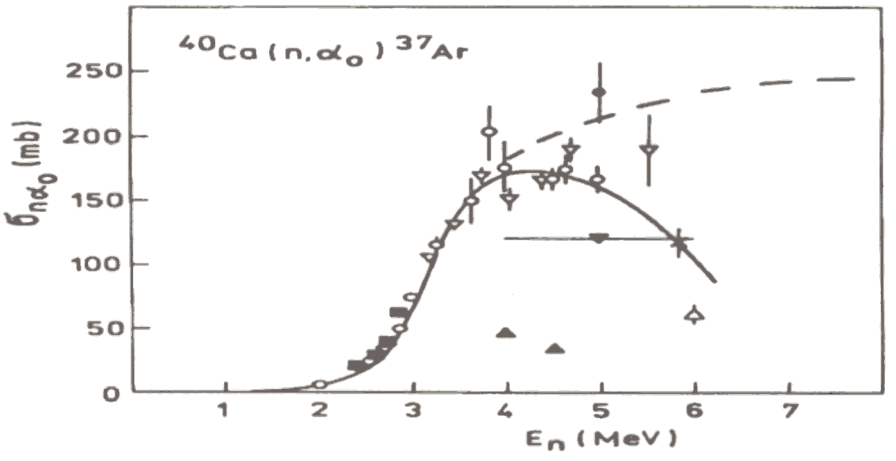

Fig. 9 The $^{40}Ca(n,\alpha_0)^{37}Ar$ reaction cross section. The experimental points ● are the FLNP data. The solid curve illustrates the results of the statistical model calculations.

Astrophysical Aspects of Neutron Physics

Cross sections for the $^{36}S(n,\gamma)^{33}$ and $^{48}Ca(n,\gamma)^{49}Ca$ reactions

Knowledge of the cross sections for neutron induced reactions with elements from the *S-Cl-Ar-Ca*-region at stellar temperatures is of importance to the study of the nucleosynthesis processes. Because the natural content of elements of this region is determined by contributions from different mechanisms (*s*- and *r*- processes, explosion burning, and cosmological synthesis following the Big Bang), one has to carry out a qualitative analysis impossible without an exact knowledge of reaction cross sections in order to analyze the mechanisms of isotope formation. This particularly concerns the problem of the formation of ^{36}S for which many theoretical models give too high a probability for. Previously, the FLNP-Karlsruhe collaboration measured the $^{36}S(n,\gamma)$ reaction cross section for kT=25 keV. This year, measurements of the cross section of this reaction were performed for kT= 151, 176, and 218 keV. Such neutron energies are mainly characteristic of the *s*-process of nucleosynthesis.

The measurements were performed with the 3.75 MeV Van-de-Graaf accelerator in Karlsruhe. A Maxwellian neutron spectrum with the thermal energy kT=25 keV was generated by the $^{7}Li(p,n)$ reaction near the threshold in a thick lithium target (30 μm). Spectra with other energies were obtained by using thinner targets (2.5 μm) and selecting the necessary proton energies. The measurements were carried out with 14 sulfur samples weighing from 20 to 150 mg.

The following cross sections for the $^{36}S(n,\gamma)^{37}S$ reaction were obtained: 187±14 μb, 81±7 μb, and 125±11 μb for the energies of 25, 151, 176, and 218 keV, respectively. The

obtained experimental values are 1.8 times smaller than the estimate previously used in calculations. This means that the ^{36}S yield from the *s*-process is larger by the same factor.

1.2.2. THEORETICAL

Nuclear Fission

Particular progress was achieved in theoretical investigations of nuclear fission. The relationship between asymptotic helicities of fission fragments and the spin projections of fissile nuclei on their axes was established. It was first shown that non-axial separation of fission fragments provides for the existence of P-even and P-odd angular correlations of fission fragments, as well as for the high values of their spins.

Development of a Modified Model of Nuclear Level Density

Following the prediction of the interacting boson model (IBM) about the asymptotic linear relationship between boson energies and the number of boson pairs of nucleons in unfilled shells, an analysis of the data on previously observed quasi-equidistant spacings of the intermediate levels in the most intense two-step cascades was performed. The comparison of the properties of these levels with the IBM predictions gives some indications that the excitations of heavy nuclei with the energies from 1-2 to 4-5 MeV demonstrated in radiative capture reactions are determined, to some extent, by excitation of the nucleon-boson condensate. The known relationships between the nucleon pairing energy, δ, and the phase transition temperature T_c=0.567δ, as well as between the critical excitation energy of the nucleus U_c and T_c: $U_c \cong aT_c^2 \cong$4-5 MeV, together with a hypothesis of the existence of a boson excitation branch, allowed us to explain the longstanding disagreement between the experimentally measured and model-predicted intensities of cascades qualitatively. This disagreement may be connected with the considerable influence, neglected in theoretical calculations, of the phase transition between the Bose and Fermi excitation branches of nuclei.

Non-Stationary Quantum Effects in Neutron Optics

The issue raised in literature of the possibility of distinguishing between pure and mixed states of a neutron beam in an experiment with the help of non-stationary quantum devices was investigated.

It was demonstrated that the long existence of a beam of particles with a non-zero density imposes certain requirements on the quantum characteristics of the beam, namely, on its density matrix. A theory of the phenomenon was developed. In the general case, a beam with modulated density exists, along which waves analogous to sound waves propagate. These waves have a discrete spectrum. The exceptions are two related limit cases: an ideally monochromatic wave which cannot be realized in practice, and a completely mixed (incoherent) state which is probably most frequent in practice. Studies of the time-space structure of the beam, together with spectrometric measurements, allowed conclusions about the density matrix type and answer the posed question.

The role of non-stationary devices is possibly reduced to the purely technical role of transforming the beam frequencies, *i.e.*, to detecting the difference between the modulator and beam frequencies.

The possibility of neutron time-focusing was discussed (together with R.Gaehler from München Technical University). It was found that the possibility of time-focusing neutrons at existing neutron sources with a relatively wide spectra of neutron velocities in the given point of space sufficiently far away from the source. Several ways of creating such time-lenses were proposed. One of them consists of significantly non-stationary action on the wave. For the relationship between the neutron source pulse duration and its image, an expression analogous to that for the usual optical magnification of a thin lens was obtained: $M = -a/b$, where a and b are the source-to-lens and lens-to-detector distances, respectively. The work may be essential for the realization of an old idea of F.L.Shapriro's of storing of UCN from a pulsed source.

Few-Body Problems in Nuclear Physics

Interaction of η-mesons with light nuclei

In recent years, this problem has been in the center of attention of theoreticians and experimentalists since one of the brightest effects of isotopic invariance violation was observed in the $d+d \rightarrow \pi^0 + {}^4He$ reaction. Non-conservation of the isospin and the existence of such a large cross section can only be explained if one assumes that the reaction goes through the creation of a virtual isoscalar η-meson which transforms into an isovector π^0-meson due to $(\eta\text{-}\pi^0)$ mixing. Up to the present time, only attempts at a simplified calculation of this two-step process in the frame of an optical model have been undertaken.

The first microscopic calculation of the subthreshold scattering of η-mesons on ${}^2H$, ${}^3H$, ${}^3He$, and ${}^4He$ nuclei was performed, discovering a quasibound state in the $\eta{}^4He$ system.

Nuclear reactions in muon molecules

Nuclei retained in molecules for a relatively long time can tunnel through the Coulomb barrier and interact with each other via nuclear forces at sub-keV energies. Such conditions cannot be created in scattering experiments. The microscopic analysis of some muon molecules allowed the discovery that among all possible nuclear reactions there is a special class of reactions with relatively large cross sections due to nuclear spectra correlation.

The structure of hypernuclei

The Skyrm-Hartry-Fok method was used to calculate the characteristics of light hypernuclei with a neutron halo (${}^{11}_{\Lambda}He$, ${}^{12}_{\Lambda}Li$, ${}^{12}_{\Lambda}Be$, ${}^{13}_{\Lambda}Be$, ${}^{16}_{\Lambda}C$). On adding a Λ–hyperon, a neutron in the halo can become either more or less bound. The characteristics of the halo strongly depend on the properties of the hyperon-nucleon interaction.

1.2.3. METHODOLOGY

Construction of the UGRA Setup

The construction work in the experimental pavilion was completed. The vacuum chamber with a rotating platform was transported from the JINR Experimental Workshops to neutron beam 6 of the IBR-30 reactor. This chamber, together with the sample movement mechanism and two detector shielding blocks, was assembled on the 250 m flight path. Assembly of the

electric drives and signaling systems was completed. The computer-aided control block was manufactured and the software for future experiments, in the main, was finished. Preparation for test experiments is under way.

Experimental Modeling to Measure Amplitudes of *n-e*-Interactions

Theoretical investigations of the influence of the thermal motion of noble gas (one-atom) atoms on the energy dependence of differential and total slow neutron scattering cross sections were completed. Two versions of experiments to measure the neutron-electron scattering length, b_{ne}, were suggested and simulated:

- measuring the total neutron cross section of the ^{86}Kr isotope, which has a very low capture cross section (~ 3mb) in the interval from 3 meV to 1 – 10 eV;
- measuring the angular anisotropy of the scattered neutrons on natural xenon (better on the $^{132,134,136}Xe$ isotopes) over the interval from 3 meV to 1 eV.

Staging of these experiments is important from the point of view of removing the considerable divergence in the experimental values of b_{ne} and refining the estimate of the mean square charge radius of the neutron.

Modernization of the ROMASHKA Setup

The purpose of this work is to transfer ROMASHKA to the mini-Crystal-Ball class. The protocol for collaboration with the Base for Development and Applications of Physics (BDAP) of the Bulgarian Academy of Sciences was signed, and the mechanical part of the new facility was designed in cooperation with specialists from BDAP. The contract for manufacturing the mechanical part to the account of the Bulgarian dues to JINR has been prepared for signing. Two new measuring modules were put into operation. The first is on the 500 m flight path to support HPGe-detector operations. The module allows multi-dimensional time-of-flight (4K channels) and amplitude (8K channels) measurements to be conducted. The second is on the 123 m flight path of beam 3. The module enables measurements of total transmission and self-indication functions following radiative capture.

Creation of the CSS Anti-Compton Gamma-Spectrometer on the Basis of an HPGe Detector and BGO Scintillators - the DELRENE Project

Calculations to optimize the geometry of BGO scintillators were performed using the GEANT computer code. Model tests of hollow light-guides were conducted. The designs of the spectrometer and its combined passive shielding were elaborated. Two PEM-125-based channels for photon registration were designed and constructed. Thirty-two crystals for the BGO scintillators were ordered and received and their parameters were measured. Manufacture of the structural elements for the spectrometer was completed. The spectrometer will be assembled and put into operation by the end middle of 1996.

Modernization of the Instrument for Measuring Angular Anisotropy of Fission Fragments from Aligned ^{235}U Nuclei

The modernization of the facility was completed: the new refrigerator for continuously maintaining a temperature of 0.1K on a sample was put into operation. New monocrystals of uranium-rubidium nitrate covered by a thin ^{235}U layer, which gives a two-bump distribution of

fission fragments, were installed. Inside the cryostat, implanted *Si*-detectors with an increased resistivity to IBR-30 gamma-pulses were assembled.

Investigation of the Subthreshold Fission of ^{234}U

An ionization fission chamber containing 0.1 g of ^{234}U isotope was manufactured. The daughter product of the α-decay of ^{238}Pu, having a ^{234}U content of over 99.8% and a considerably low (0.08%) admixture of ^{235}U, was used as the material for the chamber layers. Three series of measurements were conducted at the IBR-30 neutron booster. The preliminary results of the measurements (230 hours measuring time) are shown in Fig.10. In addition to the separate isolated resonances, in Fig.10 the first resonance cluster of ^{234}U can be clearly seen in the area around 450 - 650 eV. The measurements and data processing will be continued in 1996.

Investigations of Non-Stationary Quantum Effects in Neutron Optics

Creation of a prototype of an UCN gravitational spectrometer with interference filters was finished. The first series of test experiments was conducted at the IR-8 reactor of the RC "Kurchatov Institute". Simultaneously, investigations of the parameters of the interference filters by the method of neutron reflectometry at the IBR-2 reactor and the method of Rutherford scattering at the EG-2 electrostatic generator, was conducted in cooperation with the Scientific Department of Condensed Matter Physics FLNP. This is necessary for upgrading the technology of filter manufacture. Work to prepare new, improved filters was carried out in cooperation with the Institute for Solid State Physics of the Hungarian Academy of Sciences. An experiment to observe the dynamic multi-ray reflection of neutrons from a ferromagnetic mirror remagnetized

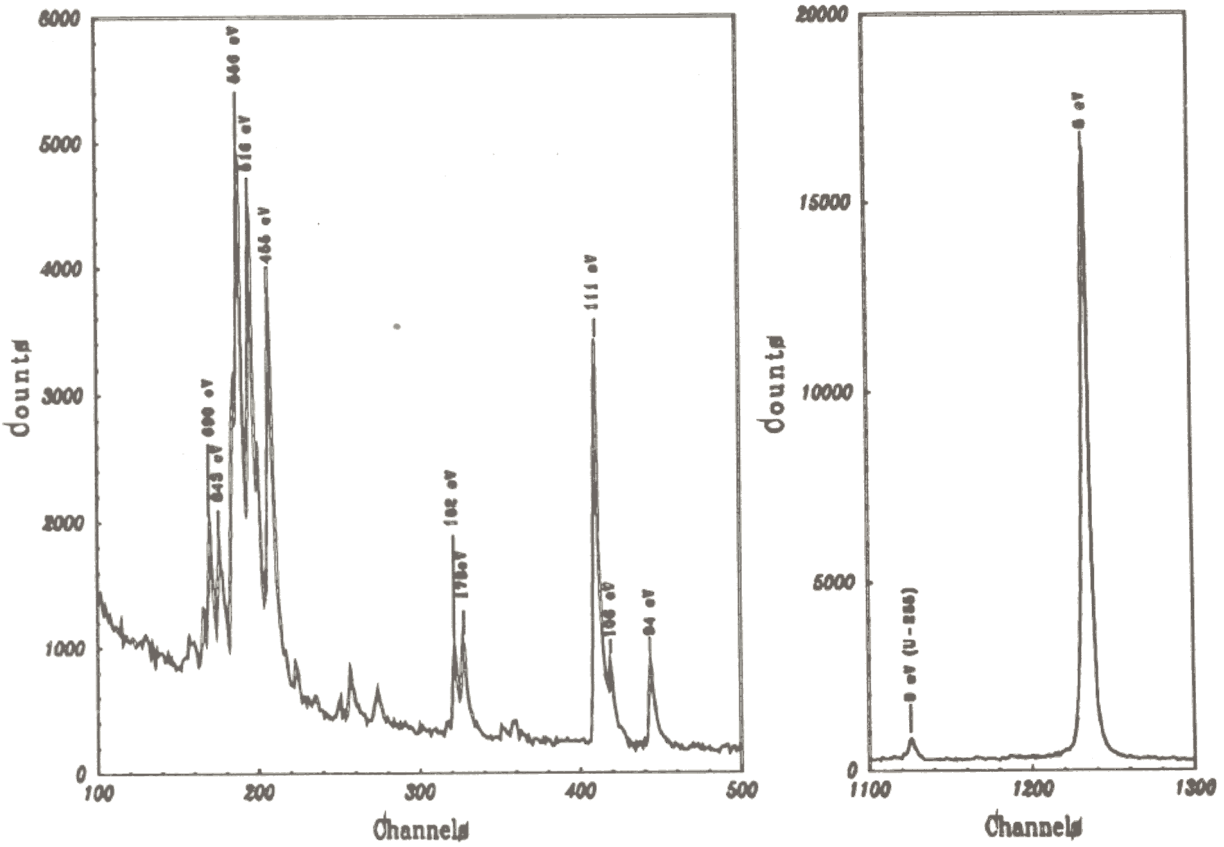

Fig. 10 The time-of-flight fission spectrum of ^{234}U in the energy range up to 1 keV.

at high frequency is under preparation. The system for generating fields with a frequency of 10 MHz and a strength on the order of 10 Gauss was constructed. Work to manufacture a mirror-sample in cooperation with the Institute of Applied Physics in Nizhnij Novgorod is under way.

Completion of the UCN Pulsed Source

In 1995, complex tests of the facility were completed in Dubna and some of the blocks were corrected. At the end of the year, the facility was moved for installation in the BIGR reactor hall at Arzamas-16.

Creation of a Facility to Search for Weak Heating of Ultracold Neutrons

In 1995, in collaboration with PNPI (Gatchina, Russia), a facility comprising 1 - a spectral filter (storage volume) with 2 - an absorber changing with height, was created and assembled at ILL (Grenoble, France). This facility allows the neutrons heated on 3 - the sample with an area up to 2 m^2 - to be registered. The registration is performed by a ^3He-based detector with variable efficiency - 4. The chamber and detector are surrounded by shielding made of cadmium and boron polyethylene. The background from the detector filled to the ^3He pressure of 400 torr, corresponding to an efficiency of 50% for thermal neutrons, was 0.02 s^{-1}. The expected effect for a foil-sample of 1 m^2 and an UCN intensity on the sample of ~1 $n \cdot cm^{-3}$ is ~1 $\cdot s^{-1}$. In this case, the entire anomaly of UCN storage can be explained by weak heating. Measuring the dependence of the detector count rate on the ^3He pressure provides the possibility of unfolding the spectrum of the heated neutrons.

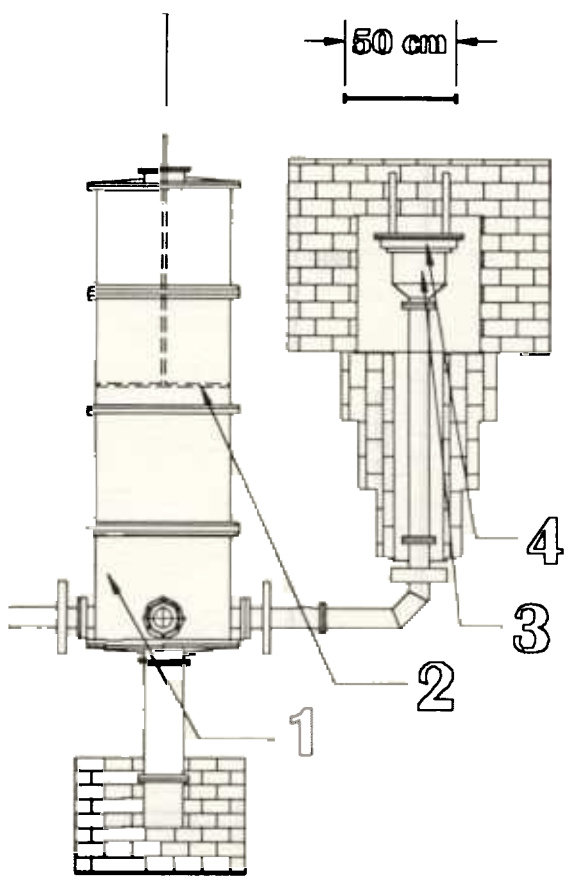

Here, the sample can have a preliminary outgasing at temperatures up to 400°C. The measurements can be conducted at sample temperature from -195°C to 400°C. The detector of heated neutrons has the same temperature.

Experiments have begun. The difference in the currently conducted experiment from the previous ones consists in the fact that the structure of the facility makes it possible to register the heated neutrons beginning from the energy of ~100 neV (5 m/s). This allows the hypothesis of weak UCN heating (to energies of $< 5 \cdot 10^{-5}$ eV) to be verified as a probable reason for the UCN storage anomaly observed in experiments with different material traps. Combining the capabilities of the facility and the record UCN flux from the ILL source gives basis for an unambiguous verification of the hypothesis.

Non-Stationary UCN Transport. Preparing Experiments of *n-n* Scattering

A method for storing UCN from a pulsed source using a mirror neutron guide and a shutter in front of the storage chamber was proposed. Preparations to conduct experimental tests of the method have started.

Calculations of non-stationary UCN storage and transport through horizontal neutron guides of different configurations and effective UCN filters were performed as well as calculation of the slow neutron background in the neutron scattering experiment at the BIGR reactor in Arzamas-16. Work to optimize the experimental geometry and calculate the detector response function was also performed.

1.3. APPLIED RESEARCH

In the reported period, the Sector of Activation Analysis and Radiation Research (AA and RR Sector) carried out investigations using the REGATA pneumatic-transport facility on beam 11 of the IBR-2 reactor in the following directions.

Neutron Activation Analysis. Data processing was completed and the results of biomonitoring of some regions in the Kola Peninsula were analyzed. For 200 soil and pine-needle samples, concentrations of 30 to 55 elements, including heavy-metal environmental pollutants, were determined. By maximums in concentration distributions, the main environmental pollution sources in the Murmansk region were identified: the big mining and non-ferrous metallurgy plants in the towns of Monchegorsk and Nickel. In the areas around these towns, concentrations of *Ni, Co, Cr, As, Se, Sb, Ag, Fe* and a number of other elements exceeded the allowed upper limit for inhabited regions. The work was carried out in cooperation with specialists from the Kola Scientific Center (KSC) of the Institute of Industrial Ecology of the North. The obtained results were presented at the international conference "Nuclear Physics for Protection of the Environment" (23-28 May, 1995, Dubna) and the national conference "Anthropogenic Soil Changes in Industrial Regions of the North" (25-27 July, 1995, Apatity) and submitted for publication.

In 1995, cooperation with KSC in investigating rare-earth element (REE) distributions in environmental samples from industrial areas in the Kola Peninsula continued. As a result, intense REE environmental pollution sources were revealed. The influence of excess REE concentrations on vegetation, animals, and man, is little studied up to now as the published data on REE contents in environmental objects are scarce. To study REE distributions, 160 soil and pine-needle samples were irradiated and gamma-spectra of the induced activity were measured. Processing of the results is under way.

In 1995, the stage of work conducted together with the Institute of the Lithosphere of Earth (ILE), RAS, to study ecosystems of the Volga and Oka river basins was competed. The results were reported at the international conference in Dubna. In continuation of this work, 100 samples of soil, sediments, and plants were measured to reveal anomalies in pollutant distributions of anthropogenic origin. The results are being processed and will be published in the ILE Report for 1995.

In the reported year, collaboration with the Institute of Chemical Kinetics and Burning, Siberian Branch, RAS (Novosibirsk) to conduct multi-element analysis of atmospheric aerosols

in some regions of Siberia, was initiated. The study of Siberian aerosols is an important and complicated fundamental problem which will be solved under the auspices of an international project "Aerosols in Siberia". Obtaining reliable data on the element composition of aerosols is an important link in these investigations, which will allow the nature and peculiarities of atmospheric pollution sources to be clarified. We investigated 150 aerosol samples from two regions in Siberia, Baikal Lake and Karasuk Lake. The results were transferred to customers for further analysis and the preparation of publications.

In the summer of 1995, members of the AA and RR Sector went on an expedition headed by Scandinavian scientists and supported by the international project "Accumulation of Heavy Metals in North Europe" to collect environmental samples in Romania and Norway. About 300 samples of soil, moss, and lichen were collected for neutron activation analysis at IBR-2.

Irradiation and neutron activation analysis of about 40 technical and jewelry crystals were conducted to investigate the origin of radiation dying and other local centers.

Radiation Investigations. In the reported year, investigations with gamma-irradiation of generation-recombination process singularities in the radiation resistant semiconducting detector material, $TlInSe_2$, continued. The experimental investigation and Monte Carlo calculations showed that the electron filling of local centers in the forbidden band of the semiconductor decreases as the photon energy of the exciting gamma radiation increases. This explains the temperature independence of the current excited by hard radiation in semiconductors such as *CdS, CdTe,* $TlInSe_2$, while the temperature dependence of the photo-current is considerable in these crystals. A paper on the investigation results was submitted to the Russian journal "Physics and Technology of Superconductors".

Together with I. L.Pisarev's group (Laboratory of Nuclear Problems, JINR) work on beam 11 to test the radiation resistance of detectors was started under the auspices of the ATLAS program.

Scientific and Methodological Developments. In the reported year, work to estimate the capabilities of the horizontal and vertical channels of IBR-2 for irradiating materials for the purposes of building new properties in those materials, producing isotopes, and conducting radiation investigations in the field of materials science.

Technical drawings of the irradiation facility for conducting radiation and radiation-analysis investigations of samples in the vertical channels of the water moderator situated behind the movable reflector were prepared and submitted to the Design Bureau.

The new experimental and technological base for the radiation investigations to be conducted in the period from 1996 to 1998 in the frame of the initiated project "Defect Formation in Strongly Anisotropic Semiconducting Crystals", is being created anew. The instrument for investigations of the Hall effect, self- and admixture-photo conductivity, and growing and intercalation of crystals of the $TlSe\text{-}TlInSe_2$ system, was assembled.

In 1995, during the reactor shut-down, the curved mirror neutron-guide (CMNG) on beam 11 of the IBR-2 reactor was adjusted with high precision. As a result, the thermal neutron yield at the CMNG exit was increased by 4 times. Additional adjustment was conducted in connection with the modernization of the instrument for measuring delayed neutron yields with uranium and transuranium nuclear targets. This work is being carried out in cooperation with Yu.S.Zamyatnin's group (FLNP).

2.1. CONDENSED MATTER PHYSICS

CONTENTS

Polarized Neutrons

Study of Depth Profiles of Elements of Thin Layer Structures Using RBS Technique
A.P.Kobzev, D.A.Korneev, O.A.Nikonov, V.A.Ul'yanov, B.G.Peskov, N.K.Pleshanov, V.M.Pusenkov, E.V.Siber Z.N.Soroko, V.G.Syromyatnikov, A.F.Schebetov

Off-Specular Neutron Reflection from Magnetic Media with Nondiagonal Reflectivity Matrices
D.A.Korneev, V.I.Bodnarchuk, V.K.Ignatovich

Investigation of the Hg-1201 structure under high external pressure by means of neutron diffraction.

V.L.Aksenov, A.M.Balagurov, B.N.Savenko, D.V.Sheptyakov
Dubna, JINR, Frank Lab of Neutron Physics, Russia
V.P.Glazkov, V.A.Somenkov
Russian Scientific Center "Kurchatov Institute", Moscow, Russia
E.V.Antipov, S.N.Putilin
Moscow State University, Department of Chemistry, Russia

$HgBa_2CuO_{4+\delta}$ is the first member of the homologous series of mercury-based superconductors[1] with general composition $HgBa_2Ca_{n-1}Cu_nO_{2n+2+\delta}$. This family of superconducting compounds displays the highest values of T_c available by now. Moreover their superconducting transition temperatures raise with the increase of external pressure[2,3] with practically the same speed for all the representatives of the series, approximately 2 K/GPa. For example it has been reported that the T_c's of above 150 K had been achieved for the compound with n=3 (Hg-1223) at external pressures higher than 10 GPa.

The increase of T_c induced by external pressure is being observed to some extent in all hole-doped superconducting copper oxides. This shows that the basic physical reason for this phenomenon is the same for all of them. It is naturally to suppose that this reason is the change in free charges concentration in the superconducting layers CuO_2 caused by changes in the interatomic distances.

Diffraction methods are providing the direct information concerning structural changes in crystals, and neutron diffraction seems to be the best method for investigations of the High-T_c compounds because it is necessary to determine the positions of the oxygen atoms with high precision. But it is quite complicated problem to obtain the information on the charge transfer even with the use of neutron diffraction because the changes of the interatomic distances are very small and the accuracy of the experimental data turns out to be insufficient. One of the ways to solve this problem is the increase of the accuracy of the data obtained, which is of course possible if the experiments are carried out at the diffractometer with the resolution (in the interlayer distances scale) not worse than 0.003. Though it is usually possible to carry out such an experiment in the range of pressures up to 1 GPa, the accuracy of the evaluated interatomic distances is quite satisfactory to make qualitative conclusions. Another possibility is in significant increase of the range of pressures at the sample (3-5 GPa) which allows to obtain necessary accuracy of data on the diffractometers with the resolution on the level of 0.01.

The structural changes in mercury-based superconductors caused by applying high external pressure have already been the subject of investigations for several teams of explorers[5,6]. In [5] the authors have investigated the crystal structures of $HgBa_2CuO_{4+\delta}$ and $HgBa_2CaCu_2O_{6+\delta}$ with a pressure up to 0.6 GPa and $HgBa_2Ca_2Cu_3O_{8+\delta}$ with a pressure up to 9.2 GPa by means of neutron powder diffraction. They have obtained the values of the compressibilities along the *a*- and *c*-axes and the bond distances compressibilities as well. In[6] the team of investigators have studied the pressure-induced structural changes in $HgBa_2Ca_1Cu_2O_{6+\delta}$ by means of neutron powder diffraction at the DN-12 diffractometer in Dubna in the pressure range 0-3.6 GPa with the use of sapphire anvil high-pressure cell. The lattice constants and bond distances compressibilities were determined and analyzed

involving quite doubtful model of disordered in the plane (*a,b*) oxygen but nevertheless the results turned out to be in general good agreement with the other data: the distance between Ba and O2 had the highest compressibility among all the other bond distances, and the compressibility of the *c*-axis is approximately twice higher than of the *a*-axis.

The structure of the compound with n=1 (Hg-1201) is the simplest among all the other compounds of the mercury series and other high-T_c's, and this is an important prerequisite for investigation of the small changes in the structure. Another important circumstance is that this compound is usually being obtained practically without any impurities and the analysis is not distorted by the signs of the other phases. As the compound with n=1 (Hg-1201) has the most simple structure among all the others, the aim of this investigation was to determine the general character of the structural behavior of Hg-1201 under applied high external pressure.

The experiments were carried out at the DN-12[4] specialized diffractometer for microsamples investigations at the IBR-2 pulsed reactor in Dubna. We used the sapphire-anvils high pressure cell to create the desirable pressures at the sample. At each pressure we have managed to perform the neutron diffraction experiment at two different angles simultaneously (usually these scattering angles values were near 45° and 90°). Such simultaneous measurements have ensured us in the correct and comparatively precise determination of experimental conditions and, thus, of the values of interest. The pressure was measured by detecting the displacement of the ruby luminescence lines and the uncertainty of these determinations was 0.03 GPa. The experiments were carried out at zero pressure in the region of d_{hkl} from 1.0 to 5.0 Å on the pure sample of the volume approximately 20 mm^3 in order to clarify the original structure and at pressures 1.47, 3.14, 4.31 and 5.07 GPa in the region of d_{hkl} from 1.8 to 5.0 Å in the high pressure cell (sample volume ≤ 2 mm^3). Rietveld refinement procedures of the diffraction patterns obtained at zero pressure possessed to estimate the values of the coordinates of atoms in the original structure. The quality of the diffraction patterns at intermediate pressures 1.47 and 3.14 GPa was not sufficient for precise determination of the lattice geometry because of the high level of background and the presence of parasitic diffraction from the sapphire single-crystal anvils but it turned out to be good enough to obtain the values of the lattice constants. Due to special improvements of the sample environment (background suppression, first of all) the quality of the diffraction patterns at higher pressures of 4.31 and 5.07 GPa turned out to be significantly better and this allowed us to carry out Rietveld refinement procedures with variation of several structural parameters, namely the *z*-coordinates of Ba and apical O atoms and lattice parameters as well. The typical view of the parts of the Rietveld refinements of the $HgBa_2CuO_{4+\delta}$ structure at zero pressure and at high pressure are shown in the fig. 1 and the detailed results of the diffraction patterns treatments are presented in the table 1.

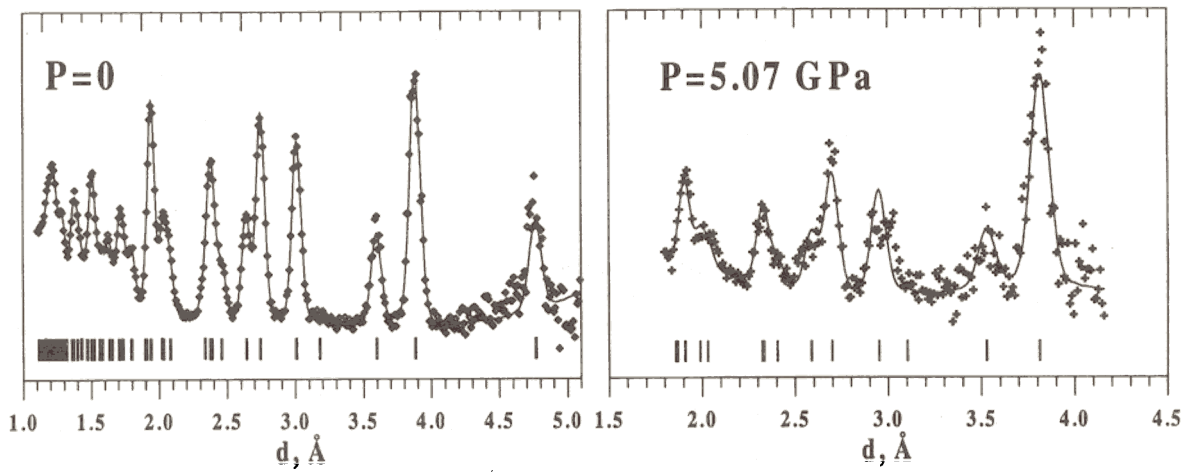

fig. 1. The parts of the Rietveld refinements of $HgBa_2CuO_{4+\delta}$ structure.

Table 1. Results of the Rietveld refinements of the $HgBa_2CuO_{4+\delta}$ structure under high external pressure.

Param.\ P(GPa)	0	1.47	3.14	4.31	5.07
a, Å	3.882(1)	3.852(2)	3.835(2)	3.826(2)	3.815(2)
c, Å	9.527(2)	9.462(8)	9.358(7)	9.335(8)	9.308(7)
V, $Å^3$	143.6	140.4	137.6	136.6	135.5
Hg, n	0.95	0.95	0.95	0.95	0.95
B, $Å^2$	1.5(3)			0.8(6)	1
Ba, z	0.2981(4)			0.299(2)	0.296(2)
B, $Å^2$	0.6			0.6	0.6
Cu, n	1	1	1	1	1
B, $Å^2$	0.5	0.5	0.5	0.5	0.5
O1, n	2	2	2	2	2
B, $Å^2$	1	1	1	1	1
O2, z	0.2078(4)			0.212(2)	0.212(2)
B, $Å^2$	1			1	1
O3, n	0.12			0.12	0.12
B, $Å^2$	1			1	1
R_w, %	4	8.5	9.2	8.8	8.8
χ^2	1.8	1.3	2.2	1.7	2.5
Cu-O2, Å	2.784			2.688	2.681
Hg-O2, Å	1.980			1.979	1.973
Ba/*l*-Cu/*l*, Å	1.924			1.876	1.899
Ba/*l*-O2/*l*, Å	0.860			0.812	0.782
Ba/*l*-Hg/*l*, Å	2.840			2.791	2.755

The main result of these experiments were the dependencies of the lattice parameters versus pressure (see fig. 2) and the dependencies of some interatomic distances in $HgBa_2CuO_{4+\delta}$ versus pressure (fig. 3, fig. 4); so we've really obtained the values of the compressibilities of the $HgBa_2CuO_{4+\delta}$ structure along *a* and *c* axes, the volume compressibility of the unit cell, and approximately estimated the compressibilities of some selected bond distances in the structure (see table 2).

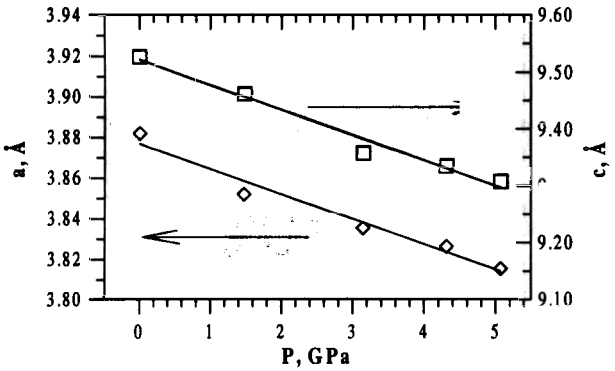

fig. 2. Lattice constants of $HgBa_2CuO_{4+\delta}$ structure versus pressure.

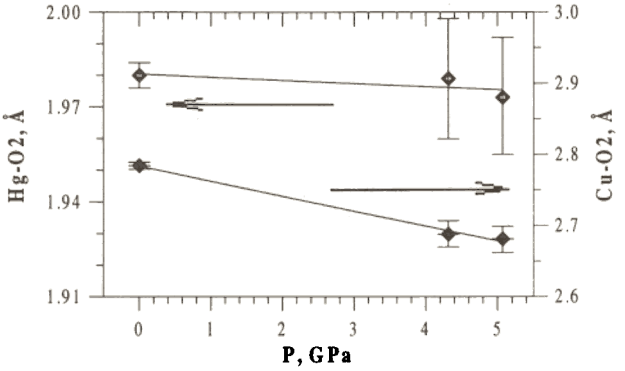

fig. 3. Dependencies of some interatomic distances in $HgBa_2CuO_{4+\delta}$ structure versus pressure.

Table 2. Compressibilities of the lattice parameters and of the unit cell volume of the $HgBa_2CuO_{4+\delta}$ structure as determined from the neutron powder diffraction data ($k_q=-(1/q)\delta q/\delta P$ (10^{-3} GPa^{-1})).

k_a	3.4
k_c	4.5
k_V	11.1
$k_{Ba/l\text{-}O2/l}$	18
$k_{Cu\text{-}O2}$	7.3
$k_{Hg\text{-}O2}$	0.7

The values of the lattice constants compressibilities are in general good agreement with those obtained earlier for the other members of the series[5,6]. The presence of small anisotropy in the lattice constants compressibilities is also in good agreement with earlier results[5,6]. Our measurements have shown that the pressure-induced changes in the $HgBa_2CuO_{4+\delta}$ structure really occur: the apical oxygen to copper atom distance sharply shortens with pressure increase (corresponding compressibility is $7.3*(10^{-3}$ $GPa^{-1})$) while the interatomic distance between O2 and Hg atoms remains practically the same.

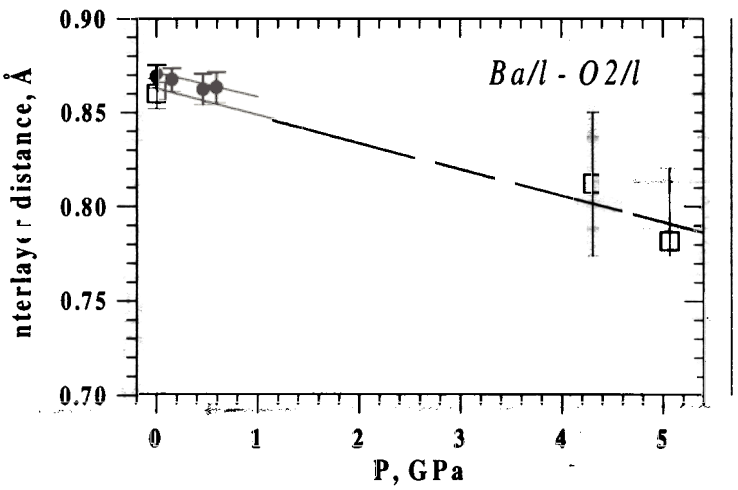

fig. 4. Dependence of Ba-O2 splitting in $HgBa_2CuO_{4+\delta}$ structure versus pressure. (● - data from[5], - current investigation)

It has been shown in the earlier works[7,8] that the value of interlayer splitting between Ba and O2 layers is the most sensitive value to the charge state of the basic and CuO_2 planes. Moreover, reasonable suggestions on the charge transfer between these two planes can be done on the basis of this splitting value. We present the dependence of this interlayer splitting on pressure in the fig. 4 together with the data

obtained in[5]. It is quite obvious that the two sets of data are giving practically the same behavior of the Ba-O2 splitting with pressure. This value is the most compressible parameter in the structure (as well as in the other members of the Hg-based compounds): $k_{Ba\text{-}O2} \approx 18$. It can be calculated that the corresponding value from[5] is approximately $k_{Ba\text{-}O2} \approx 15$.

From the charge balance analysis it follows that the decrease of Ba-O2 splitting corresponds to the charge transfer from the HgO_δ reservoir to the CuO_2 plane. In order to estimate this charge transfer it is possible[8] to use the empiric equation $\Delta = -0.045 + 0.2475Q$ which puts up the correlation between the splitting of the Ba-O2 layers and the charge transfer between the neighbouring HgO_δ and CuO_2 planes. Using this equation and our results we obtained that at external pressure of 5.07 GPa the charge equal to 0.13 elementary charges travels to the CuO_2 planes. This value after being normalized to the 1 GPa pressure is close to those obtained in[8] for Y-123, Y-124 and Hg-1212. This flow of charge from basic layers to the superconducting ones causes the lowering of the formal charge of copper atoms which results in the increase of the onset temperature. These speculations explain qualitatively the growth of T_c with pressure the observations of which had been reported about elsewhere[2,3].

Acknowledgements

We thank V.A.Alyoshin and D.A.Mikhailova for sample preparation.

References

1. E.V.Antipov, S.N.Putilin, Priroda (in Russia), 10 (1994) 3
2. C.W. Chu, L.Gao, F.Chen, Z.I.Huang, R.L.Meng and Y.Y.Xue, Nature, (London), 365 (1993) 323
3. M.Nunez-Regueiro, J.Tholence, E.V.Antipov, J.Capponi and M.Marezio, Science 262 (1993) 97
4. V.L.Aksenov et al, High Press. Res. 14 (1995) 181
5. B.A.Hunter, J.D.Jorgensen, J.L.Wagner, P.G.Radaelli et al, Physica C 221 (1994) 1
6. V.L.Aksenov et al, High Press. Res. 14 (1995) 127
7. S.Sh.Shilshtein, A.S.Ivanov, V.A.Somenkov, Physica C, 245 (1995) 181
8. S.Sh.Shilshtein, IAE Communications, 5339/9, Moscow, 1995

PHASE TRANSITION IN AC_{60} (A=K,Rb) FULLERIDE CRYSTALS

V.L. Aksenov, Yu.A. Ossipyan*, V.S. Shakhmatov

Frank Laboratory of Neutron Physics, JINR, Dubna
*ISSP, RAS, Chernogolovka, Russia

From experimental investigations, e.g., [1], it is known that the phase transition (PT) from the high temperature face-centered cubic phase of the Fm3m (O_h^5) symmetry to the low temperature polymeric-like phase of the Pnnm (D_{2h}^{12}) orthorhombic symmetry is observed in AC_{60} (A=K,Rb) fulleride crystals.

Inter-arrangement of the crystal cells of the above two phases is shown in Fig. 1.

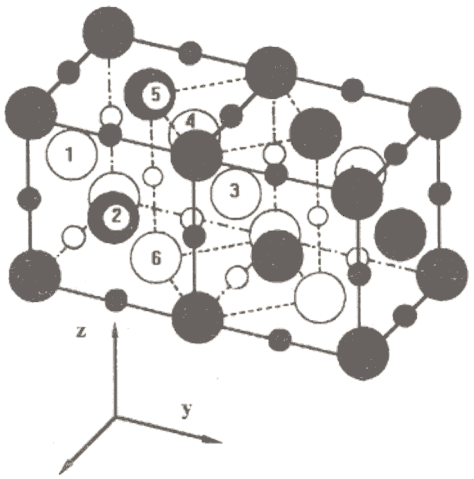

Fig. 1. Inter-arrangement of crystal cells in the Fm3m and Pnnm phases. Large circles refer to C_{60} molecules, smaller circles refer to metal atoms. Black circles indicate metal atoms and C_{60} molecules situated on visible faces of two face-centered cubic cells in the Fm3m phase. The Pnnm phase crystal cell is shown by dashed lines. The C_{60} molecules creating the octahedral environment for the metal atom are denoted by the numbers 1,...,6.

The A C_{60} compounds exhibit a number of very interesting physical properties. In the Fm3m high temperature phase, these compounds demonstrate strong localization of electrons, while in the polymeric-like phase, the A C_{60} compounds are quasi-one-dimensional metals. Moreover, at low temperatures the metallic state is unstable with respect to the formation of spin or charge density waves [2].

In our paper [3], the Landau phenomenological theory of PT to a polymeric-like phase in A C_{60} (A=K,Rb) crystals is developed on the basis of symmetry analysis. By analysis of the interactions between order parameters, probable PT connected

changes in the subsystem of metal atoms are investigated. The developed theory predicts the partial ordering of alkali metal atoms over the positions allowed in the octahedral environment of C_{60} molecules (Fig. 2).

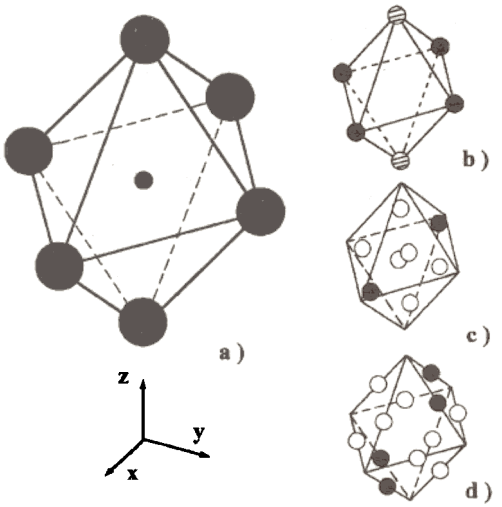

Fig.2. Possible types of positions for metal atoms (smaller circles) in the octahedral environment of C_{60} molecules (large circles): a) The central position **1b**; b), c) and d) are the **6e**, **8f** and **12i** positions, respectively.

A metal atom in the octahedral **1b** center position (Fig.2a) experiences no structural changes following PT. If a metal atom occupies a noncentral position, then partial ordering over the positions indicated in Figs. 2b, c), and d) takes place following PT. For the **6e** position, the partial ordering of the metal atoms either on the horizontal plane (dark circles) or over two positions situated above or below the plane (shaded circles) takes place. For the **8f** and **12i** positions (Fig. 2c and d), the occupied positions are shown by dark circles.

At decreasing temperature the appearance of another structural PT, which leads to complete ordering of the metal atoms, is also possible.

References

1. P.W. Stephens, G. Bortel, G. Faigel et al., *Nature*, **370**, 636 (1994).

2. O. Chauvet, G. Oszlanyi, L. Forro et al., *Phys. Rev. Lett.*,**72**, 2721 (1994).

3. V.L. Aksenov, Yu.A. Ossipyan, V.S. Shakhmatov, *JETP Letters*, **62**, 428 (1995) and
Preprint JINR, E17-95-426, Dubna, 1995.

Precision neutron diffraction structural study of the high-T_c superconductor $HgBa_2CuO_{4+\delta}$

A.M.Balagurov, V.V.Sikolenko, V.G.Simkin
141980 Dubna, JINR, Frank Lab of Neutron Physics, Russia

V.A.Aleshin, E.V.Antipov, D.A.Michajlova, S.N.Putilin
119899 Moscow State University, Department of Chemistry, Russia

F.Bouree
91191 Gif-sur-Yvette, LLB, France

The new mercury superconductors, belonging to a series of the general formula $HgBa_2Ca_{n-1}Cu_nO_{2+2n+\delta}$, with n=1,2,3 etc., were discovered in 1993[1]. The highest transition temperature, 134 K, was found for n=3. It increases up to 150 K under pressure of 11 GPa and this value is a record for high-T_c materials at present.

The structure of Hg-based compounds is being investigated by all possible methods, neutron diffraction among them. Several questions are still open, first of all about the exact oxygen content and its connection with T_c, about the mercury occupancy factor, and the reason for the high mercury temperature factor.

At FLNP, the studies of these new compounds were initiated in 1994 and continued in 1995. These studies are carried out in collaboration with the MSU Department of Chemistry of and the Russian Scientific Center of Kurchatov Institute. In 1995, four $HgBa_2CuO_{4+\delta}$ (Hg-1201) samples were studied: sample A with $T_c \approx 71$ K, m=2.09 g, sample B with $T_c \approx 83$ K, m=2.05 g, sample C with $T_c \approx 98$ K, m=1.93 g and sample D with $T_c \approx 96$ K, m=1.84 g. The last was prepared by a special method that resulted in an unconventional relation between the *a* and *c* lattice parameters. The main goal of this study was determination of the T_c dependence on oxygen content.

Neutron diffraction experiments with those samples were performed on the high resolution Fourier diffractometer (HRFD) at the IBR-2 pulsed reactor in Dubna and the 3T2 diffractometer at the Orphee reactor in Saclay. Diffraction pattern measurements were done with HRFD at room temperature for samples A-D and at 8 K for sample B. With 3T2, the measurements were made of sample A at room temperature and at 8 K. All the observed diffraction lines were accounted for by the expected Hg-1201 structure with the symmetry of space group *P4/mmm*. The MRIA and FULLPROF programs were used for processing data. A refinement of the Fourier spectra was carried out in the 0.81 - 2.09 Å interval with 110 peaks from Hg-1201. An example of the measured diffraction pattern can be seen in Fig.1. The refinement was done for the *z*-coordinates of Ba and O2 atoms, for the occupancy factors of Hg and O3 atoms, and for temperature factors of all atoms except O3. The determined structural data, together with selected interatomic and interlayer distances, are given in Table 1. The small amount of O3 atoms in the structure did not allow the exact value of the temperature factor, B_T(O3), to be found, though the correlation with the O3 occupancy factor, n(O3), was not very high. Thus, the variation of B_T(O3) over wide limits did not change n(O3) more than the limit of one standard deviation. A much stronger correlation was found between B_T(Hg) and n(Hg) (Fig.2). Moreover, for these two parameters, the minimum in χ^2 and R-factors values is not very pronounced.

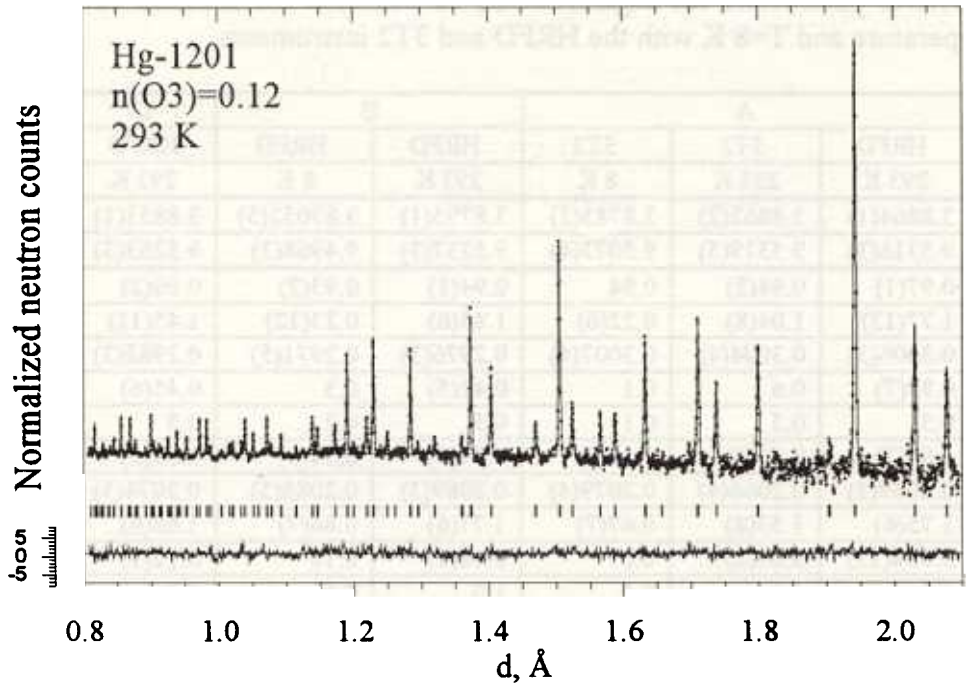

Fig. Diffraction spectrum from $HgBa_2CuO_{4.12}$, measured with the HRFD diffractometer and processed by the Rietveld method.

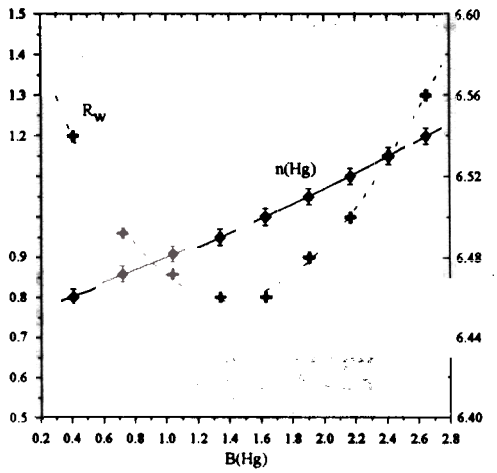

Fig. 2 Mercury occupancy factor n(Hg) (left scale) and weighted R_w-factor (right scale) as functions of a fixed value of B_T(Hg) for sample C.

On the whole, the structural results are in good accordance with published data[2-4] and, especially, with the data of Ref.[5] All features of the Hg-1201 structure and their dependence on temperature and oxygen content announced in[4] were confirmed.

We would like to draw special attention to the deficiency of the Hg position and the large temperature factors of the Hg and O2 atoms. The first was already mentioned in papers[6] and[7]. The attempts to explain it as a substitution of mercury for impurity atoms (copper or carbon) lead to contradictions with other data[6]. The low temperature data show that B_T(Hg) and B_T(O2) become much smaller at T=8 K. So, we have come to the conclusion that the mercury deficiency is real and the temperature motion of the Hg and O3 atoms is actually high at room temperature.

Both for our samples and the samples studied in[5], the linear dependence between oxygen content and the values of the *a* and *c* parameters can be seen. The T_c value depends strongly on n(O3), as shown in Figure 3, where our data and data from[5] are displayed. As it was predicted, both curves are hill-like, though their maximums are shifted.

Table 1. Structural parameters for $HgBa_2CuO_{4+\delta}$ as obtained for samples A - D at room temperature and T=8 K with the HRFD and 3T2 instruments.

Sample	A			B		C	D
Instrument	HRFD	3T2	3T2	HRFD	HRFD	HRFD	HRFD
Param./ T, K	293 K	293 K	8 K	293 K	8 K	293 K	293 K
a, Å	3.8864(1)	3.8862(2)	3.8783(2)	3.8795(1)	3.87052(5)	3.8851(1)	3.8851(1)
c, Å	9.5316(3)	9.5319(5)	9.5073(4)	9.5237(3)	9.4968(3)	9.5263(3)	9.5202(3)
Hg, n	0.97(1)	0.94(2)	0.94	0.94(1)	0.93(2)	0.96(2)	0.91(2)
B, $Å^2$	1.77(12)	1.04(8)	0.22(6)	1.45(6)	0.23(12)	1.45(11)	1.09(15)
Ba, z	0.3006(3)	0.3004(4)	0.3007(4)	0.2976(3)	0.2971(5)	0.2982(3)	0.2981(3)
B, $Å^2$	0.89(7)	0.6	0.1	0.42(5)	0.3	0.45(6)	0.29(7)
Cu, B, $Å^2$	0.5	0.5	0.1	0.5	0.2	0.5	0.5
O1, B, $Å^2$	1.06(7)	0.70(8)	0.38(8)	0.77(5)	0.34(8)	0.64(6)	0.29(7)
O2, z	0.2059(3)	0.2066(4)	0.2079(4)	0.2089(3)	0.2088(5)	0.2074(3)	0.2082(3)
B, $Å^2$	1.75(6)	1.53(8)	0.67(7)	1.77(6)	0.86(7)	1.68(6)	1.58(7)
O3, n	0.054(11)	0.07(2)	0.07	0.18(1)	0.18	0.12(1)	0.11(1)
B, $Å^2$	1.0	1.0	0.5	1.0	0.5	1.0	1.0
R_w	0.068			0.059	0.056	0.065	0.077
χ^2	1.06	1.18	1.21	1.78	1.06	1.07	1.11
Cu-O2, Å	2.803(3)	2.797(4)	2.777(4)	2.772(3)	2.765(5)	2.787(3)	2.778(3)
Hg-O2, Å	1.963(3)	1.969(4)	1.977(4)	1.990(3)	1.983(5)	1.975(3)	1.982(3)
Hg-Cu, Å	4.766	4.766	4.754	4.762	4.748	4.762	4.760
Ba// - Cu//, Å	1.901(3)	1.903(4)	1.895(4)	1.928(3)	1.927(5)	1.922(3)	1.922(3)
Ba// - O2//, Å	0.903(4)	0.894(5)	0.882(5)	0.845(4)	0.839(7)	0.865(4)	0.856(4)
Ba// - Hg//, Å	2.865(3)	2.863(4)	2.859(4)	2.834(3)	2.821(5)	2.834(3)	2.838

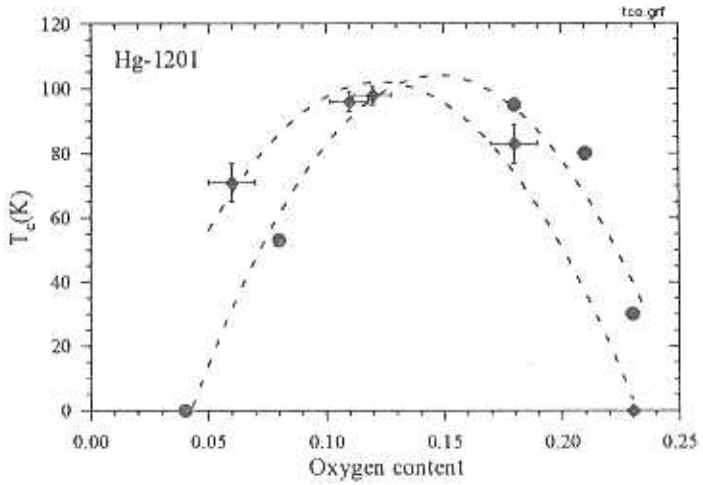

Fig. 3 T_c as a function of oxygen content for our samples (◊) together with point (δ=0.23) from[4] and for samples from paper[5] (•). The dashed curves are eye guides.

For the studied interval of oxygen content, the most pronounced changes can be found in the interlayer Ba - O2 distance, namely ~0.06 Å. It is ~10 times larger than the change in the *c* lattice parameter. This fact is in accordance with the idea published in[8] that this distance is the most sensitive one to charge changes in the neighboring layers. But the experimental decrease in this distance with increasing of δ does not coincide to the calculated value if the valence of the O3 atoms is put at −2. The coincidence can be achieved following the suggestion that ν(O3)≈−0.98. This value is in good accordance with the formal valence calculations performed in[5], where for ν(O3) the value of −0.90 was found.

In structural Hg-1201 papers, the question about the exact cation content of the compound is under very active discussion. Direct refinement attempts using the Rietveld

method failed due to the small number of additional atoms and the influence of experimental error. More information can be obtained after calculating the scattering-density maps, especially of experimental and calculated difference densities. The very high resolution of HRFD offers the possibility of drawing these maps. The sensitivity of this method is illustrated in Fig.4, where the difference map for the basal plane sample A is shown. The O3 atom is seen very clearly; its peak amplitude is ~2.5 times higher than the highest background peaks. It means that atoms with a coherent scattering length of ~0.6 (carbon, for instance) can be found for a concentration of around 3%. As an example, the experimental scattering-density map for the x=y, $0 \leq z \leq 0.5$ section is shown in Fig.5.

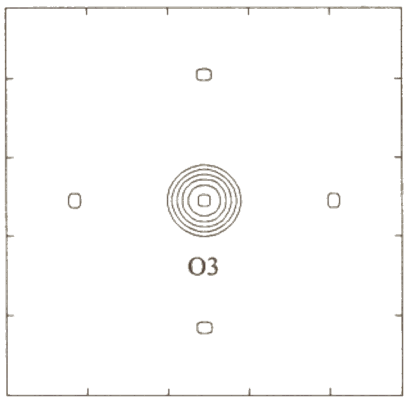

Fig. 4 Difference scattering-density map for the basal plane of sample. Oxygen O3 was removed from the for calculation of F_{hkl}.

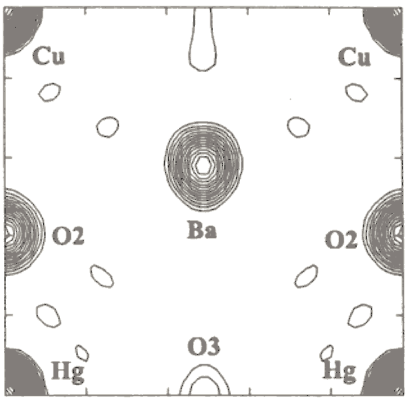

Fig. 5 Experimental scattering-density map for the diagonal crosssection x=y, $0 \leq z \leq 0.5$ of sample C.

References

1 S.N.Putilin, E.V.Antipov, O.Chmaissem and M.Marezio, Nature (London), 362 (1993) 226.
2. J.L.Wagner et al., *Physica C*, 210 (1993) 447.
3. O.Chmaissem et al., *Physica C*, 212 (1993) 259.
4. S.M.Loureiro et al., *Physica C*, 243 (1993) 1.
5. Q.Huang, J.W.Lynn, Q.Xiong, C.W.Chu, *Phys. Rev.*, B52 (1995) 462.
6. E.T Alexandre, S.M.Loureiro, E.V.Antipov et al., *Physica C*, 245 (1995) 207.
7. V.L.Aksenov, E.V.Antipov, A.M.Balagurov et al., *High Press. Res.*, 14 (1995) 127.
8. S.Sh.Shilstein, A.S.Ivanov, V.A.Somenkov, *Physica C*, 245 (1995) 181.

Structure of Graphitized Carbon Black Aggregates in Triton X-100/Water Solutions by Small Angle Neutron Scattering.

Vasil M. Garamus, Frank Laboratory of Neutron Physics Joint Institute for Nuclear Research, Dubna, Russsia; Jan Skov Pedersen Risø National Laboratory, Roskilde, Denmark; Leonid L. Bulavin, Kiev University, Kiev, Ukraine; Tamara V. Karmazina Institute of Colloid Chemistry and Chemistry of Water, Kiev, Ukraine.

Small angle neutron scattering method gives unique information about inner structure of carbon black (CB) particles [1]. The measurements of CB/Triton X-100/water solutions were continue of the such kind experiments at Risø National Laboratory performed by us [2]. The main conclusions of Ref. [2] are that the presence of CB particles shift CMC of Triton X-100 and fractal like CB particles with adsorbed layer of Triton X-100 and Triton X-100 micelles are situated at solutions.

In present measurements the experimental beam time was 18 h at half reactor power (1 MW) that is why only two experiments were performed in two different contrasts 30% and 60% heavy water.

The views of all curves agree with obtained previously [2]. In 30% heavy water solution we can observe only CB particles and in case 60% CB particles with adsorbed layer of Triton X-100 and Triton X-100 micelles give contributions to scattering curves.

The lower part of curves (q=0.008-0.02 $Å^{-1}$) were analysed by simple fractal expression:

$$d\Sigma(q)/d\Omega \sim q^{-D},$$

where D is the fractal dimension. The obtained values of D are 3.44±0.06 and 2.74±0.04 for 30% and 60% respectively together with early obtained [2] point that the compensation point is situated between 75 and 100% heavy water content.

The experimental scattering curves obtained in this experiment and previously [2] were modelled by expression:

$$d\Sigma(q)/d\Omega = A_1\Delta^2\rho_{CB}\Phi^2(q,<R>,\sigma,L)S(q,D,\zeta) + A_2\Delta^2\rho_{TP}F^2_{el}(q,a,\nu) + A_3\rho^2_sF^2_{sph}(q,r) + A_4,$$

where first term describe the scattering from fractals consist of polydisperse primary spherical particles with average radius <R> and dispersion σ, L - width of Triton layer, ζ is the maximum size of fractal structure; the second term is the scattering of ellipsoid of rotation Triton X-100 micelles with little semiaxis a and ratio between axis ν; the third term is a scattering from spherical voids which present in CB particles; A_4 is residual background.

The experimental data and model curves are represented at figure which shows good agreement between it.

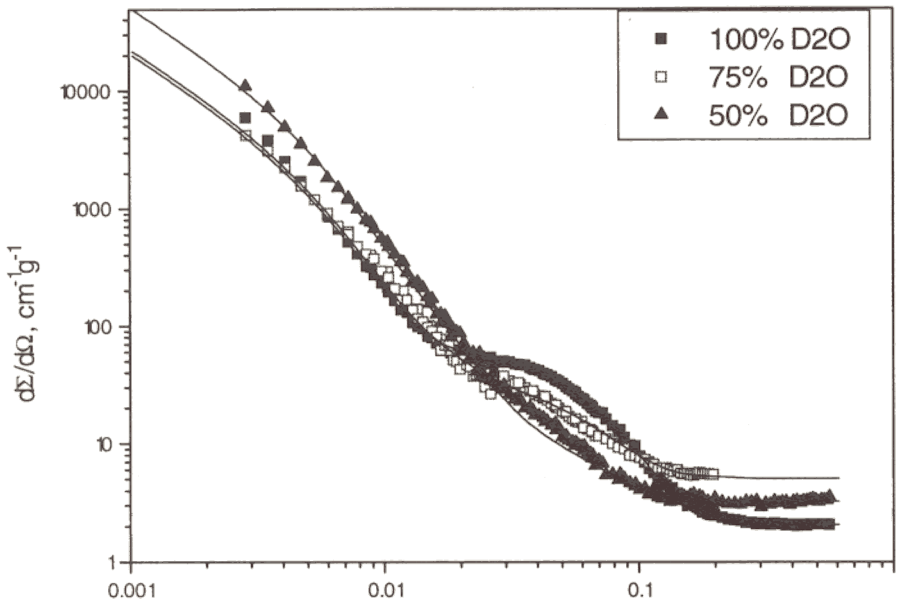

Small angle neutron scattering by dispersion of 10 g/l CB in 1.84 g/l Triton X-100/water solution with different contrast and model (solid lines).

The fractal dimension is found to decrease for increasing CB concentration from D = 3.4 at h = 0.01 to D = 2.9 at h = 0.05, the maximum size of fractal aggregate increases from 150 Å to 200 Å. The primary CB particles have wide size distribution and it's average size (80 Å) slightly decreases with CB concentration. The degree of occupation of CB surface by surfactant molecules is 10% and stays the constant with varying CB and surfactant concentration. The micelle structure is found same to it's structure in surfactant/water solutions. The volume fraction of voids does not exceed 1% of CB volume fraction.

1. Hjelm R. P. Jr., Wampler W. A., Seeger P. A. / J. Mater. Res., 1994, v. 9, p. 3210-3222.
2. Garamus V.M., Pedersen J.S. 2.7.6 "Carbon Black Dispersion in Non-Ionic Surfactant Water Solutions" "Annual Progress Reports of Department of Solid State Physics 1 January - 31 December 1994" ed. P.-A. Lindgard, K. Bechgaard, K. N. Clausen, R. Feidenhans'l, and I. Johannsen, Riso National Laboratory, Roskilde, Denmark, 1995 p.98

Structure of mixed multilayers of palmitoyloleoylphosphatidylcholine and oligooxyethelene glycol monododecyl ether determined by x-ray and neutron diffraction.

G. Klose[1], A. Islamov[2], B. Koenig[1] and V. Cherezov[2].

(1) University of Leipzig, Germany.

(2) LNP JINR Dubna, Russia.

Structure analysis of the lipid multilayers modified by nonionic surfactant was carried out at DN-2 diffractometer for studying several fundamental questions concerning structural and dynamical properties of lipid/water interfaces, understanding intermembrane interactions and the nature of so-called hydration forces.The structure of palmitoyl-oleoylphosphatidylcholine lipid (POPC) containing nonionic surfactant of the type $C_{12}H_{25}O(CH_2CH_2O)_nH$ ($C_{12}E_n$) was studied at the relative humidities RH=85%, 97% and at the molar ratio surfactant/lipid $R_{A/L}$=0.5,1, with n=2,4 and 6, where n is number of hydrophilic oxyethelene moieties. Partially deuterated surfactants $C_{12}H_{25}O(\mathbf{CD_2CD_2O})_nH$ ($C_{12}E_n$-d4n) and $C_{11}H_{23}\mathbf{CD_2}O(CH_2CH_2O)_nH$ ($C_{12}E_n$-d2) were used to determine the location of surfactants in lipid matrix. Fig.1. presents strip-function models of deuterated segments together with electron density profiles of POPC/$C_{12}E_n$ bilayers determined by x-ray diffraction. It was shown that α-methylene position ($C_{12}E_n$-d2 label) is anchored near the boundary of the hydrophobic core of lipid matrix, the oxyethelene moieties($C_{12}E_n$-d4n label) are mainly located in the polar membrane/water interface. With increasing humidity , molar ratio surfactant/lipid and number of oxyethelene moieties n, the partial lose of areas under strip-models is observed. This can be explained by the high degree of static disorder or/and motional freedom of surfactant moieties in the lipid matrix.

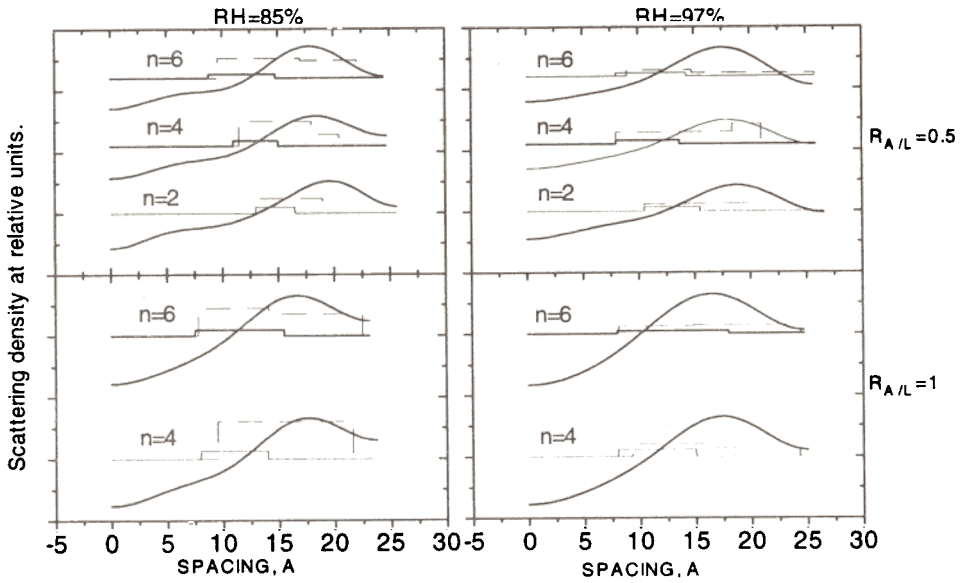

Fig.1. Strip-function models of deuterated segments $C_{12}E_n$-d2(solid line) and $C_{12}E_n$-d4n (dashed line) are presented together with electron density profiles of POPC/$C_{12}E_n$ bilayers at the relative humidities RH=85% and 97%, molar ratio surfactant/lipid $R_{A/L}$=0.5 and 1, n=2,4 and 6. Dramatical decrease of the area under deuterated label evidences about high degree of disorder of oxyethelene moieties in the lipid bilayer.

Partially unfolded state of lysozymes in dimethylsulphoxide with a well developed secondary structure

M.V.Avdeev*, M.D.Kirkitadze**, D.A.Prokhorov**, I.N.Serdyuk*, A.A.Timchenko**

* Frank Laboratory of Neutron Physics, Joint Institute for Nuclear Research, Dubna
** Institute of Protein Research, Puschino

A structural description of intermediate states realized upon spontaneous protein folding is ultimately essential for an understanding of protein self-organization rules. In most cases, however, kinetic intermediates have life times too short to be fully studied. It is more fruitful to find experimental conditions where the intermediates are stable. An example are low-molecular alcohols that stabilize the protein intermediate called a 'molten globule'. The action of dimethylsulfoxide (DMSO) on protein structure is the most interesting. It was shown for hen-egg white lysozyme (HEWL) that the helicity of unfolded protein in DMSO becomes somewhat higher than the helicity of the native one, and the protein forms a gel at low pH. These facts are indicative of great changes in the protein conformation and strong intermolecular interactions. Up to now, no structural information about these states has been available.

To fill this gap, we used neutron scattering from a solution of HEWL in DMSO and light water. The use of X-ray scattering for these purposes is practically impossible because of the high absorbance of X-rays by DMSO. The scattering experiments of HEWL in 70% DMSO at pH 2.5 and pH 2.0 have been performed. The latter case corresponds to the case of gel formation. The range of scattering vectors was 0.008 - 0.25 $Å^{-1}$. Figure 1 presents the scattering curve of HEWL in 70% DMSO at pH 2.5 plotted on Kratky coordinates. Such a plot makes it possible to distinguish the globular structure from the unfolded one. The wide plateau on this plot represents a coil-like structure. On the contrary, the globular structure shows a complex picture in this region, as can be seen from Fig.2 for the globular chaperonin GroEL measured simultaneously with HEWL.

Analysis of the plot in Fig.1 shows a plateau with a small incline. It indicates that the coil-like structure of the lysozyme molecule differs from the ideal coil. From the Guinier plot in the small-angle region, it is possible to evaluate the radius of gyration and intensity at the zero scattering angle I(0). Knowing I(0) it is easy to calculate the molecular mass of the protein. Such calculations have been made and it appears that lysozyme in 70% DMSO consists of about two monomers and its radius of gyration Rg is 35 Å. Such an Rg value unambiguously means that the conformation of the protein is not compact, in contrast to the 'molten globule' state. It is possible that the conformation of HEWL in DMSO resembles an early stage of protein folding where, according to some

investigators, unfolded conformation with native-like helices is formed. Further model calculations can clarify this question.

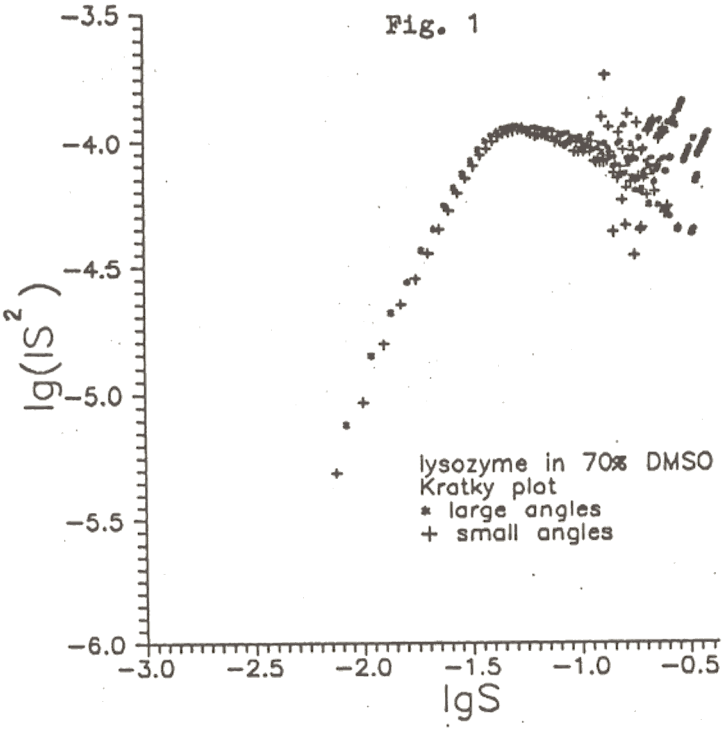

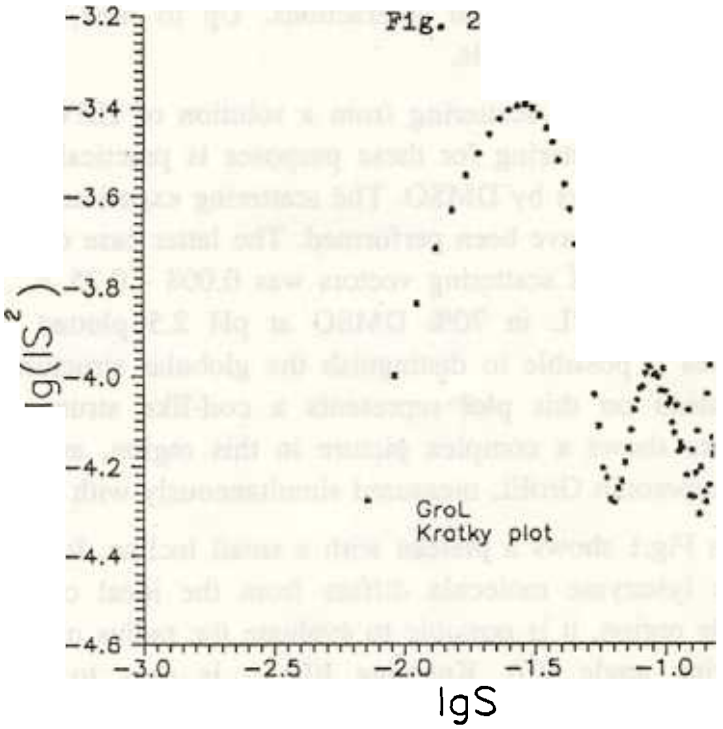

Some problems appeared upon measuring the gel-like form of the protein, but they can be easily solved after some changes in the program of data treatment. The above results will be published in the journal of Biofizika.

References

[1] K.Braig, Z.Otwinowski, R.Hegde, D.C.Boisvert, A.Joachimiak, A.L.Horwich, P.B.Sigler Nature, 371, 578-585 (1994)

[2] L.M.Gierasch, Z.Wang, J.Hunt, S.J.Landry, A.Weaver, J.Deisenhofer, Prot. Engineering 8 suppl.,14 (1995)

[3] K.Braig, M.Simon, F.Furuya, J.F.Hainfeld, A.L.Horwich, Proc. Natl. Acad. Sci. USA, 90, 3978-3982 (1993)

[4] Y.Igarashi, K.Kimura, K.Ichimura, S.Matsuzaki, T.Ikura, K.Kuwajima, H.Kihara, Biochemistry (1995, in press)

[5] D.I.Svergun J.Appl.Cryst. 24, 485-492 (1991)

Ammonium dynamics in $K_{1-x}(NH_4)_xI$ mixed salts at 10 K.

I. Natkaniec[&], L.S. Smirnov, S.I. Bragin, A.I. Solov'ev

Frank Laboratory of Neutron Physics, JINR, 141980 Dubna, Russia
&-On leave from H. Niewodniczanski Institute of Nuclear Physics, 31-342 Krakow, Poland

The $K_{1-x}(NH_4)_xI$ mixed salts have attracted increasing interest because they exhibit a low-temperature orientational glass phase devoid of long range order. The orientational degrees of freedom involved in the disordered frozen state are related to induced electric dipoles associated with the ammonium tetrahedra [1]. The x-T phase diagram of the $K_{1-x}(NH_4)_xI$ solid solution has been determined in [2] as consisting of three concentration ranges at low temperatures. At high concentrations ($x > x_c \cong 0.75$), ammonium ions are ordered as in pure NH_4I in a slightly distorted CsCl structure of tetragonal symmetry. For $0.3<x<x_c$ an orientational glassy phase with short range antiferroelectric order manifests itself in a NaCl type cubic structure. At cooling, below $x \cong 0.3$, the transition is no longer collective but is replaced by a single ion freezing.

The low energy rotational tunnelling transitions ($\Delta E < 1$ meV) have been investigated by the inelastic incoherent neutron scattering (IINS) method for $x<0.30$, but the rotational tunnelling states of ammonium ions in a diluted solutions of $K_{1-x}(NH_4)_xI$ are still not well understood [3,4]. The IINS studies of the localised dynamics in the dipolar $K_{1-x}(NH_4)_xI$ glass within the range $0.05<x<0.70$ show three distinct ammonium excitations at ca. 10, 21 and 31 meV, which are interpreted in terms of the so-called "triple-approach model" assuming that the tetrahedral ammonium ions adopt the C_{3v} symmetry site in the crystal [5].

We have studied the $K_{1-x}(NH_4)_xI$ system in the full concentration range on the NERA spectrometer at the IBR-2 pulsed reactor [6]. The IINS spectra were measured for concentrations x=0.0, 0.05, 0.15, 0.30, 0.45, 0.60, 0.80 and 1.0 at temperatures of 10, 80 and 290 K, respectively. The G(E) weighted phonon density of states obtained from the IINS spectra at 10 K are presented in Fig. 1.

The G(E) of pure potassium iodide exhibits two bands with energies of 5.8 and 13.2 meV, which correspond to the acoustic and optic phonon branches, respectively, in accordance with ref. [7]. For ammonium concentrations below x_c, corresponding G(E) functions display an additional low energy excitation at ca. 2.5 meV, in comparison to the results of ref. [5]. The low energy bands at ca. 2.5 and 9 meV are present only in the G(E) of the disordered phase. In the ordered, phase translational and torsional ammonium vibrations are marked by ν_5 and ν_6, respectively. The ν_5 band broadening with increasing ammonium concentration and in the ordered phase demonstrates two maxima. The average energy of the translational ammonium vibrations slightly decreases with ammonium concentration. The energy of the torsional excitations ν_6 changes from 36.5 meV in the ordered phase to ca. 30 meV in the disordered phase. The width of these bands increases with decreasing ammonium concentration.

The concentration dependencies of the energies of the ammonium excitations in the $K_{1-x}(NH_4)_xI$ mixed salts at 10 K are presented in Fig. 2 and are compared with the results of ref. [5].

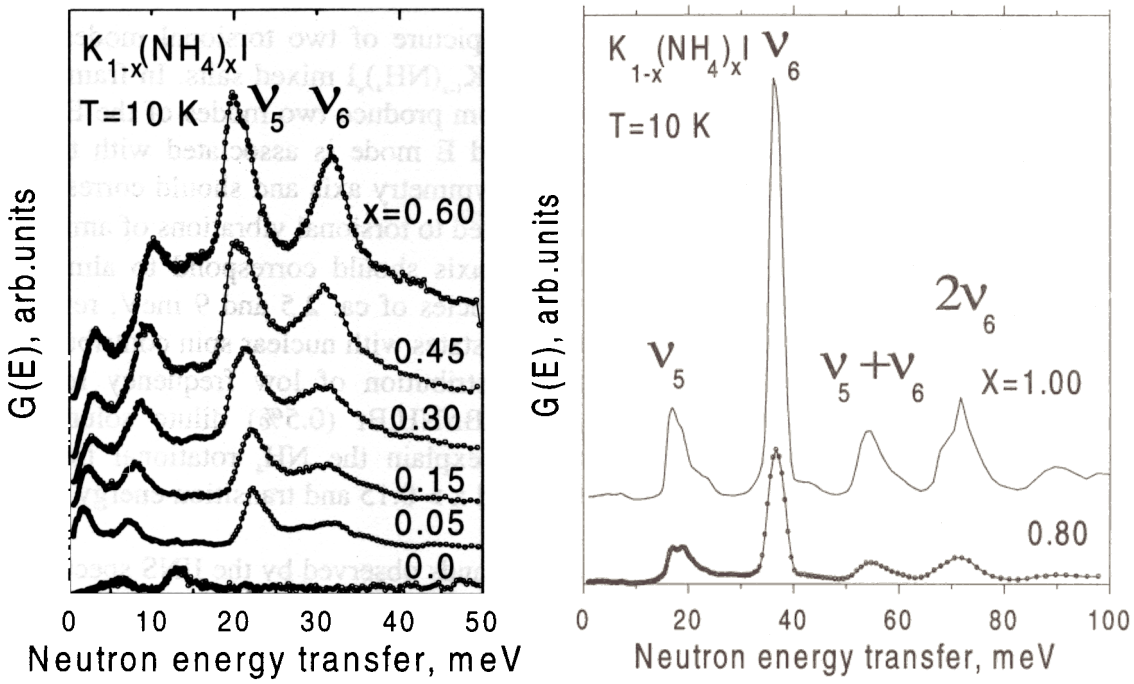

Fig. 1. The concentration dependence of the G(E) spectra for the $K_{1-x}(NH_4)_xI$ samples at 10 K.

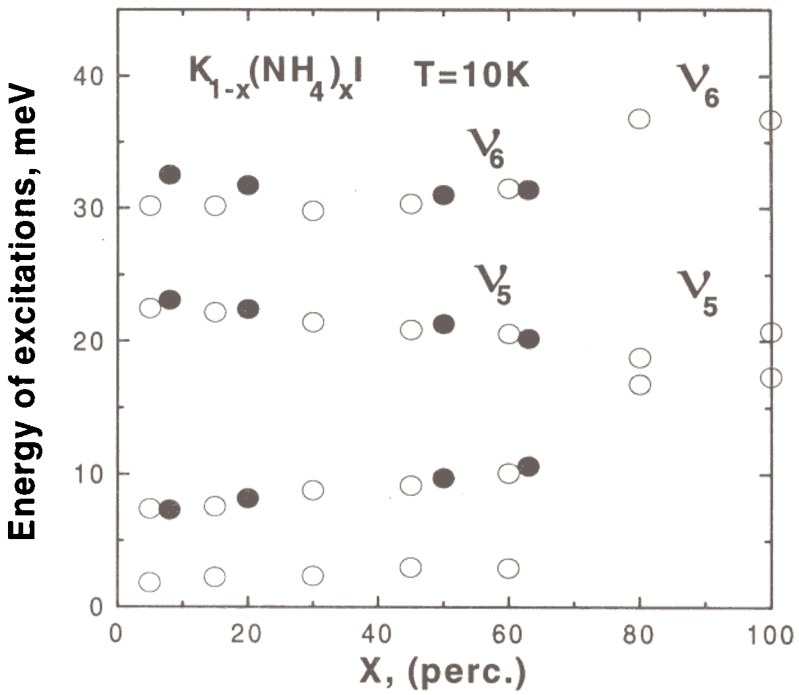

Fig. 2. The concentration dependence of the excitation energies of ammonium ions in $K_{1-x}(NH_4)_xI$ mixed salts (O- our results, O- results of ref. [5]).

Our results do not confirm the simple picture of two torsional modes of the ammonium ions in the disordered phase of the $K_{1-x}(NH_4)_xI$ mixed salts. In frame of the C_{3v} model, the three rotational degrees of freedom produce two modes of the E and A_2 character, respectively. The doubly degenerated E mode is associated with torsional vibrations about axes perpendicular to the C_{3v} symmetry axis and should correspond to the ν_6 band at ca. 30 meV. The A_2 mode associated to torsional vibrations of ammonium ions with their dipole oriented along the C_{3v} axis should correspond to almost free rotation. Possibly, two bands at the low frequencies of ca. 2.5 and 9 meV, reflect the rotational tunnelling spectrum of NH_4 free rotor states with nuclear spin contributions in the C_{3v} symmetry site. Similarly, a broad distribution of low frequency rotational excitations of NH_4 has been observed in KBr/NH_4Br (0.5%) dilute solution [8]. However, this model was not acceptable to explain the NH_4 rotational tunnelling excitations in the $K_{1-x}(NH_4)_xI$ mixed salts for and $x > 0.15$ and transition energy below 1 meV [3].

It is not doubt that both low frequency bands observed by the IINS spectroscopy in the disorder phase of the $K_{1-x}(NH_4)_xI$ mixed salts correspond to localised dynamics of ammonium ions in crystalline lattice. However, their concentration dependence is even more clear than for higher frequency modes and reflect ammonium-ammonium interactions. This implies that the C_{3v} rotational potential for NH_4 ions directly depends on such interactions. Direct ammonium-ammonium interactions contradict the presentation of this mixed salt as a pure dipolar glass. More detailed studies of the shape, width and intensity of these bands in dependence on concentration and temperature should explain the nature of these interactions and its role in the formation of the orientational glassy state in mixed ammonium salts.

REFERENCES

1. I. Fehst, R. Bohmer, W. Ott, A. Loidl, S. Haussuhl, C. Bostoen, Phys. Rev. Lett., **64** (1990) 3139-3142.
2. J.F.Berret, C.Bostoen, B.Hennion, Phys.Rev., **B46** (1992) 13747-13750.
3. C.Bostoen, G.Coddens, W.Wegener, J.Chem.Phys., **91** (1989) 6337-6345.
4. R.Mukhopadhyay, J.Tomkinson, C.J.Carlile, Europhys.Lett., **17** (1992) 201-206.
5. J.Tomkinson, B.A.Dasannacharya, P.S.Goyal and R.Chakravarthy, J.Chem.Soc.Faraday Trans., **87** (1991) 3431-3433.
6. I. Natkaniec, S.I. Bragin, J. Brankowski, J. Mayer, Proc. ICANS-XII, Abingdon 1993, RAL Report 94-025, Vol. I. p.89-96.
7. G.Dolling, R.A.Cowley. C.Schittenhelm, and I.M.Thorson, Phys. Rev., **147** (1966) 577-582.
8. A. Inaba, H. Chihara, J.A. Morrison, H. Blank, A. Heideman, J. Tomkinson, J. Phys. Soc. Japan, **59** (1990) 522-531.

Investigation of the librational spectrum of deuterated thiocyanate ammonium.

L.S. Smirnov, I. Natkaniec[&], S.I. Bragin

Frank Laboratory of Neutron Physics, JINR, 141980 Dubna, Russia.
&-On leave from H. Niewodniczanski Institute of Nuclear Physics, 31-342 Krakow, Poland

Thiocyanate ammonium, NH_4SCN, undergoes phase transitions from the tetragonal phase I with space group D_{4h}^{18} through the orthorhombic phase II with space group D_{2h}^{11} to the monoclinic phase III with space group C_{2h}^{5} during cooling at 390 and 360K, respectively. The phase transition from the tetragonal phase I to the orthorhombic phase II is due to the ordering of molecular SCN^- ions and the phase transition from the orthorhombic phase II to the monoclinic phase III is due to the ordering of the molecular NH_4^+ ions. The contribution of ammonium ions to the phase transitions of NH_4SCN was investigated with the help of inelastic incoherent neutron scattering in [1]. In this work, the librational spectrum of ammonium was determined.

In order to be sure that energies in the region from 300 to 400 cm^{-1} are indeed librational energies it is necessary to carry out the investigation of ammonium dynamics with inelastic incoherent neutron scattering of deuterated ammonium thiocyanate. It is known that the librational energies of deuterated ammonium decrease by 1.4 times and this method is used to identify rotational states.

In a recent report the results of the inelastic incoherent neutron scattering (IINS) investigation of the deuterated thiocyanate ammonium in the monoclinic phase at 9K are presented. The G(E) vibrational density of state weighted on amplitude of atom vibrations, obtained from the IINS spectra for ND_4SCN and earlier for NH_4SCN [1] are presented in Fig. 1. The optical translational and librational energies determined for deuterated and protonated ammonium are summed in the Table.

Table. Energies of $N(H/D)_4$ (are given in cm^{-1})

Modes	NH_4SCN	ND_4SCN	E(H)/E(D)
ν_5	179	168	1.065
	193	182	1.060
ν_6	318	235	1.353
	351	256	1.371
	380	278	1.366
	409	300	1.363

The obtained relations of E(H)/E(D) for ν_5 and ν_6 are in accordance with the band identification done in [1].

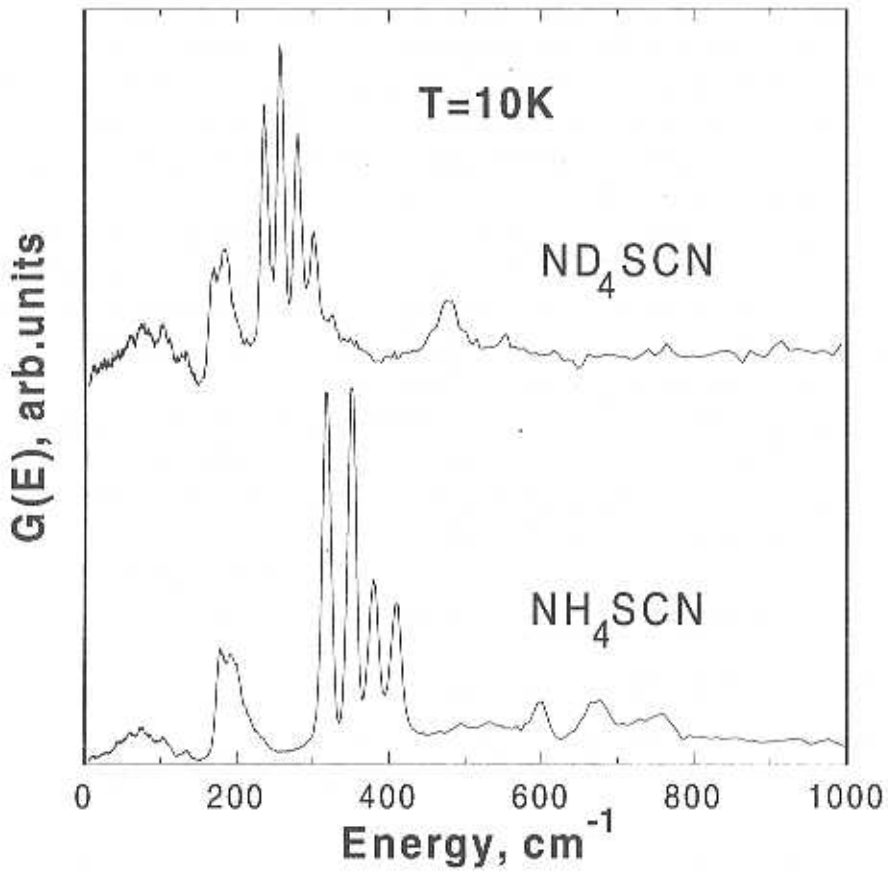

Fig. 1. The comparison of G(E) spectra for NH_4SCN and ND_4SCN at 10 K.

Reference:

1. I. Natkaniec, L.S. Smirnov, A.I. Solov'ev, Physica **B 213&214** (1995) 667-668.

DENSITY OF VIBRATIONAL STATES OF HIGHLY DISPERSE CARBONS.

1. Nanodisperse diamonds

I.Markichev*, E.Sheka*, A.Muzychka** and V.Khavryutchenko**

(*) *Russian Peoples' Friendship University, Moscow*
(**)*LNP, JINR, Dubna*

Nano-size carbons have recently attracted a great attention due to promising perspectives of their large application in science and technology. This is mainly due to a large variety of carbon nanospecies: from nanodiamonds and nanographites compositions to fullerenes. This variety of nanospecies, having sometimes a similar appearance, in its turn, has put a problem of the species identification and sertification. A lot of IR and Raman spectroscopic studied has been undertaken to tackle the problem for the last few years. However, the above optical methods occurred to be unsufficient in some cases. Besides that, optical methods are mainly related to bulk vibrations of the species while the surface and its vibrations play an important role for nanospecies. These facts have necessitated a performance of a series of nanospecies vibrational spectra studies using the technique of inelastic neutron scattering (INS), which has highlighted itself as an appropriate tool for both bulk and surface nanospecies vibrations investigation [1].

Below a series of experiments is presented which was carried out for the following carbon nanospecies:

- nanodisperse diamond of different grain size and of different origin;
- exfoliated graphite;
- graphitized black;
- endogenic carbon dust;
- carbon heterosorbents.

This report presents the results obtained for nanodiamonds. Experiments were carried out on INS spectrometer KDSOG-M at T=80K. Three samples were studied.

Sample 1 was obtained in the course of a blow-driven reaction between trinitritoluene and hexan. It consists of particles with the diameter of 35-40Å in average. According to X-Ray study, the particles have a diamond-like structure. Their surface is partially graphitized. Sample mass is of 39.4 gr, measuring time is 5 hours. The sample was provided by Physical Department of the Moscow State University.

Samples 2 and 3 are commersial syntethic diamonds produced in the Institute of superhard materials of the national Ac.Sci. of the Ukraine. They differ by the average grain size which is of 60-40 mcm for sample 2 (it will be called below as a macrodiamond) and is much less for sample 3, corresponding to the specific area value

of 187 m^2/gr. The both samples masses are of 20 and 19 gr, respectively. Measuring time was 8 hours in both cases.

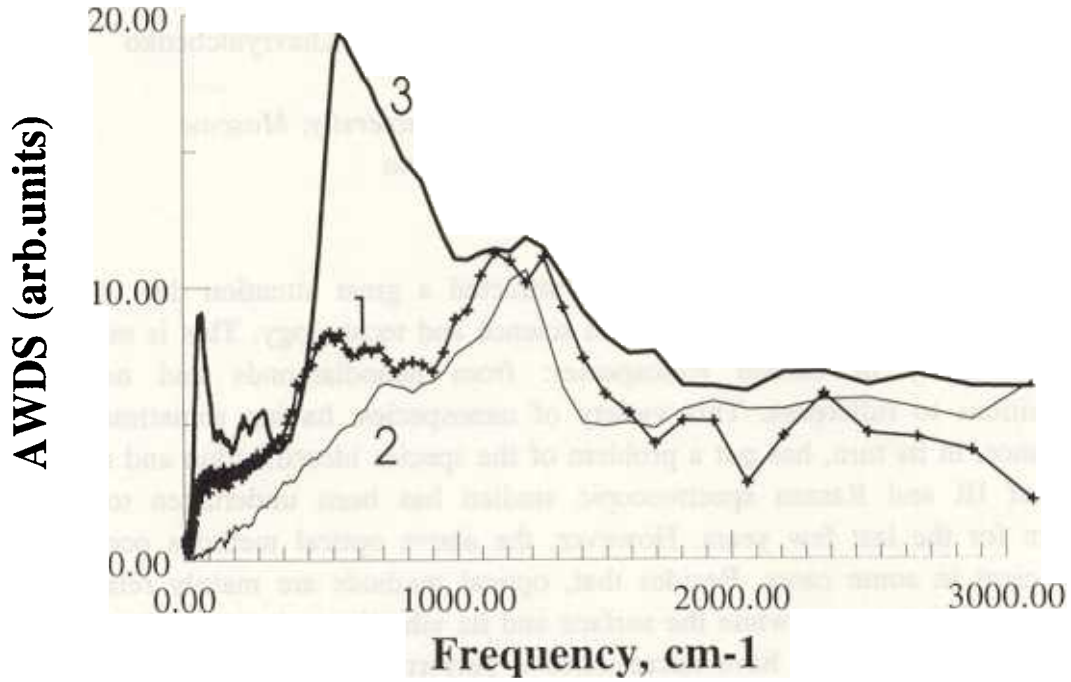

Fig.1

Fig.1 presents the sample spectra of double-amplitude weighted density of vibrational states (AWDS) normalized per 100 gr of mass and 1 hour of measuring time. The spectra numbering in Fig.1 corresponds to the sample numbering. As expected, the spectrum of macrodiamond (sample 2) is of the lowest intensity among the spectra set. This is due to the fact that this spectrum corresponds to bulk vibrations only while the other two spectra, related to more disperse species, are composed of both bulk and surface vibrations. In the latter case the vibrations of the surface zone as whole are implied. Spectrum 2 fits well the DOS of bulk vibrational states for diamond [2]. Its shape has a peculiar two-hump structure with maxima positioned at 700 and 1200-1250 cm-1. A sharp decreasing of the spectrum intensity is observed over 1300 cm-1.

To analyse spectra 1 and 3 means to decompose them into the spectra of their constituents, primarily into spectra of bulk and surface vibrations. To obtain the atter spectra, it is necessary to substract spectrum 2 which presents the spectrum of the bulk modes, from spectra 1 and 3. Fig.2. shows a residual spectrum (3) - (2). The spectrum (1) - (2) has the same shape but is less by intensity. The residual spectrum in Fig.2 in the main spectral region up to 1200 cm-1 is fully similar to a well known spectrum of a quenched water (see, for example, [1]) so that it should be attributed to a confined water in the body of both nanodiamond powders. Further investigation should answer

a question what kind of nano-scale porous or capilar structure is responsible for catching water inside the powder of nanodiamonds.

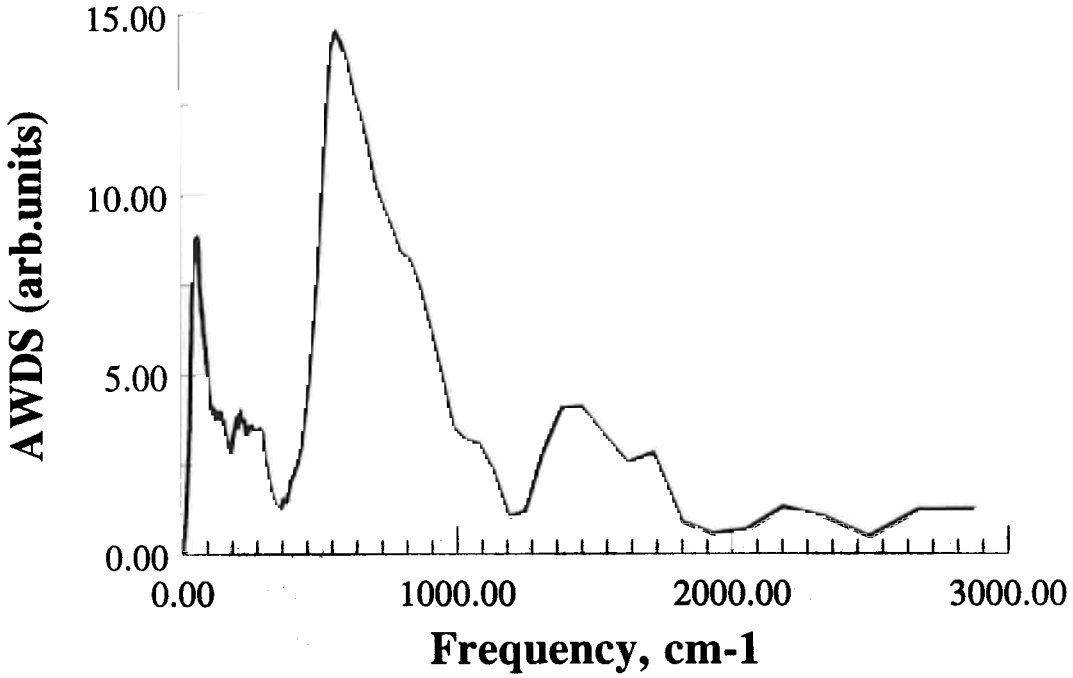

Fig.2

1. E.F.Sheka, V.D.Khavryutchenko and I.V.Markichev, Russian Chemical Reviews, 64 (5), 389-414 (1995)

2. P.Pavone, K.Karch, O.Schutt, W.Windl, D.Strauch, P.Gianozzi and S.Baroni, Phys.Rev.B48, 3156 (1993).

The Interaction of Oxygen (Nitrogen) with Hydrogen in Ti, V and Ta.

V.V.Sumin, Ch.Gantulga

LNP, JINR, Dubna, Russia

The fast ion channelling (FIC) showed than hydrogen mores from tetrahedral positions to the octahedral in V-O-H solid solution (SS) or low symmetrical positions in Ta-N SS. [1] due to O(N)-H interaction.

So oxygen or nitrogen locate in the octahedral positions the FIC method can not determine exactly the hydrogen location.We check these statements by INS.

Sample preparations. The vanadium was alloyed by the ultimate concentration of oxygen α-phase (6 at%). The sample was charged by hydrogen at 800^0C and water quenched.

One tantalum sample was alloyed preliminary by 3 at% of vanadium and then saturated by nitrogen and hydrogen from the gas phase and water quenched from 800^0C. Vanadium and nitrogen in Ta form additional defect complex, which captures hydrogen. Titanium sample was prepared by melting Ti with TiN to concentration $TiN_{0.05}$ and charged by H. All the samples was single phase as was determined by neutronography.

V - O - H system

In this system the formation of β–V_2H hydride was studied by INS. Due to high luminosity of the KDSOG-2M local mode of hydrogen in the octahedral sites can be measured during 1 hour. So the process of β- V_2H formation was studied at gradual cooling of the samples from room temperature to 210^0K (Fig.1,2). Oxygen courses the substantial influence on this process first of all, the LM energies change by different lows (Fig.3).

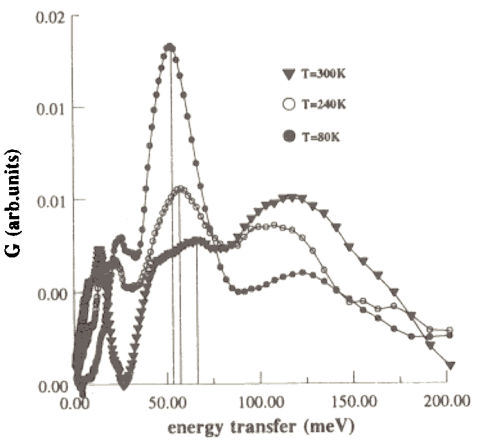

Fig.1 The partial hydrogen function of state (PHFS) in VO H at 300K, 240K and 80K

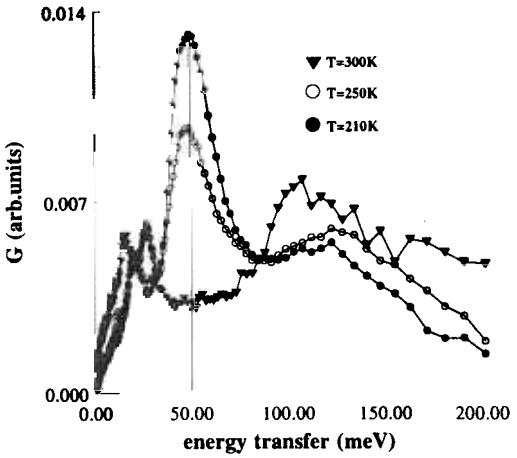

Fig.2 The PHFS in $VH_{0.01}$ at 300K, 250K and 210K

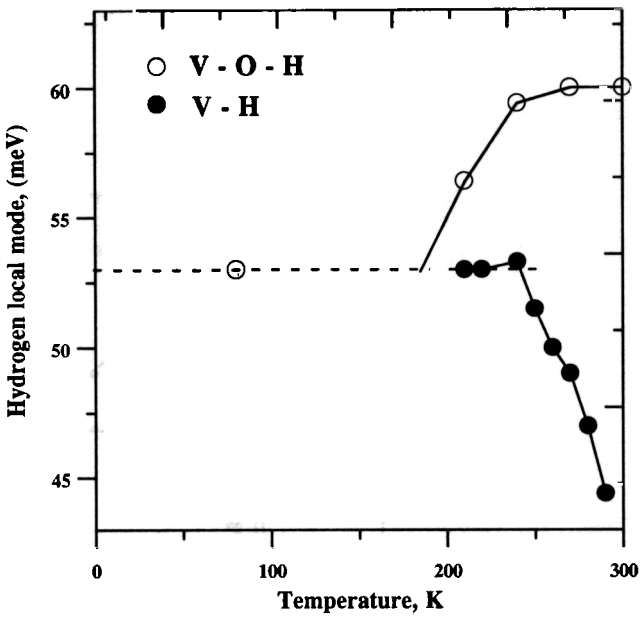

Fig.3 The dependence of LMP versus temperature for the $VO_{0.06}H_{0.03}$ (open circle) and $VH_{0.01}$ (dark circle).

In binary $VH_{0.01}$ system the hydrogen local mode positions (LMP) increase from 45 meV at room temperature to 53 meV at 240^0K and stay constant at more lower temperature. According to [2] hydrogen precipitates into hydride at 260^0K for 1 at% concentration in V. Before this temperature LMP changes can be explained by the preparation of hydrogen atoms to phase transition. This process accompanies by grows of the tetragonality VH_x SS [3]. Fukai [3] proposed that 1T→4T(O) transition perponsed for this tetragonality. We confirm this proposal by INS.

In the case of ternary $VO_{0.06}H_{0.03}$ system, LMP's decries from 63 meV to 53 meV (Fig.3). Oxygen keep hydrogen in SS down to 190^0K. That is on 50^0K lower than for binary V-H system in spite of the greater H concentration in ternary SS.

Both for binary or ternary systems hydrogen takes participation not only in LM but in resonance - like lattice vibrations (RLLV) (Fig.1,2). The positions of this RLLV depend on temperature and close to the predict value 16 meV [4].

$TaN_{0.02}H_{0.045}$ and $TaV_{0.03}N_{0.02}H_{0.02}$ solid solutions.

The binary $TaH_{0.045}$ SS changes essentially the LMP at low temperature due to formation of β-TaH hydride (Fig.4).

In contrary to that the nitrogen contained alloys do not change the LMP at low temperatures (Fig.5,6). From these facts we conclude that N-H or V-N-H interactions keeps hydrogen in SS.

Moreover in $TaV_{0.03}N_{0.02}H_{0.02}$ alloy the hydrogen LM split into three peaks as for ε-V_2H hydride. The model calculation for microcrystal showed that such split can be explained by N-H or H-H interactions throw the deformation fields.

Increasing of deformation fields for nitrogen in Ti with comparison to the fields in Ti-O SS causes the increase the amount of residual hydrogen in octahedral sites of Ti-N SS (Fig.7, peak at 90 meV). So in Ti-N SS this amount is nearly 25%, but for the Ti-O SS it is 7% only [5]. The most part of hydrogen both in the Ti-N and Ti-O SS is in the hydride phases (Fig.8, peak at 153 meV).

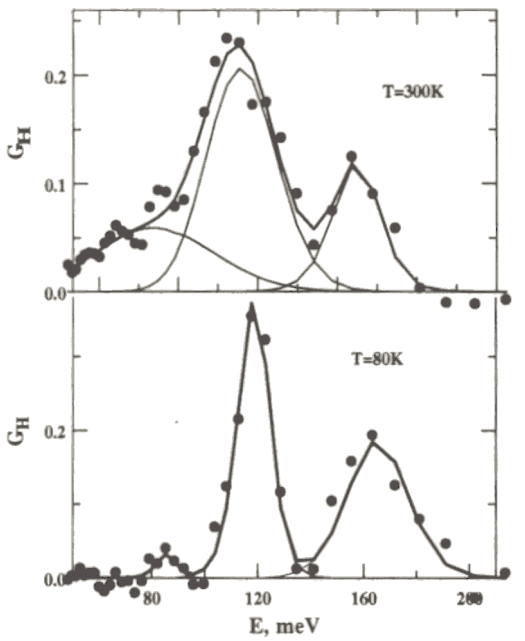

Fig.4 The PHFS in $TaH_{0.045}$ at 300K and 80K

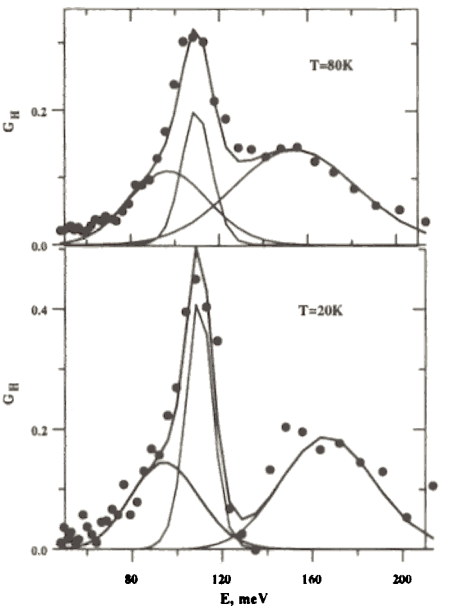

***Fig.5** The PHES in $TaV_{0.03}N_{0.02}H_{0.02}$ at 80K and 20K*

***Fig.6** The PHFS in $TaN_{0.02}H_{0.045}$ at 300K, 80K and 20K*

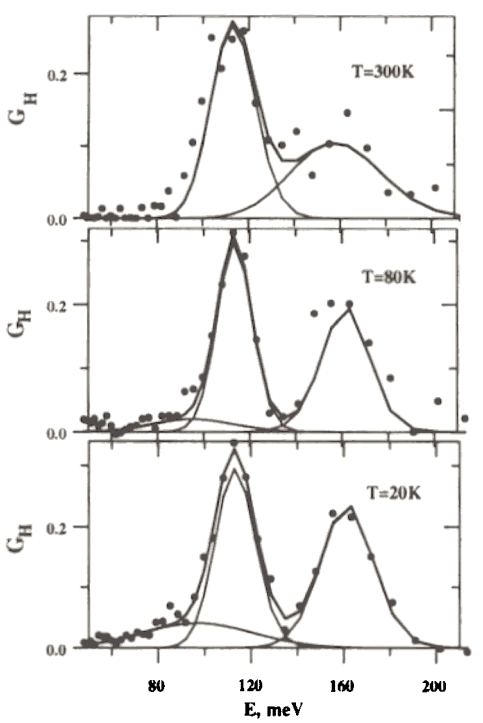

***Fig.7** The PHFS in Ti-N ss at 300K, 210K, and 80K*

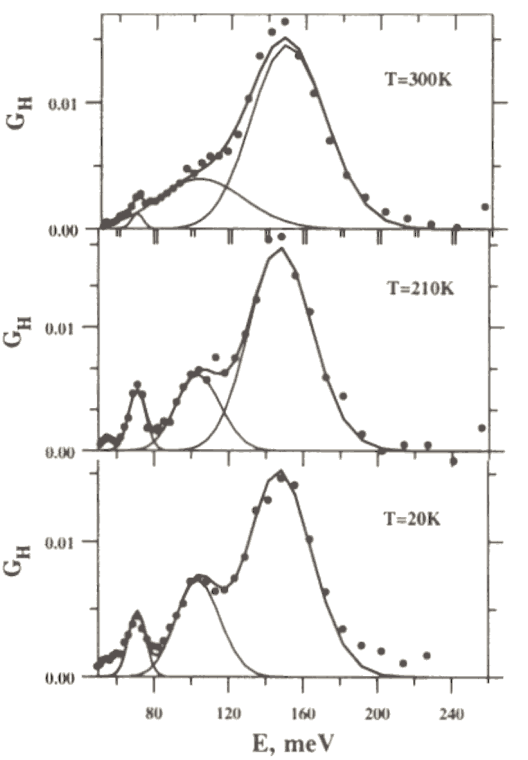

. Literature.

1. Carstanjen H.D., Interstitial Positions and Vibrational Amplitudes of Hydrogen in Metals Investigated by Fast Ion Channelling. Phys.Stat.Sol. (a), 1980, 59, p11-25
2. Hydrogen in Metals, Springer-Verlag, 1978, v2, p51.
3. Suqimoto H. and Fukai Y., Theory of Light Interstitials in BCC Metals, Phys.Rev.B, 1980, v22, p670-680.
4. Schober H.R., Lottner V., Lattice Dynamical Aspects of H in V, Nb, Ta and Pd., Z.Phys.Chemie New Folge, 1979, v114, p203-212.
5. Belushkin A.V., Morozov S.I., Natkanec I., Sumin V.V., Study of the Hydrogen Vibration spectra in Ti-O solid solution by INS. Rapid Communications of JINR, P14-86-41, Dubna, 1986, p8

The $S(q)$ Structural Factor of Liquid ^{4}He for Small q

Zh.A.Kozlov

Frank Laboratory of Neutron Physics, JINR, Dubna, Russia

Bijl [1], Feynmann [2], and Pitayevskii [3] obtained the following expression for $S(q)$ at small wave vectors q and $T \to 0$

$$S(q) = \frac{\hbar q}{2Mc} \qquad (1)$$

under the assumption that only one-photon processes contribute to the $S(q)$ structural factor of liquid ^{4}He. At $T \neq 0$, $S(0) = \rho k_B T K_T$ [4], where ρ is the density of ^{4}He atoms, k_B is Boltzman's constant, and K_T is the isothermic compressibility.

To verify the validity of expression (1), we did the following. Data on integral intensities at T=0.42; 1.45; 2.05, and 2.21 K in [5,6] was obtained by summing all of the neutron scattering components measured in [5, 6]. The heating part of the scattering law was accounted for using a detail equilibrium relation. The phonon regions of these data for $q \approx (0{,}1 \div 0{,}6)$ Å^{-1} were described by two functions:

$$Z_1(q) = a_1 + a_2 q,$$

$$Z_2(q) = b_1 + b_2 q + b_3 q^2,$$

where a_i and b_i are constants. Statistical criteria for the approximation precision χ_1^2 were obtained. Then, the temperature dependence for the so-called variance ratio $v^2 = \chi_1^2/\chi_2^2$. was built. The variance ratio characterizes the deviation degree of experimental data from a straight line.. Figures 1 a, b illustrate the dependencies of the integral intensities on the phase vectors and the description of phonon areas using a straight line for T=0.42 K and a curved line for T=2.21 K. Figure 1 c shows the dependence of v^2 on T. The equality $v^2=1$ means that experimental data on S(q) can be described unambiguously using a straight line. As is seen from Fig. 1, at increasing of temperature below the λ-point, sufficiently smooth bending of the curve changes for a sharp jump at the phase transition point T_λ. The circle at T=0 K was drawn from theoretical considerations.

As a result, we can state that in the phonon region, the dependence of the statistical structural factor on the wave vector of liquid ^{4}He smoothly tends to a straight line at decreasing temperature. At the same time, the intensity of inelastic neutron scattering has a tendency to decrease to zero at a decrease in the temperature and wave vector. Note that elastic scattering is not observed in the scattering of neutrons in superfluid ^{4}He. Thus, dependence (1) was experimentally confirmed.

References

1. Bijl A.- Physica, 1940, vol.7, p.869.
2. Feynman R.P.- Phys. Rev., 1954, vol.94, p.262.
3. Pitaevskii L. P.- ZhETF, 1956, vol.31, p.536 (in Russian).
4. Price P.J.- Phys. Rev., 1954, vol.94, p.257.
5. Blagoveshchenskii N.M., Bogoyavlenskii I.V., Karnatsevich L.V., Kozlov Zh.A., Kolobrodov V.G., Priezzhev V.B., Puchkov A.V., Skomorokhov A.N., Yarunin V.S.- Phys. Rev. B, 1994, vol.50, p.16550-16565; Preprint JINR P3-94-125, Dubna, 1994 (in Russian).
6. Kozlov Zh. A., Russian J. Particle and Nucleus, 1996, v.6 (in Russian).

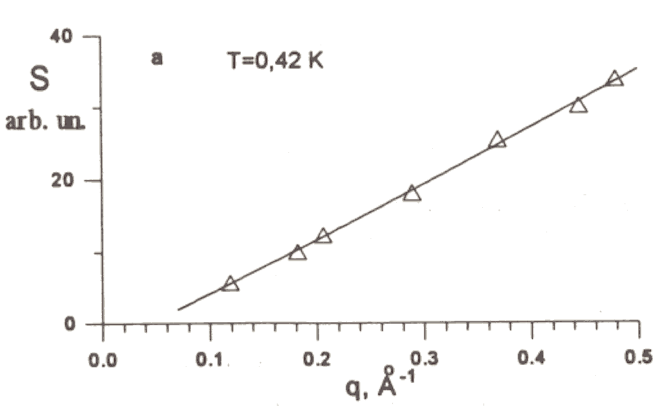

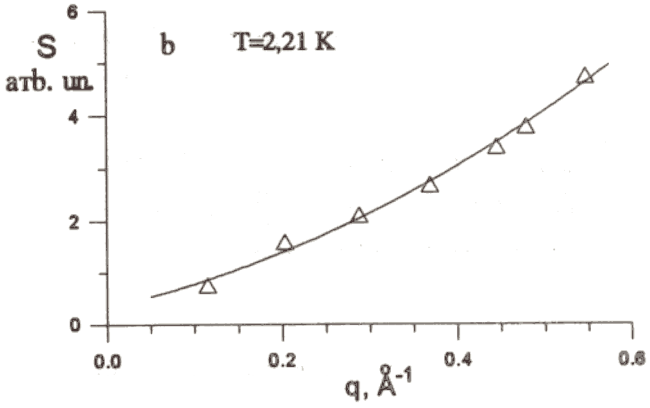

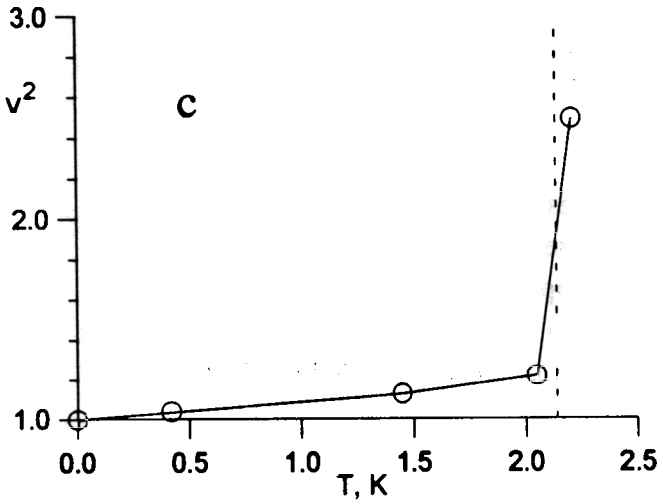

Fig. 1. a, b. The dependencies of the integral intensities on q for T=0.42 and 2.21 K, and the curves which describe the phonon region. c. The dependence of v^2 on T.

Study of depth profiles of elements of thin layer structures using RBS technique

Kobzev A.P., Korneev D.A., Nikonov O.A.(JINR)
Ul'yanov V.A., Peskov B.G., Pleshanov N.K., Pusenkov V.M., Siber E.V.,
Soroko Z.N., Syromyatnikov V.G., Schebetov A.F.(PNPI, Gatchina)

At the present time polarizing devices on the basis of supermirrors are widely used to obtain neutron polarized beams. Supermirrors represent aperiodic multilayered structures of alternating magnetic and nonmagnetic layer structures with the thickness changing according to the appropriate law from 75 A to 700A. To produce highly effective polarizing supermirrors, it is necessary to select the elementary composition of FeCo/TiZr, Co/Ti layers in such a way that the difference between a nuclear and magnetic potential should be equal to a nuclear potential of nonmagnetic ones. The layers themselves and their boundaries are not ideal due to roughness and mixture of materials at the boundaries as they are being deposited, as well as different kinds of admixtures appear (O, Ar, C, N and others). Moreover, while the polarizing devices are in use in real conditions, oxidation of the upper layer takes place which worsens the polarizing properties of mirrors too.

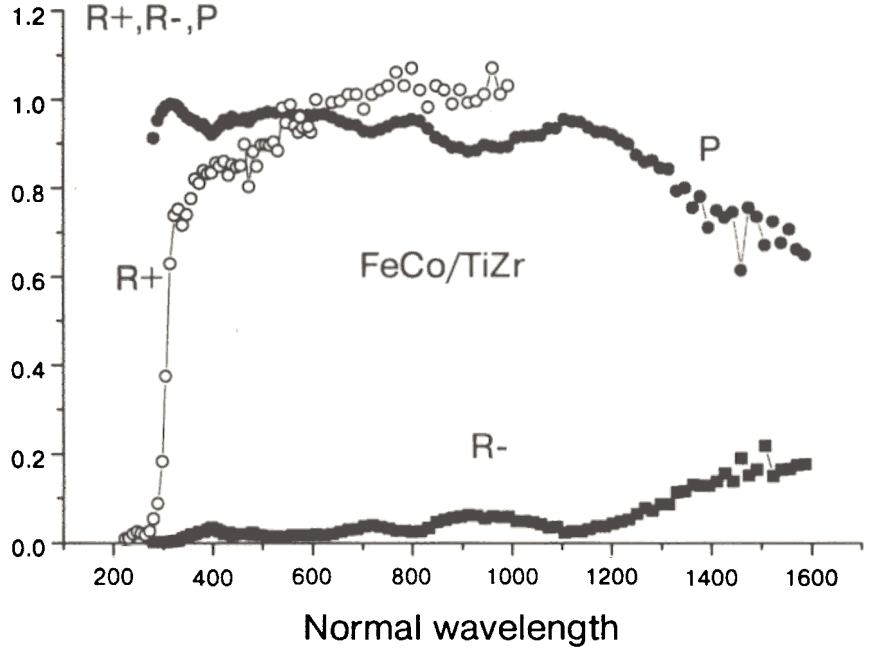

Fig.1. Reflection coefficients for two spin components and polarizing capability of supermirror.

As an example, Fig.1 shows the reflection curves for the two spin components R^+,R^- and the polarizing efficiency of a supermirror with the layers FeCo/TiZr. One can see that the polarizing efficiency of a mirror has gaps which are probably connected with the imperfection of the element composition of layers reflecting neutrons with λ =400-700A. These data have been obtained at the reflectometer at the WWR-M reactor in Gatchina.

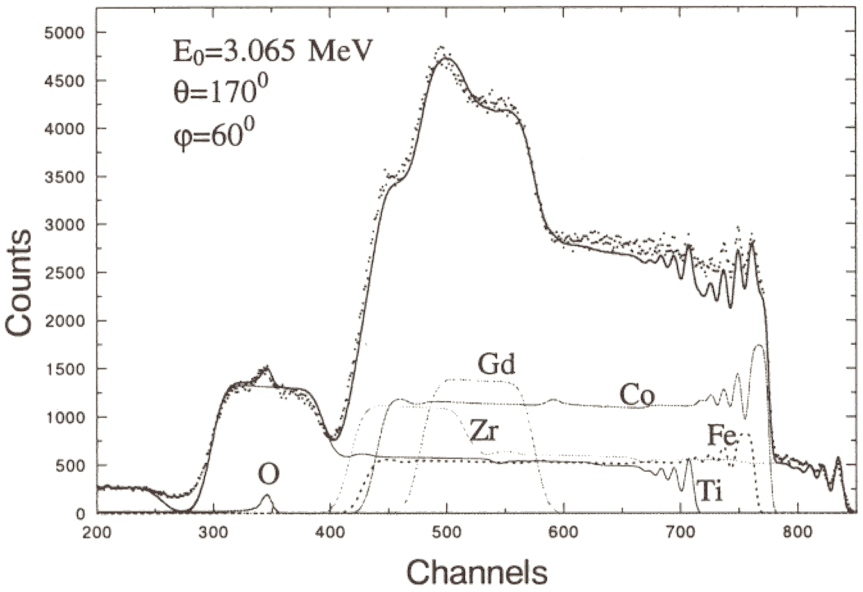

Fig.2. Experimental and calculated spectra of scattered ions $^4He^+$ for supermirror.

Depth profiles of elements in multilayered structures have been studied using the RBS technique at the electrostatic generator EG-5 FLNF. Fig.2 shows one of the experimental spectra, partial spectra of all elements involved in the composition of different mirror layers, as well as the resulting spectrum calculated for an appropriate model. The calculated spectrum has been obtained as a result of the variation of model parameters (composition and layer thickness) up to the achievement of the best description of the experimental spectrum. The peak in Fig. 2, corresponding to the resonance scattering of helium ions on oxygen, shows its composition in the first layer of the multilayer structure. The spectra at higher energies have been measured to analyse the following layers. As it has been seen, a sample can be analysed at its whole depth up to the substratum (glass). Changing experimental conditions, one can achieve the resolution in tens of angstroms, i. e. to observe separate layers.

Thus using the non-destructive technique one can obtain a full depth profile of all main and admixed elements in the composition of multilayered structures. The obtained results permit us to understand the reasons of imperfection of polarized neutrons and to introduce some changes in the manufacturing process.

Off-specular Neutron Reflection from Magnetic Media with Nondiagonal Reflectivity Matrices

Dmitri A. Korneev[1], Victor I. Bodnarchuk[1], Vladimir K. Ignatovich[2]
[1]*Laboratory of neutron physics, JINR, 141980 Dubna Moscow reg., Russia*
[2]*Research Reactor Institute Kyoto University Kumatori-cho, Senan-gan, Osaka 590-04, Japan.*
(Received February 1, 1996)

The reflection of neutrons from magnetic substances is described using the reflection matrix with nondiagonal, in general, matrix elements which determine neutron spin reverse. In external field the spin reverse is accompanied by changes of the neutron kinetic energy and reflection angle. The particular case of reflection from a magnetic mirror with magnetization noncollinear to the external field is considered. The probability of spin reverse and a deviation of reflection angles from the specular one are calculated. The experiment to observe this effect is described and its results are reported.

KEYWORDS: thermal neutrons, magnetic scattering, polarization, optical potential

§1. Introduction

Since the time of the first works by Hughes and Burgy[1)] specular reflection has been used to polarize neutrons. With polarized neutrons one can investigate, for instance, magnetization profiles of films and multilayered systems[2-6)]. It was pointed out[7-13)] that reflection from films with noncollinear magnetic structures is more complicated than reflection from films with collinear ones. In noncollinear case the reflection is characterized by the reflection matrix:

$$\hat{R} = \begin{pmatrix} R_{++} & R_{+-} \\ R_{-+} & R_{--} \end{pmatrix}$$

with nonzero elements R_{+-} and R_{-+}. To measure all matrix elements in $\hat{R}$ is the main goal of polarized neutron reflectometry.

In the next section, the angular characteristics of reflection with spin-flip in external fields are considered. In the third section, the matrix elements of $\hat{R}$ and the intensities of constituent beams for the case of reflection from a magnetic mirror with magnetization noncollinear to the external field are calculated. In the fourth section, the experiment to observe the off-specular reflection is described

§2. Angular splitting of the reflected beam

The reflection of neutrons from an interface in an external magnetic field can be off-specular (though coherent) if it is accompanied by spin flipping[7,9)]. In general, the incident beam after reflection undergoes triple splitting, as shown in fig. 1. It contains the middle part which is specular and two side lobes which are off-specular and perfectly polarized. The intensity of the side lobes are determined by the matrix elements R_{+-} and R_{-+} of the matrix $\hat{R}$ and by incident beam polarization. If the incident beam is perfectly polarized, one of the side lobes vanishes. If the incident beam is nonpolarized, two side beams in weak external fields have almost equal intensities. The splitting of the beam takes place because of spin flipping, energy conservation and the conservation the of components of neutron momentum parallel to the interface.

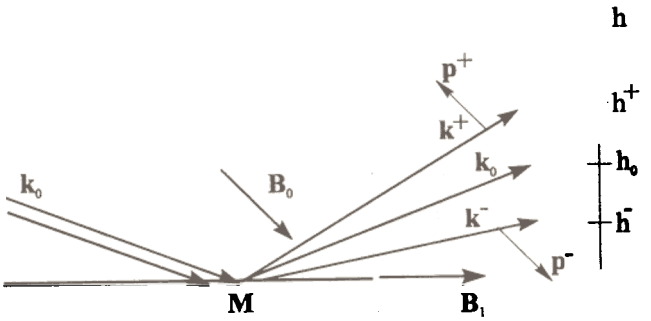

Fig. 1. Following the reflection from a magnetized mirror with the magnetization **M** noncollinear to the external magnetic field $\mathbf{B}_0$ the nonpolarized incident neutron beam with a wave vector k_0 splits into three beams. Two off-specular beams with the wave vectors k^+ and k^- are ideally polarized. The splitting of the beam gives the distribution over height h of the reflected neutrons and it can be measured by a moving or a position sensitive detector.

Let us denote $\mathbf{k}=(\mathbf{k}_\parallel, \mathbf{k}_\perp)$ the wave vector of the incident neutron with the $\mathbf{k}_\perp$, $\mathbf{k}_\parallel$ being its normal and parallel to the surface components. In the external field **B** the neutron has the potential energy $-\sigma\mathbf{B}$, where **B** is measured in $\hbar^2/2m\mu$ (m, μ are the neutron mass and magnetic moment, respectively) and σ are the Pauli matrices. On spin reverse the potential energy changes in magnitude by ①2B. Because of energy conservation it changes the kinetic energy: $k^2 \to k^2$①2B. In the reflection from an interface the components $\mathbf{k}_\parallel$, are also conserved. Thus the change of the kinetic energy means the change in the normal component $\mathbf{k}_\perp$: $k_\perp \to k_\perp^\pm = \sqrt{k_\perp^2 \pm 2B}$, and as a result to change in the reflection angle. It is not difficult to calculate the angular deviation of shifted beams. For a small grazing angle $\phi_0=10^{-2}\div10^{-3}$ we have

$$\frac{\Delta\phi^\pm}{\phi_0} = \frac{\Delta k^\pm_\perp}{k_\perp} = \sqrt{1 \pm 2B/k^2} - 1$$
$$= \sqrt{1 \pm 1.47\cdot10^{-10} B_0 \lambda^2/\phi_0^2} - 1$$

Here the neutron wavelength λ is measured in Angstroms, B in Gauss, and ϕ_0 in radians.

The dependence of relative splitting $\Delta\phi^\pm/\phi_0$ on λ and B is shown in fig.2.

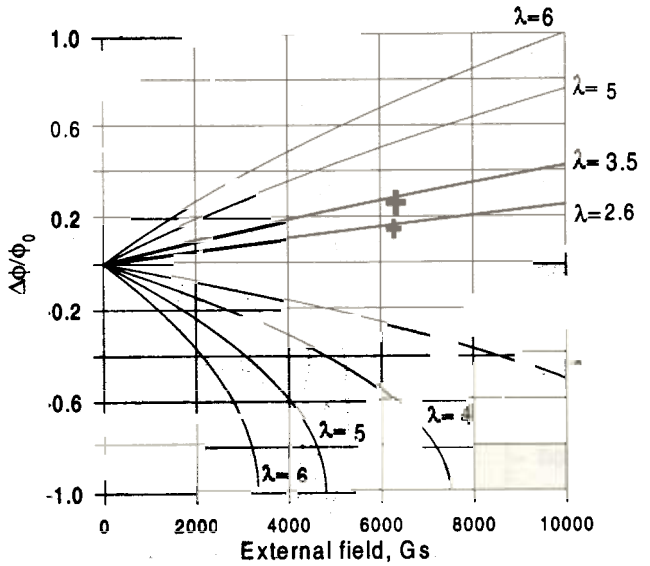

Fig.2. The relative angular splitting of spin reversed beams in dependence on λ (in Angstroms) and the external magnetic field for ϕ_0=4.2mrd. The crosses are the experimental points (see sec. 4).

If the external field is sufficiently large, spin reverse is forbidden for $\Delta\phi<0$.

§3. Matrix $\hat{R}$

Let us find the solution of the Schrödinger equation in presence of the external magnetic field $\mathbf{B}_0$ and a magnetized reflecting mirror:

$$(\Delta - u\theta(z>0) + \sigma\mathbf{B}(z) + k^2)\psi = 0$$

where u is an optical potential of the mirror, which is supposed to fill the half space z > 0, θ is a step function equal to unity when the unequality in its argument is satisfied and to zero in the opposite case,

$$\mathbf{B}(z) = \mathbf{B}_0\theta(z<0) + \mathbf{B}_1\theta(z>0),$$

and $\mathbf{B}_1$ is the magnetic induction of the mirror. We consider the case when $\mathbf{B}_0$ unparallel to $\mathbf{B}_1$. The solution is: $\psi(\mathbf{r}) = \exp(i\mathbf{k}_1\mathbf{r}_1)\xi(z)$, where

$$\xi(z) = \theta(z<0)[\exp(i\hat{k}_\perp^+ z)\xi_0 + \exp(-i\hat{k}_\perp^+ z)\hat{R}\xi_0] + \theta(z<0)\exp(i\hat{k}'^+_\perp z)\hat{T}\xi_0$$

$\hat{R}$, $\hat{T}$ are reflection and transmission matrices, $\hat{k}_\perp^\pm = \sqrt{k_\perp^2 \pm \sigma B}$, $\hat{k}'^\pm_\perp = \sqrt{k_\perp^2 - u \pm \sigma B}$, and ξ is the spinor state of the incident particle. For simplicity in the following, we shall omit the subscript ⊥.

Matching of the wave function at the interface z=0 for arbitrary ξ_0 gives two equations for $\hat{R}$ and $\hat{T}$:

$$\hat{I} + \hat{R} = \hat{T},\ \hat{k}^+(\hat{I} - \hat{R}) = \hat{k}'^+.$$

The solution of these equations can be represented as follows:

$$\hat{R} = (\hat{k}^+ + \hat{k}'^+)^{-1}(\hat{k}^+ - \hat{k}'^+),\ \hat{T} = (\hat{k}^+ + \hat{k}'^+)^{-1}2\hat{k}^+$$

Here we shall consider in details only the matrix $\hat{R}$.

It is possible to get rid of the matrices σ in the denominator by representing $\hat{R}$ in the form

$$\hat{R} = (\hat{k}^- + \hat{k}'^-)(\hat{k}^+ - \hat{k}'^+)/N \equiv \hat{A}/N$$

where, N is the number and it is useful to calculate it as a matrix element:

$$N = \langle + | k^+k^- + \hat{k}'^+\hat{k}'^- + \hat{k}'^- k^+ + k^-\hat{k}'^+ | + \rangle,$$

where $|\pm\rangle$ represent the eigen states of the matrix $\sigma\mathbf{B}_0$:

$$\sigma\mathbf{B}_0|\pm\rangle = \pm B_0|\pm\rangle.$$

Evaluation gives

$$N = (k^+ + k'^+)(k^- + k'^-) - (k'^- - k'^+)(k^+ - k^-)\sin^2(\chi/2)$$

where $k^\pm = \sqrt{k^2 \pm B_0}$ and $k'^\pm = \sqrt{k^2 - u \pm B_1}$ are the c-numbers now, and χ is the angle between vectors $\mathbf{B}_0$ and $\mathbf{B}_1$. The numerator of (3.2) can be reduced to the form:

$$\hat{A} = k^-k^+ - k'^-k'^+ + \hat{k}^-\hat{k}'^+ - \hat{k}'^-\hat{k}^+ =$$
$$= k^+k^- - k'^+k'^- + (1/2)(k'^- + k'^+)(\hat{k}^+ - \hat{k}^-)$$
$$-(1/2)(k'^+ - k'^-)(\hat{k}^-\sigma\mathbf{b}_1 + \sigma\mathbf{b}_1\hat{k}^+)$$

where the first two terms do not contain the σ matrices at all, and $\mathbf{b}_1$ is the unit vector in the direction of $\mathbf{B}_1$.

Now we are calculate matrix elements of $\hat{A}$

$$\langle\pm|\hat{A}|\pm\rangle = (k^- \pm k'^-)(k^+ \mp k'^+) \pm (k'^+ - k'^-)(k^+ + k^-)\sin^2(\chi/2),$$

$$\langle\mp|\hat{A}|\pm\rangle = -(k'^+ - k'^-)k^\pm \sin\chi,$$

In the case of χ=0 (and the similary for χ=π) the matrix $\hat{R}$ becomes diagonal with the elements:

$$R_+ = (k^+ - k'^+)/(k^+ + k'^+),\quad R_- = (k^- - k'^-)/(k^- + k'^-)$$

For the general case the final expressions for the matrix elements of $\hat{R}$ are:

$$R_{\pm\pm} = \frac{1}{C}\left\{R_\pm \mp \frac{(k'^+ - k'^-)(k^+ + k^-)}{(k^- + k'^-)(k^+ + k'^+)}\sin^2(\chi/2)\right\}$$

$$R_{\pm\mp} = \frac{1}{C}\left\{\frac{(k'^+ - k'^-)k^\mp}{(k^- + k'^+)(k^+ + k'^+)}\sin\chi\right\}$$

$$C = 1 - \frac{(k'^+ - k'^-)(k^- - k^+)}{(k^- + k'^-)(k^+ + k'^+)}\sin^2(\chi/2).$$

These formulas are useful to calculate the beam splitting, but the notations are not appropriate for an experimerit, becuase both spin states in the incident beam are characterized by the sam wave vector $\mathbf{k}^+ = \mathbf{k}^- = \mathbf{k}$ with a given normal component k. Thus, if we consider the splitting of the part of the beam initially polarized along the field, we must replace k^2-B_0 by k^2 which means shifting of all k^2 in (3.5) by $+B_0$. Thus, $\mathbf{k}^+$ for that part of the beam becomes, $k^+ = \sqrt{k^2 + 2B_0}$, and $k'^\pm = \sqrt{k^2 - u \pm (B_1 \pm B_0)}$. For the part of the incident beam polarized in the opposite direction we must take $k^+ \equiv k$ and then, $k^- = \sqrt{k^2 - 2B_0}$, and $k'^\pm = \sqrt{k^2 - u \pm (B_1 \mp B_0)}$.

It is easy to estimate the intensity of reflected beams in the case when the inside field is strong enough to make k'^- be imaginary, and leave k'^+ to be real. In the first

approxirnation with respect to B_0/k^2 the denominator can be replaced by 1, and the intetisity of the off-specular beam become proportional to

$$|R_{-+}|^2 = k^2\left|\frac{-(k'^- - k'^+)}{(k^+ + k'^+)(k^- + k'^-)}\sin\chi\right|^2 = \frac{\gamma B_1 \sin^2\chi}{2(u+B_1)},$$

where $\gamma=|2k/(k+k'^+)|^2\approx 1$.

§4. Experiment

The experiment was performed at the time-of-flight reflectometer of polarized neutrons at the IBR-2 reactor in Dubna.

The sample was a thin anizotropic FeCo film on a glass substrate. The external field was applied either parallel to the anizotropy axis in the film plane ($\chi=0$) or at an angle of 76deg. to it (out of plane). The magnitude of the external field could be varied in the range 0.01÷7kGs. The polarized neutron beam with a wide Maxwellian spectrum was incident on the film at a grazing angle ϕ_0=4.2mrd. The polarization of the beam P(λ) was a monotonous function decreasing from P=0.98 at λ=1.8Å to P=0.5 at λ=7Å. The detector with a cadmium slit of 0.5mm width was placed at 2.68m from the sample. Thus, the angular aperture of the detector was $\delta\phi$=0.18mrd. To determine the reflection coefficients the intensity of the incident and reflected neutrons were measured at different orientation and magnitudes of the external field B.

For $\chi=0$ the dependence of $N_+R_{++}+N_-R_{-+}$ on the wavelength was measured. Here $N_\pm(\lambda)$ are proportional to the intensities of the incident neutrons with two spin projections on the external field, and $R_\pm$ are the squares of modules of the related reflection amplitudes.

For χ=76deg., the angular distributions of the reflected neutrons were measured for two magnitudes of the external field: 0.2 and 6.3kGs. (fig.3). In the field H=6.3kGs, off-specular neutrons were observed at $\phi>\phi_0$. To determine the dependence of $\Delta\phi=\phi-\phi_0$ on λ the energy range of counted neutrons was restricted to two intervals $\Delta\lambda_1$ and $\Delta\lambda_2$ around λ_1=2.6Å and λ_2=3.5Å respectively. The measured ratio of the magnitudes $\Delta\phi_1(\lambda_1)$ and $\Delta\phi_2(\lambda_2)$ (fig.3b) satisfies the relation $\Delta\phi_1(\lambda_1)/\Delta\phi_2(\lambda_2)=(\lambda_1/\lambda_2)^2$ with the precision better than 5%, and corroborates the quadratic dependence of $\Delta\phi$ on λ. The measurements of $\Delta\phi$ at fixed λ and different B corroborate the linear dependence $\Delta\phi\propto B$.

For the fixed position of the detector at $\Delta\phi$=0.7mrd and two magnitudes of the external field: B=6.3 and 3.2kGs the spectral dependence of the square modules of R_{++}, R_{+-}, and R_{-+} were measured (fig. 4). The spectral interval of the measurments was determined by the angular detector aperture $\delta\phi$=0.18mrd.

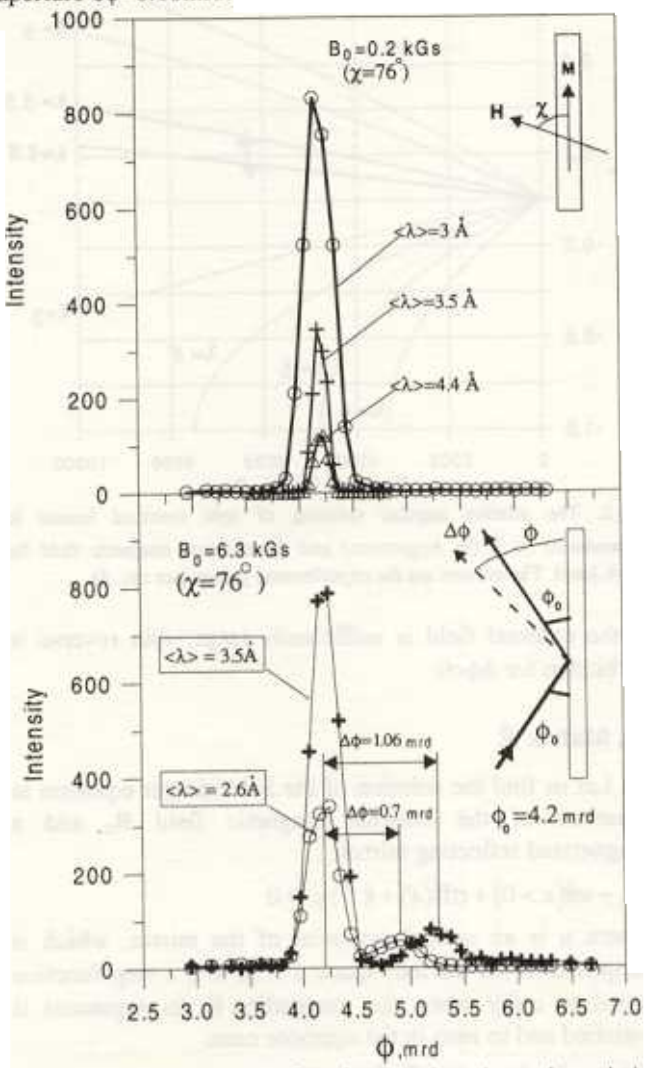

Fig.3. The dependence of the reflected neutron intensity on the angle ϕ of detector positioning.
a) B=0.2kGs, χ=76°, the detector aperture $\delta\phi$=0.18mrd, the grazing angle of the incident beam is ϕ_0=4.2mrd. The intensitydistribution maximums for different λ are observed at the same specular angle $\phi=\phi_0$.
b) B=6.3kGs, χ=76°, $\delta\phi$=0.18mrd , ϕ_0=4.2mrd. The angular distribution of the reflected intensity for two different intervals of λ. In the vicinity of the specular beam($\phi=\phi_0$), off-specular ones appear. The angular shift $\Delta\phi=\phi-\phi_0$ has the quadratic dependence on averaged wavelength $<\lambda>$.

The probabilities $|R_{\uparrow\downarrow}(\lambda)|^2$ were also measured at $\delta\phi$=1.06mrd for two magnitudes of the external magnetic field (fig.5). The position and spectral width of the functions $R_{\uparrow\downarrow}(\lambda)$ corroborate the expected theoretical dependence $\Delta\phi\propto B\lambda^2$. It is evident that measurment of nondiagonal elements $|R_{\uparrow\downarrow}(\lambda)|^2$ in a wide spectral interval of λ and in the off-specular direction requires detector with wide angular aperture contrarily to the measurment of the sum $N_+R_{++}(\lambda) + N_-R_{-+}(\lambda))$ in the specular direction.

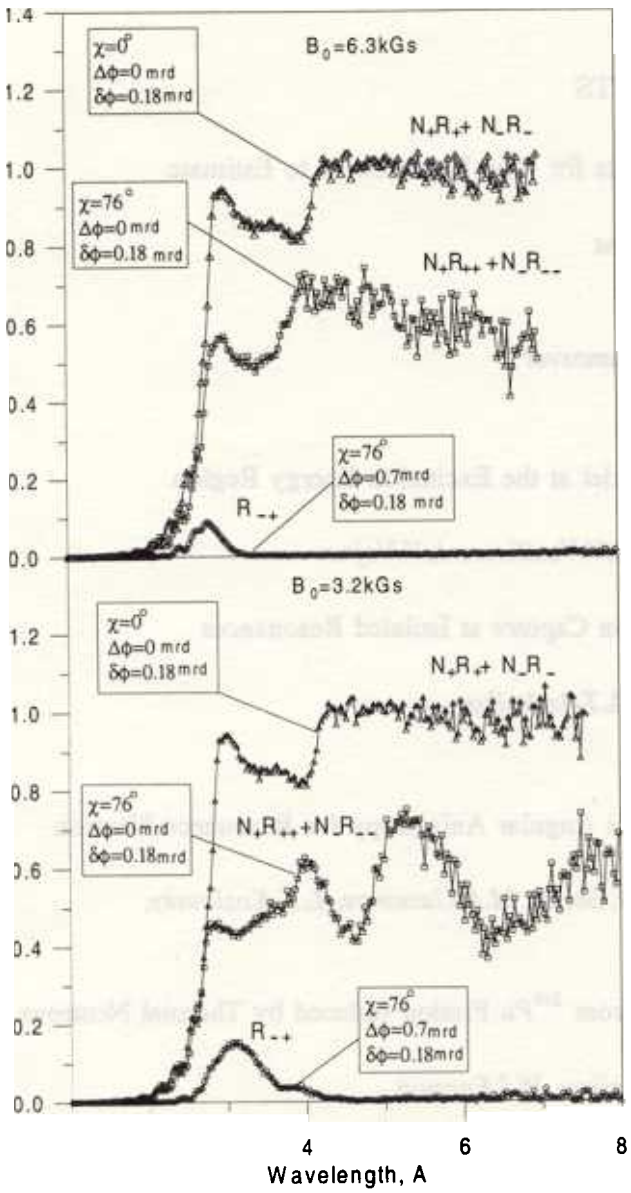

Fig.4. The wavelength dependence of $N_+R_{++}N_-R_-$ in the specular direction $\phi=\phi_0$ for $\chi=0$ and $\chi=76$deg. and of $|R_{-+}|^2$ for $\chi=76$deg in the off-specular direction ($\Delta\phi=0.7$mrd.). a) B=6.3kGs, b) B=3.2kGs.

§5. Conclusion

The obtained experimental data demonstrate that the relectometry in high external fields (B>2kGs) from noncollinear structures with nondiagonal reflection matrices reveals strong angular dispersion of the reflected neutrons with reversed spins. For the case of nonpolarized incident beam the observation of this dispersion gives the opportunity to measure the nondiagonal elements $R_{\phi(\omega)}(\lambda)$ in the off-specular beams and the sum $1/2(R_{++}(\lambda)+R_{--}(\lambda))$ in the specular one. It also gives the opportunity to get information on the distribution of magnetization in films using nonpolarized neutrons.

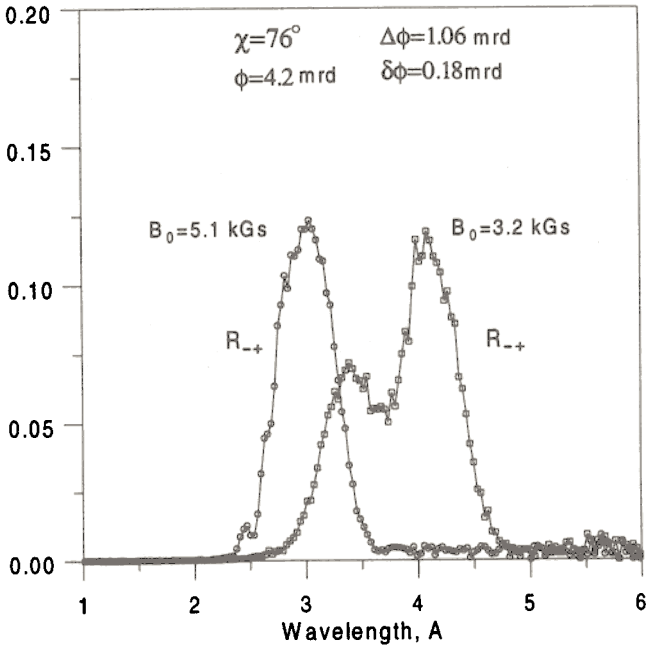

Fig.5 The dependence of $|R_{-+}|^2$ on λ for $\Delta\phi=1.06$mrd and two fields: B=5.1 kGs, and B=3.2kGs. The shift and broadeniag of the spectral interval for the weaker field corroborate the dependence $\Delta\phi\propto B\lambda^2$. The bell shaped forms of both spectra are related to the small aperture $\delta\phi=0.18$mrd of the detector.

Acknowledgments

One of the authors (V.K.I.) wants to express his gratitude to I.Carron for his invaluable assistance.

1) Hughes D.J., Burgy M.T., Phys. Rev. 81 (1951) 498.
2) Felcher G.P., Hildeke R.O., Crawford R. Haumann J., Kleb R. and Ostrowski G. Rev.Sci.Instr. **58** (1987) 609.
3) Korneev D.A., Pasyuk V.V., Petrenko A.V., and Dokukin E.B., "Neutron refectivity studies on superconducting, magnetic and absorbing thin films on the polarized neutron spectrometer at the pulsed reactor IBR-2" in H.Zabel,I.K.Robinson(Eds.) "Surface X-ray and neutron scattering" (Proceedings of the 2nd Int.Conf.,Bad Honnef, Germany, June 25-28, 1991), p.213-217
4) Lauter H.J., Bland J.A.C., Bateson R.D., and Jonson A.D. "Magnetic properties of ultrathin Co/Ag films investigated by polarized neutron reflection" Ibid, p. 219
5) Endoh Y., "Neutron reflection studies on magnetic superlattice", in Neutron Optics Devices and Applications, C.Majkrzak, J.Wood, Editors, Proc. SPIE 1738, 224-232 (1992)
6) Fitzimmons M.R., Smith G.S., Pynn R., Nastasi M.A., Burkel E. Physica B **198** (1994) 169.
7) Ignatovich V.K. Pis'ma ZhETP **28** (1978) 311 (see Sov. JETP Lett.).
8) Korneev D.A. Poverchnost' **2** (1989) 13 (in Russian).
9) Ignatovich V.K. "The Physics of Ultracold Neutrons" Claren-don Press, Oxford, 1990.
10) Majkrzak C.F. "Polarized neutron reflectometry" Physica B **173** (1991) 75.
11) Korneev D.A., Chernenko L.P. "Neutron diffraction opticsof films with noncollinear magnetic depth structure", in Neutron Optics Devices and Applications, C.Majkrzak, J.Wood, Editors, Proc. SPIE 1738, 468-476 (1992)
12) Zabel H. " Spin polarized neutron reflectometry of magnetic films and superlattices" Physica B 198 (1994) 156.

2.2. NEUTRON NUCLEAR PHYSICS

CONTENTS

The Problem of the Neutron Charge Radius and Proposals for New Experiments to Estimate the n, e Amplitude

V.G.Nikolenko, A.B.Popov, G.S.Samosvat, T.Yu.Tretyakova

The total neutron scattering length b for bound atoms is described in terms of nuclear interaction with the nucleus and electromagnetic interaction with the nucleus and the electron shell, for example, in [1]. In the case of nuclei with $\vec{I} = 0$ and without taking Schwinger scattering into account the total neutron scattering length is

$$b \quad b_N \quad b_{ne} Z[1 \quad f(\vec{q})] \ ,$$

where

$$b_{ne} = b_F + b_I$$

is the neutron-electron scattering length determined from experiments.

Here:

b_N is the nuclear scattering length (with negligible contribution of the neutron polarizability);

b_F is the Foldy scattering length

$$b_F = \frac{e\mu}{\hbar c} \equiv \frac{\gamma e^2}{2mc^2} \simeq -1.468 \ \cdot 10^{-3} fm; \tag{3}$$

b_I is the so-called intrinsic neutron-electron scattering length

$$b_I \quad \frac{1}{3}\frac{me^2}{\hbar^2} < r_{in}^2 > \tag{4}$$

$< r_{in}^2 >$ is the intrinsic mean square charge radius;

$f(\vec{q})$ is the atomic form factor.

The known value of b_{ne} allows (3) and (4) to be used to estimate the intrinsic mean square charge radius (rms) of the neutron:

$$< r_{in}^2 >= \frac{3\hbar^2}{me^2} b_I = 86.4(b_{ne} - b_F) \qquad fm^2. \tag{5}$$

The experimental estimates of b_{ne} presented in literature may be grouped near two values:

$$b_{ne} \quad (\ 1.59 \pm 0.04) \cdot 10^{-3} \quad fm \qquad ([2], [3])$$

$$b_{ne} \quad (-1.31 \pm 0.03) \cdot 10^{-3} \quad fm \qquad ([4], [5])$$

These quantities give contradictory values for $< r_{in}^2 >$.

$$< r_{in}^2 >= -0.0105 \pm 0.0034 \quad fm^2 \qquad \text{for (6)} , \tag{8}$$

$$< r_{in}^2 >= +0.0136 \pm 0.0026 \quad fm^2 \qquad \text{for (7)} . \tag{9}$$

The first value corresponds to previous considerations of the neutron as an object with a central positive charge and an enveloping negatively charged mesonic cloud. In modern quark models of hadrons there are also suggestions of such a charge distribution . A recent experimental result [6] was obtained from the total cross section measurement for a liquid mixture of even isotopes of lead and it gives $b_{ne} = -1.38 \pm 0.04 \quad mfm$, which corresponds to $< r_{in}^2 >= 0.008 \pm 0.003 \quad fm^2$. To control these contradictions of experimental data one needs to repeat the measurements using the same methods. This has been done for the total cross section measurement of lead. The next problem is to check the results for the scattering of thermal neutrons by noble gases.

Following [7], we recall the main equations for differential and total neutron cross sections for treatment of the thermal motion of gas atoms. The differential cross section for the neutron at angle θ with respect to the incident neutron direction is

$$\sigma(V_0 \to V, \vec{\Omega}_0 \to \vec{\Omega}) = \frac{\sigma_0}{4\pi}\Big(\frac{A+1}{A}\Big)^2 F(V_0, V, \theta, A) , \tag{10}$$

where

$$F(V_0, V, \theta, A) = \frac{1}{\sqrt{\pi} V_0 B_0} \frac{V^2}{\sqrt{V^2 + V_0^2 - 2VV_0\cos\theta}} * \\ exp\Big\{ \frac{-(V^2 - V_0\frac{A-1}{A+1} - \frac{2VV_0\cos\theta}{A+1})^2}{4(\frac{A}{A+1})^2 B_0^2 (V^2 + V_0^2 - 2VV_0\cos\theta)} \Big\} \tag{11}$$

Here $B_0 = \sqrt{\frac{2kT}{Am}}$, T is the temperature of the target gas and m is the neutron mass.

In order to obtain the ratio of neutron scattering at different angles, one needs to integrate expression (13) over V at fixed angles

$$R = \frac{\int_0^\infty F(V_0, V, \theta_1, A) dV}{\int_0^\infty F(V_0, V, \theta_2, A) dV} = \frac{F_s(V_0, \theta_1, A)}{F_s(V_0, \theta_2, A)}. \tag{12}$$

Now we can write the differential cross section for the scattering of neutrons by the atoms of a monoatomic gas, taking into account the n, e interaction in the form:

$$\frac{d\sigma}{d\Omega} = [b_N^2 + 2b_N Z b_{ne} f(E_r, \theta_{cm})] F(V_0, V, \theta) , \tag{13}$$

where $f(E_r, \theta_{cm})$ is the atomic form factor corresponding to the relative energy of motion (between the atom and the neutron) E_r and to such scattering angle θ_{cm} in the center-of-mass system, which leads to the scattering angle θ in the laboratory one. Our calculations of average form factors using the Monte-Carlo method and considering the thermal motion, show that the average form factor values agree with a good precision with the form factor values in the laboratory system taken directly for E_0 (V_0) and θ. For this

reason the neutron intensity ratio with n, e scattering and thermal motion contributions may be written as

$$R = \frac{b_N^2 F_s(V_0, \theta_1, A) + 2 b_N b_{ne} Z f(V_0, \theta_1)}{b_N^2 F_s(V_0, \theta_2, A) + 2 b_N b_{ne} Z f(V_0, \theta_2)} .$$

For the total cross section without n, e scattering, using (13) one can obtain

$$\sigma_s = \sigma_0 \frac{1}{x_0}[(x_0 + \frac{1}{2Ax_0}) erf(\sqrt{A} x_0) + \frac{1}{\sqrt{\pi A}} e^{-Ax_0^2}] \equiv \sigma_0 F_t(V_0, A) , \qquad (15)$$

where $x_0 = \frac{V_0}{V_T}$ and $V_T = \sqrt{\frac{kT}{m}}$. Introducing n, e scattering by analogy with eq.(17), we can write

$$\sigma_s \quad 4\pi b_N^2 F_t(V_0, A) + 8\pi b_N b_{ne} Z f_t(E).$$

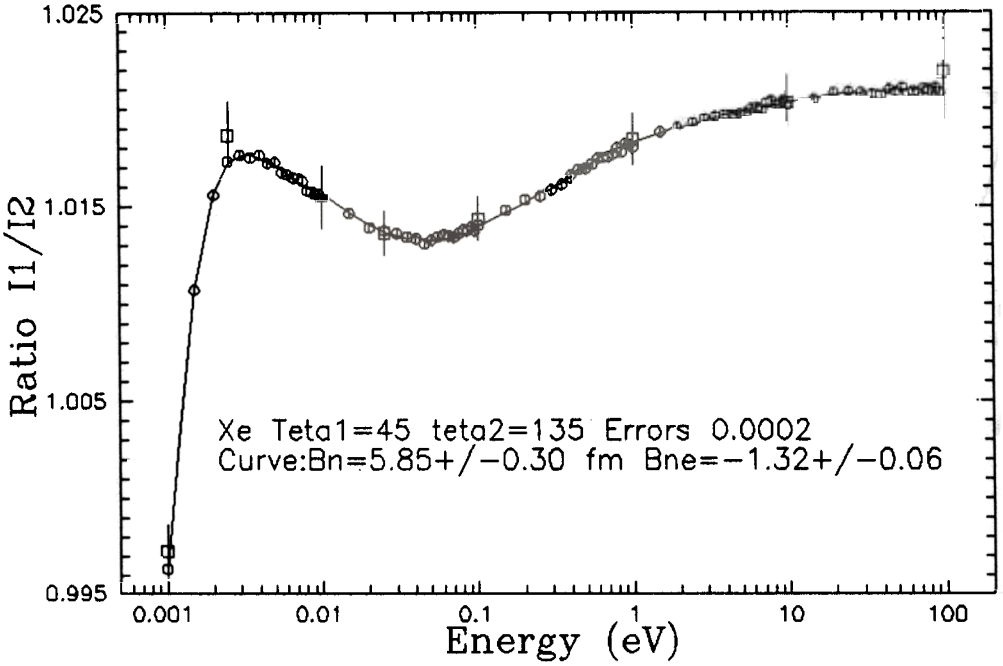

Fig.1. Intensity ratio $R(E)$ for angles of 45^0 and 135^0. The squares is the result of Monte Carlo calculation.

Fig.1 shows the energy dependence of the intensity ratio of the neutrons, scattered by Xe at 45^0 and 135^0. Calculations were carried out using (14). The abrupt decay of R in the region below 5 meV is determined by the kinematic factors $F_s(V_0, \theta)$ for pure nuclear scattering. In the energy region above 10 eV, the curve R approaches the value for scattering by atoms at rest.

The depth of minimum $R(E)$ at $E \sim 0.05$ eV is the contribution of n, e scattering with a relative value of $\sim 5.10^{-3}$.

If it is assumed that $R(E)$ can be measured with errors of 2.10^{-4} (in Fig.1 random points are within such accuracy limits), so the converse analysis of pseudo experimental data using the FUMILI-code (the curve in Fig.1) shows that b_{ne} may be extracted only with the same accuracy as b_N, because the linear correlation between b_{ne} and b_N appears in the $R(E)$ analysis. For measurements it is better to use the heavy isotopes of Xe, because they do not have neutron resonances in the eV region.

For $R(E)$ analysis it is convenient to use the region below 0.1 eV, because then there is no necessity to make corrections for changes in detector efficiency for neutrons scattered at 45^0 and 135^0.

We obtained for Xe at $E = 0.05$ eV that

$R = 1.021$ without n, e scattering and thermal motion consideration,

$R = 1.020$ considering thermal motion, only,

$R = 1.013$ with both n, e scattering and thermal motion.

So, at the maximum of the n, e scattering effect the anisotropy $R - 1$ due to going from a center-of-mass system to the laboratory one is equal to 0.021. The correction for the thermal motion reduces this value by 0.001 and the searched for effect by 0.007 more.

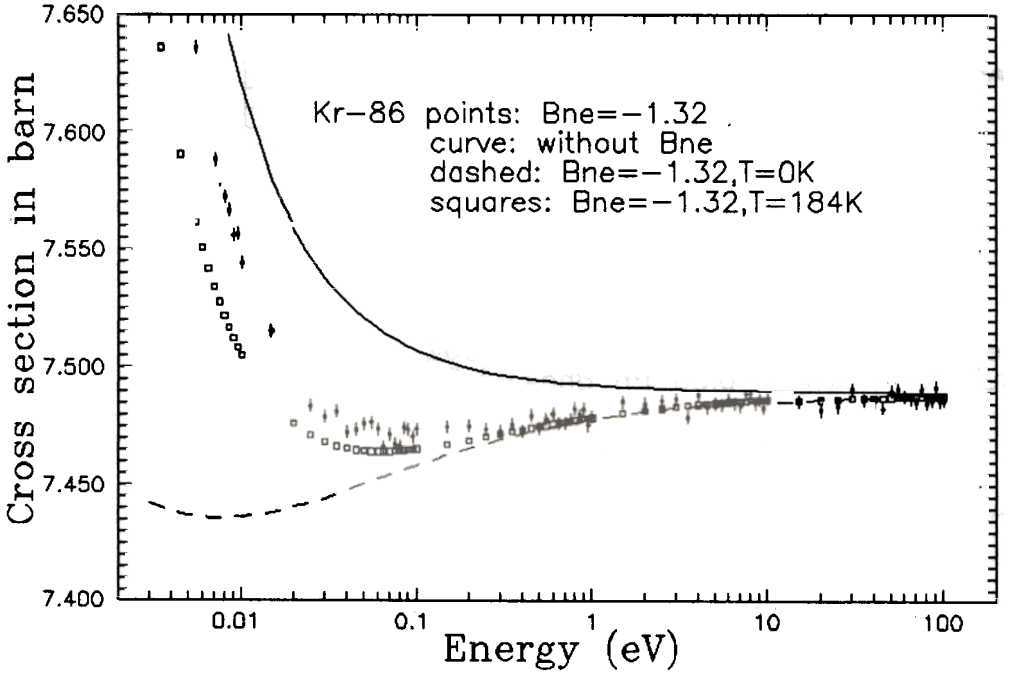

Fig.2. The shape of total cross sections at low energies in relation to the consideration of thermal motion and n, e scattering contributions.

Measurement of the total cross section for the ^{86}Kr isotope has been more promising. This isotope has a small thermal capture cross section 3 ± 2 mb [8] so the total cross section has been determined, in general, by scattering. Energy dependences of σ_t calculated for some hypothetical cases are shown in Fig.2. Points show $\sigma_t(E)$, calculated by equation (19) for the fixed parameters $b_N = 7.73$ fm and $\sigma_{0\gamma} = 2$ mb ($\sigma_\gamma = \sigma_{0\gamma}/\sqrt{E}$), by the factor of 4 more than for the pure ^{86}Kr isotope, $b_{ne} = -1.32$ mfm, and statistically scattered

with an error of 2.5 mb. The solid curve displays $\sigma_t(E)$ at $b_{ne} = 0$, that is, the case without n, e scattering. The dashed curve corresponds to $\sigma_t(E)$ for the case without the thermal motion of gas atoms (calculated by eq.(16 at $T \to 0$). One can see, that in the region 0.1 eV, the real contribution of n, e scattering is 35 mb, of which 15 mb are compensated for by the thermal motion effect of the atoms. For lower energies the contribution of n, e scattering arises, but it is overlapped considerably by the thermal motion effect. So, at $E = 0.001$ eV, $\sigma_{ne} \sim 55$ mb, whereas the thermal motion contribution is more than 100 mb. In Fig.2 the squares show the case corresponding to a gas temperature of $184^0 K$ (provided that the gas is cooled by liquid xenon). These data essentially improve the problem of estimating the n, e amplitude.

If data covered the region $0.003 - 10$ eV and even $0.003 - 1$ eV, b_{ne} can be obtained with an accuracy of $\sim 5\%$. In this case the capture cross section can be extracted with an accuracy of 10%. If the data below 0.01 eV are absent, then the errors of b_{ne} and $\sigma_{0\gamma}$ increase by ~ 2 times. In this case it is desirable to know the value of $\sigma_{0\gamma}$ from addition measurements of σ_t in the millivolt region, which can improve the accuracy of the b_{ne} estimation.

The Russian Gov. Fund for Stable Isotopes has 10 g samples of ^{86}Kr with 99.97% enrichment. A $S \sim 1.7$ cm^2 sample can be prepared and its transmission may be $T \sim 0.74$. To attain an accuracy of up to 2.5 mb for such T, the statistic has to be $\sim 3.10^8$ per point. With the mirror neutron guide tube of the IBR-2 reactor in the interval of $3 - 25$ meV, such a statistic may be achieved in twenty four hours; in 4 days at the IBR-30 booster for a flight path of 10 m and in the region of $0.005 - 10$ eV.

References

1] V.F.Sears, Phys.Reports, **141**, p.281, 1986

[2] E.Melkonian, B.M.Rustad, W.W.Havens, Phys.Rev, **114**, p.1571, 1959

[3] Yu.Alexandrov, T.Machekhina, L.Sedlakova, L.Fykin, Yadernaya Fisika, **20**, p.1190, 1974

[4] V.E.Krohn, G.R.Ringo, Phys.Rev.,**D8**, p.1305, 1973

[5] L.Koester, W.Waschkowski, A.Kluver, Physica, **B137**, p.282, 1986

[6] S.Kopecky, P.Riehs, J.Harvey. Proceedings Int. Conf. on Nuclear Data for Science and Technology. Gatlinburg, May 1994, p.233

7] V.Turchin, Medlennye nejtrony, Gosatomisdat, Moskva,1963

[8] S.Mughadghab et al. Neutron Cross Sections, Academic Press, 1984

INVESTIGATIONS OF NEUTRON ELECTRIC POLARIZABILITY IN 1995

T.L.Enik, L.V.Mitsyna, V.G.Nikolenko, A.B.Popov, G.S.Samosvat
Frank Laboratory of Neutron Physics,
Joint Institute for Nuclear Research, Dubna, Russia

As far as we know, only one experimental work [1] on the neutron electric polarizability α_n has been performed during the last year. This work has relatively low statistical accuracy but, together with more precise work [2], plays an essential part in further advance of the α_n determination. The neutron total scattering cross section for ^{208}Pb, free of contributions from all known resonances, was obtained in [1] at 13 energies between $1\,eV$ and $25\,keV$ with errors of $3-18\,mb$ and in [2] at 100 energies between $50\,eV$ and $40\,keV$ with errors of $\sim 2\,mb$.

The authors of [2] analyzed their cross section by the "mathematical" formula

$$\sigma(E) = \sigma(0) + ak + bk^2 + ck^4, \qquad (1$$

fitted four coefficients of (1) and found for the polarizability

$$\alpha_n = (1.20 \pm 0.15) \cdot 10^{-3} fm^3, \qquad (2)$$

using only the quantity of a.

An alternative, more "physical" method of $\sigma(E)$ analysis was applied in [1]

$$\sigma(E) = \frac{4\pi}{k^2} sin^2(-ka_{pot}) + \frac{12\pi}{k^2} sin^2\delta_1, \qquad (3)$$

where

$$a_{pot} = R' - hE - a_p P,$$

$$a_p = -\frac{6}{5}\frac{\alpha_n M_n}{R_N}\left(\frac{Ze}{\hbar}\right)^2$$

$$P = \frac{5\pi}{18} kR_N - \frac{5}{21}(kR_N)^2 + \frac{2}{243}(kR_N)^4 -$$

$$\delta_1 = -kR + arctg(kR) + arcsin\frac{(kR)^3 R_1^\infty}{1+(kR)^2},$$

$Z = 82, R_N = 7.1 fm, R = 8.0 fm, R_1^\infty = 0.21, M_n$,$E$ and k are the neutron mass, energy and wave number. There are three parameters to be fitted, R', h and α_n. The purpose of the h parameter is to take into account the energy

dependent contribution of distant resonances. It can be expressed to the first power of the E/E_0 approximation via the sum

$$h = 2276\frac{A+1}{A}\sum\frac{g\Gamma_n^{(0)}}{E_0^2} fm/eV \qquad (4)$$

through all s–wave resonances not taken into account in the $\sigma(E)$ calculation. We used expression (3) for three different tasks.

I. The first task was to obtain the values of the three parameters described the Dubna data [1] on $\sigma(E)$. We found R' and a strong correlation between α_n and h, so that $h \geq 11 \cdot 10^{-7} fm/eV$, unless $\alpha_n < 0$. Such large h is unexpected and testifies that some resonances were not taken into account. For comparison: even the strongest and nearest resonance at 507 keV gives $h = 6.6$ *) and a negative "dummy" resonance at $E_0 = -1.9MeV$ from [3] only 1.2.

II. The second task of (3) was to examine the validity of approximation (1) and the sense of its coefficients obtained in [2]. We decomposed (3) in terms up to sixth power of k and found the following:

1) The coefficients of (1) $\sigma(0), a, b$ from [2] give

$$R' = (9.5696 \pm 0.0021) fm, \quad \alpha_n = (1.18 \pm 0.15) \cdot 10^{-3} fm^3, \quad h = 19.0 \pm 0.6. \quad (5)$$

2) These three values give in their turn a coefficient c larger by $\sim 25\%$ than was obtained in [2], signifying the deficiency of c not only for p–wave contribution but for k^4- term of $sin^2(-ka_{pot})/k^2$, as well.

3) The terms with k^5 and k^6 are small indeed, giving contributions to $\sigma(40keV)$ of less than $1\,mb$.

4) The term with k^3, as the term with k, is proportional to α_n and the former reaches $\sim 12\%$ of the latter at $E = 40\,keV$.

III. The third task of (3) was to analyse $\sigma(E)$ measured in the work [2]. Having no primary data, we calculated 100 values of $\sigma(E)$ for E from 0.4 to $40\,keV$ according to (1) with the coefficients given in [2] and spread them randomly with a standard deviation of $2\,mb$. The fitting of three parameters to this set of $\sigma(E)$ points gave

$$R' = (9.5684 \pm 0.0007) fm, \quad \alpha_n = (1.70 \pm 0.21) \cdot 10^{-3} fm^3, \quad h = 20.4 \pm 0.4. \quad (6)$$

We then added to (3) the resonance and interference terms for one resonance with a given E_0 and $\Gamma_n^{(0)}$ and tried to fit R', α_n, E_0, $\Gamma_n^{(0)}$ at the fixed $h = 0$. There is strong correlation between E_0 and $\Gamma_n^{(0)}$ and no evident minimum of χ^2.

*) We omit $10^{-7} fm/eV$ units for h here and below

According to the level scheme of ^{209}Pb [4], the best candidate for the unknown resonance is the only $1/2^+-$ level below neutron binding energy at $2.03\,MeV$, i.e. the same negative "dummy" resonance at $-1.9MeV$ from [3]. Fixing $E_0 = -1.9\,MeV$ gave

$$R' = (7.048 \pm 0.040)fm, \quad \alpha_n = (1.66 \pm 0.21) \cdot 10^{-3} fm^3$$
$$h = 0, \quad \Gamma_n^{(0)} = (2170 \pm 34)eV \tag{7}$$

Such a high quantity for $\Gamma_n^{(0)}$ of a resonance does not seem unacceptable, because the one–particle Wigner limit for a nuclear radius of $8\,fm$ is $\sim 2300\,eV$ and the $4s_{1/2}$ level at $2.03\,MeV$ has a spectroscopic factor close to 1 [5].

Summarizing, we should say:

1 Most probably (see points 2) and 4) above), the cross section $\sigma(E)$ and result (2) for polarizability α_n are somewhat wrong.

2. Success in searching for the true α_n can come only if the k^3-term is added to (1) for $\sigma(E)$ analysis, and if more definite information on the s–wave resonances of ^{208}Pb is obtained.

Referenses

[1] T.L.Enik, L.V.Mitsyna, V.G.Nikolenko, A.B.Popov, G.S.Samosvat, P.Prokofjevs, A.V.Murzin, W.Waschkowski. ISINN–3: Neutron Spectroscopy, Nuclear Structure, Related Topics, JINR E3–95–307, Dubna, 1995, p.238.

[2] J.Schmiedmayer, P.Riehs, J.A.Harvey, N.W.Hill. Phys. Rev. Lett. 1991, v.66, p.1015.

[3] D.J.Horen, C.H.Johnson, J.L.Fowler, D.A.MacKellar, B.Castel. Phys. Rev. C, 1986, v.34, p.429.

[4] Table of Isotopes, ed.by C.M.Lederer, V.S.Shirley, 7^{th} Edition, York, 1978.

[5] D.G.Kovar, Nelson Stein, C.K.Bockelman. Nucl Phys. A, 1974, p.266.

MAIN PECULIARITIES OF THE CASCADE γ-DECAY OF HEAVY NUCLEI AT THE EXCITATION ENERGY REGION OF 1 TO 5 MeV

S.T. Boneva, V.A. Khitrov, Yu.V. Kholnov, A.M. Sukhovoj, E.V. Vasilieva, A.V. Vojnov

Frank Laboratory of Neutron Physics, Joint Institute for Nuclear Research, Dubna, 141980, Russia

The excitation region of 1-2 to 4-5 MeV in a heavy (for example, $A > 100$) nucleus corresponds to a principle change in its properties. Here, the levels of simple and known structures are transformed into compound-states. This complex process is very difficult for both detailed experimental study and interpretation of the data observed.

For instance, the following questions are raised:

a) Which components of the cascade intermediate level wave function dominate the matrix elements of γ-transitions populating and depopulating this level?

b) What density of intermediate levels can be excited in the slow neutron radiative capture reaction?

New information concerning these questions was obtained at FLNP JINR recently. It was previously noted [1] that the appearance of the most intense cascades in the spectra is not random - these cascades (their intermediate levels) can be arranged in "bands" with practically equidistant spacings. In each studied nucleus, two (sometimes more) such "bands" are revealed with possible equidistance periods of 270 to more than 1000 keV. If it is actually so, then the states differing in structure by 1,2,... phonons play an important role in the γ-decay process the excitation region under discussion. But, if the decay scheme contains more than one hundred intermediate levels of the most intense cascades, then the question of establishing the fact of the "regularity" of observing such "bands" cannot have a clear and unambiguous answer, even in principle. It means that the final conclusion about the existence of such vibrational excitations can be derived only after observing them in different resonances of the same nuclei.

Nevertheless, analysis of the data on the two-step cascades following thermal neutron capture provides arguments in favour of this effect [1] and allows one to explain its possible nature. The Interacting Boson Model [2] predicts that the boson energy must asymptotically and linearly depend upon the the number of boson pairs, N_b, in unfilled nucleon shells. Such a dependence is shown in fig.1. It is seen that:

a) the linear relation between the equidistance period, T, and N_b is, in fact, observed (although with some variations);

b) the energy of corresponding bosons for cascades of the $E1+E1$ and $M1+M1$ types exceeds that for cascades of $E1+M1$-transitions;

c) the equidistance period for even-even nuclei is larger than that for even-odd and odd-odd nuclei.

This situation can be qualitatively explained by accounting for known nuclear properties: the energy of octupole phonons, whose contribution to the wave function structure of levels can cause the width enhancements and the observed equidistance in the case of the $E1+E1$ and $M1+M1$ cascade transitions, exceeds the energy of quadrupole phonons. But,

the observation of enhanced equidistant cascades of $E1+M1$-transitions can be explained solely by the contributions of quadrupole phonons.

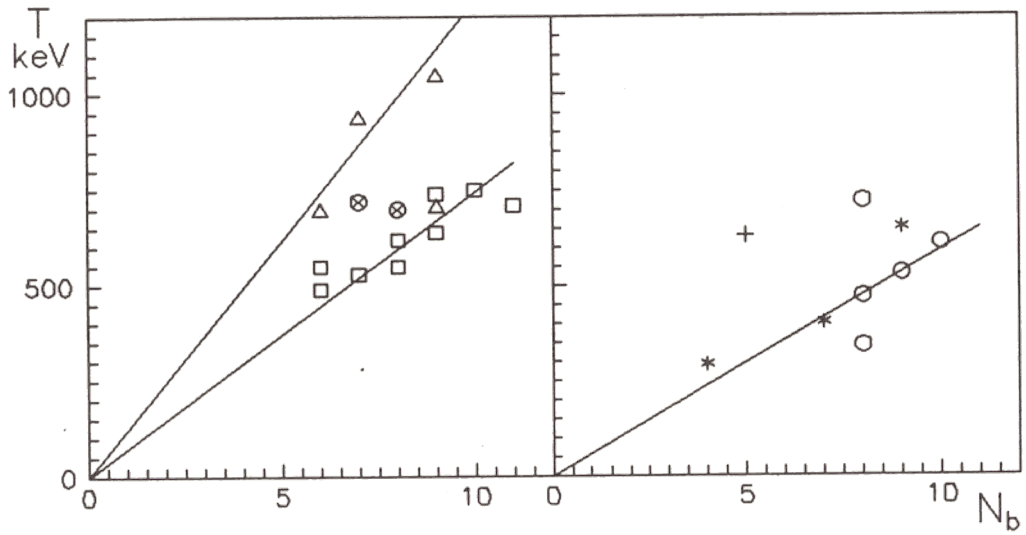

Fig.1. The value of the most probable equidistance period, T, as a function of the number of boson pairs, N_b, in unfilled shells. □ - even-even nuclei, cascades of $E1+M1$-transitions; △ - even-even nuclei, + - even-odd nuclei, cascades of $E1+E1$- or $M1+M1$-transitions; ◯ - even-odd nuclei with $\Gamma_n^o/ < \Gamma_n^o > > 1$; ×- preliminary data for odd-odd nuclei; ⊗ - ϵ_d values for the $^{110,112}Cd$ nuclei. Line - extrapolation of possible dependence.

On the other hand, the interaction of quasiparticles with phonons changes the energy of the latter, which permits one to explain the lesser T value for nuclei with one or two odd nucleons.

The presence of levels differing in structure by 1,2,... phonons in the excitation spectrum means that the energy of the captured neutron passes to the excitation of the nucleus as the whole, but not to the excitation of quasiparticle states. If this is true, then one should consider the nucleus as a system characterized by a lower temperature than follows from generally conceived notions. A lower nuclear temperature unambiguously leads to a decrease in the density of excited states. As an example, figure 2 shows the number of intermediate cascade levels observed in 100 keV energy intervals as a function of the excitation energy of the ^{198}Au compound-nucleus. Experimental data (points) are compared with the model [3,4] calculated values. As seen from the figure, the experimental level density is less than that predicted by the Fermi-gas model with a backshift [3].

Usually, such a situation is interpreted as an "omission" of levels excited by cascades whose intensities are less than the sensitivity limit of the spectrometer. This is not the only explanation, however. Figure 3 shows the sum intensities of two-step cascades to several low-lying (energy is less than 680 keV) levels of the ^{198}Au nucleus as a function of their primary transition energy. Experimental intensities (histograms) are compared with calculated intensities (smooth lines). Curve 3 was calculated using a combined level density: the experimental density was used below the excitation energy of 3 MeV; the level

density above this energy was found within the exponential interpolation to experimental values at the excitation energies of 3 and 6.5 MeV, respectively. As can be seen, the "combined" model gives considerably better agreement with the experiment.

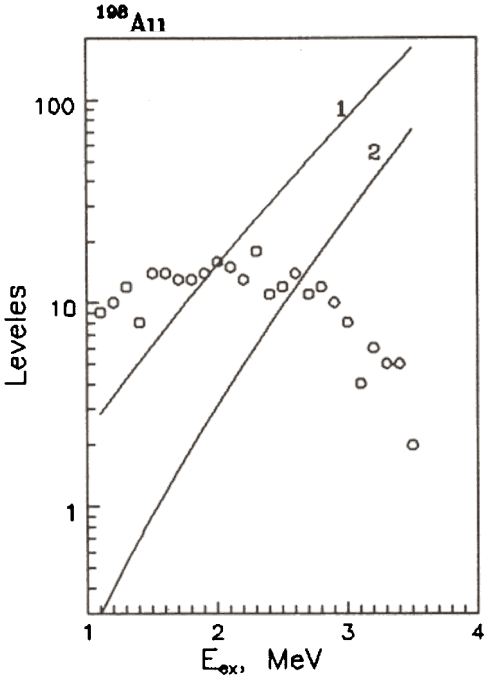

Fig.2. Number of observed levels in ^{198}Au for the excitation interval of 100 keV (points). Curves 1 and 2 represent the BSFG (ref.[3]) and the Ignatyuk thermodynamical model (ref.[4]) predictions for negative parity.

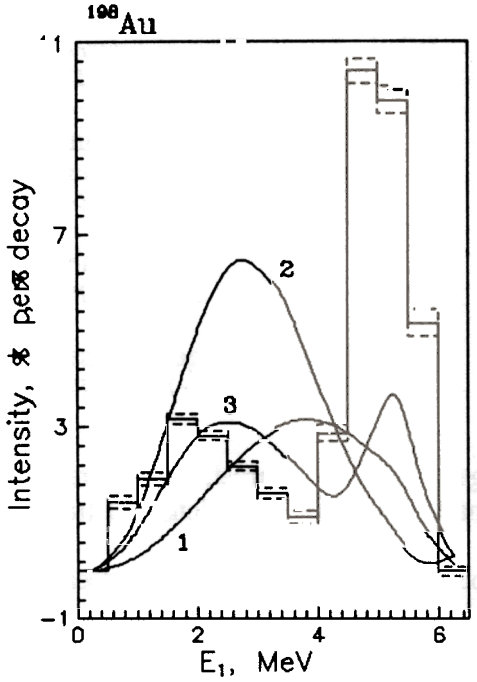

Fig.3. Distribution of total two-step cascade intensities (in % per decay) in ^{198}Au as a function of primary transition energy. The histogram represents the experimental intensities summed in energy bins of 500 keV; the statistical errors are shown. Curves 1 and 2 correspond to predictions according to models mentioned in refs.[3,4] respectively. Curve 3 represents the calculation within the "combined" model.

Summarizing, one can state that quadrupole (and possiply octupole) multiphonon excitations determine, in considerable measure, the properties of a nucleus above an excitation energy of about 1-2 MeV.

And as a consequence, the density of states excited in the (n, γ)-reaction is considerably less than what follows from the Fermi-gas model (which does not take into account the correlated motion of nucleon pairs).

References

[1] E.V.Vasilieva et al., Bull. of the Rus. Acad. of Scien., Physics, 57, 1582 (1993)

[2] F.Iachello, A.Arima, The interacting boson model, Cambridge University Press, Cambridge, 1987

[3] W.Dilg et al., Nucl. Phys., A217, 269 (1973)

[4] A.V.Ignatyuk et al., Yad. Fiz., 21, 485 (1975)

PHOTON STRENGTH FUNCTIONS OF ^{159}Gd STUDIED FROM NEUTRON CAPTURE AT ISOLATED RESONANCES OF ^{158}Gd

Stanislav Pospíšil, Jiří Kubašta
Faculty of Nuclear Sciences and Physical Engineering, Czech Technical University
Břehová 7, CZ-115 19 Prague 1, Czech Republic

František Bečvář
Faculty of Mathematics and Physics, Charles University
V Holešovičkách 2, CZ-180 00 Prague 8, Czech Republic

Huynh Thuong Hiep
Institute of Physics, Hanoi, Vietnam

Sergey Aleksandrovich Telezhnikov
Joint Institute for Nuclear Research, 141 980 Dubna, M.O., Russia

Keywords: gadolinium 158 target, neutron reactions, resonance neutrons, capture, gadolinium 159, prompt gamma radiation, E1 transitions, M1 transitions, level widths, strength functions

Although many studies of gamma decay of highly excited states in medium and heavy nuclei have already been undertaken, see, e.g., [1-5], the available experimental data concerning this subject are still far from providing a reasonably full picture of this process. In particular, the well-known discrepancy between the measured photon strength and the strength calculated within the frame of Brink's model has remained an open problem for more than three decades. While it is evident that for some nuclei Brink's model in its formulation [6] based on a simple idea of purely Lorentzian electric Giant Dipole Resonance (GDR) leads to overestimating the photon strength [1-3,5], in view of the limited number of nuclei studied it is not quite certain that the deficit of experimental photon strength does indeed belong exclusively to spherical and transitional nuclei, as suggested by the existing experimental data [3-5]. There is an evident need of further data for deformed nuclei, which motivated us to undertake the present study.

The experiment was carried out at the JINR Pulsed Fast Reactor IBR-30 which worked as a booster in conjunction with 40 MeV electron linac LUE-40. The sample consisted of 48.56 g of Gd_2O_3 enriched in ^{158}Gd to 97.7%. The time-of-flight resolution power of 70 ns/m allowed us to accumulate γ-ray spectra for 12 isolated neutron *s*-wave resonances with $J^{\pi}=1/2^{+}$ at energies of 22.3, 101.1, 242.7, 277.2, 344.8, 409.1, 503.3, 588.5, 692.9, 847.3, 917.1, and 1068.0 eV [7]. However, the resonance at energy 847.3 eV has a small contribution of the next weak unresolved resonance at energy 869.3 eV. Relative intensities of primary transitions to final levels of ^{159}Gd below 1150 keV were determined, the total area under 7 low-energy γ-lines at 467.2, 524.5, 537.1, 551.0, 601.8, 677.4, and 715.2 keV being adopted as a measure of neutron capture rate. A separate run was undertaken using a composite sample consisting of a layer of enriched Gd covered on the back side by a layer of natural boron. Comparing the yields of γ-rays, resulting from deexcitation of the product of the ^{10}B(n,α)^{7}Li* reaction, and 5943.0 keV γ-rays, accompanying the neutron capture in ^{158}Gd at isolated 22.3 eV resonance, absolute intensity I_{γ} = 0.100±0.015 γ's per neutron captured was determined for the corresponding 5943.0 keV transition and a given resonance. This intensity was then used as a reference value to convert the relative intensities of primary transitions into the absolute intensity scale. Assuming that a total radiation width of each resonance is equal to the average value of this quantity, $\langle\Gamma_{\lambda\gamma}\rangle_{\lambda}$ = 0.105±0.010 eV, deduced from the data in [7], the absolute primary intensities were transformed into partial radiation widths $\Gamma_{\lambda f}$, where λ and f are labels of neutron resonance and final level, respectively.

Multipolarities (*E1* and *M1*) of primary transitions to the individual final levels f were determined on grounds essentially similar to those adopted in the well-known technique of average resonance capture [8]. Besides that, for some final levels f additional information on multipolarity was gained from analysis of fluctuations of $\Gamma_{\lambda f}$ for fixed f and variable λ, assuming that these quantities fluctuate according to Porter-Thomas distribution, i.e. χ^2 distribution with the number of degrees of

freedom ν = 1. We found 8 primary *E1* transitions populating ^{159}Gd levels below 1150 keV whose energies are 5943.0, 5434.7, 5384.7, 4881.7, 4863.5, 4832.2, 4803.3, and 4796.9 keV. A conservative analysis of the sensitivity of our experiment indicated that these levels form a full set of $J^{\pi} = 1/2^-,3/2^-$ levels within the given range of excitation. This statement could be made with a statistical significance of 98.5%. Similarly, we observed 9 primary *M1* transitions populating levels below the same limit with energies 5341.1, 5295.9, 5198.1, 5161.0, 5083.0, 4987.0, 4971.0, 4939.7, and 4814.4 keV.

The partial radiation widths obtained were used to calculate the values of photon strength function defined conventionally as

$$S_\gamma(E_\gamma) = \frac{\langle \Gamma_{\lambda\gamma f} \rangle_\lambda}{D_J E_\gamma^3} \qquad (1)$$

where $\langle\rangle_\lambda$ denotes averaging over resonances, D_J is the average spacing between neighbour resonances of a given spin ($J^{\pi} = 1/2^+$) and E_γ is γ-ray energy. The deduced values of $S_\gamma(E_\gamma)$ are plotted in Fig. 1 for *E1* and in Fig. 2 for *M1* transitions, respectively.

In the case of *E1* radiation these values are compared with the predictions of Brink's model in its above-outlined formulation by Axel [6], and also with predictions of the alternative model of Kadmenskij *et al.* [9] based on the theory of Fermi liquid. In view of missing data on photoabsorption in ^{159}Gd, parameters of the GDR used for calculation within these two models were taken from data in [10] for photoabsorption in neighbour nucleus ^{159}Tb. In our case the region of excitation of final levels overlaps the pairing energy of ^{159}Gd at most by 300 keV, and for this reason the nuclear temperature does not play a noticeable role while calculating photon strength within the alternative model [9]. Note that in other situations, e.g., when data from two-step γ-cascades are studied [11], this is not the case.

The data of $S_\gamma(E_\gamma)$ for *M1* transitions are compared with an energy-independent value, based on systematization of McCullagh [2] within the strongly simplified single-particle Weisskopf model. The average is $(1.5\pm0.3)\times10^{-8}$MeV^{-3}, as obtained from the data in Fig. 2. This value corresponds to previous estimates given in [2].

From Fig.1 it is evident that, except for one primary transition (E_γ = 5384.7 keV) which populates the level at 558.2 keV, our data are fully compatible with Brink's model [6] based on the use of purely Lorentzian GDR [10] (i.e., with a constant damping width). On the other hand, our data are in sharp contradiction with predictions of the alternative model of Kadmenskij *et al.* [9]. This finding thus corroborates tentative conclusions made in previous works [5,12] that the noted deficit of the *E1* photon strength is characteristic only of spherical and transitional nuclei. Nevertheless, the strange behaviour of the noted transition to the 558.2 keV level is not understood. The existence of a doublet structure near energy of 5384.7 keV seems improbable.

Acknowledgement

This work has been supported by the Committee of the Czech Republic for Cooperation with the Joint Institute for Nuclear Research at Dubna, under a Grant from the Ministry of Industry and Trade of the Czech Republic.

References

[1] CARPENTER, R. T., Argonne National Laboratory Reports Nos. ANL-6589 (1962) and ANL-6797 (1963).

[2] McCULLAGH, C. M. - STELTS, M. L. - CHRIEN, R. E., Phys. Rev. C**23** (1981) 1324.

[3] RAMAN, S., in *Proceedings of the Fourth International Symposium on Capture Gamma-ray Spectroscopy and Related Topics, Grenoble, 1981,* edited by T. von Egidy, F. Gönnenwein, and B. Maier, IOP Conference Proc. No.62, Institute of Physics and Physical Society, London (1982) 357.

[4] KOPECKÝ, J. - UHL, M., Phys. Rev. C **41** (1990) 1941

[5] BEČVÁŘ, F. - MONTERO-CABRERA, M. E. - HUYNH THUONG HIEP - TELEZHNIKOV, S. A., in *Proceedings of the Sixth Conference on Capture Gamma-ray Spectroscopy, Leuven, 1987,* edited by K. Abrahams and P. van Assche, Institute of Physics Conference Series No.88, Bristol and Philadelphia (1988) S649-S651.

[6] AXEL, P., Phys. Rev. **126** (1962) 671

[7] MUGHABGHAB, S. F. - DIVADEENAM, M. - HOLDEN, N. E., in *Neutron Cross Sections, vol. 1, Neutron Resonance Parameters and Thermal Cross Sections, Part B Z=61-100,* Academic Press (1981).

[8] CHRIEN, R. E., in *Neutron Induced Reactions,* Proceedings of the Europhysics Topical Conference, Smolenice 1982, edited by P. Obložinský, Physics and Applications Vol. 10, Institute of Physics EPRC, Bratislava (1982) 189.

[9] KADMENSKIJ, S. G. - MARKUSHEV, V. P. - FURMAN, V. I., Yad. Fiz. **37** (1983) 277 (Sov. J. Nucl. Phys. **37** (1983) 165).

[10] BERMAN, B. L., in *Atlas of Photoneutron Cross Sections Obtained with Monoenergetic Photons,* Atomic Data and Nuclear Data Tables **15** (1975) 319-390.

[11] BEČVÁŘ, F. - CEJNAR, P. - CHRIEN, R. E. - KOPECKÝ, J., Phys. Rev. C **46** (1992) 1276.

[12] KOPECKÝ, J. - UHL, M. - CHRIEN, R. E., Phys. Rev. C **47** (1993) 312.

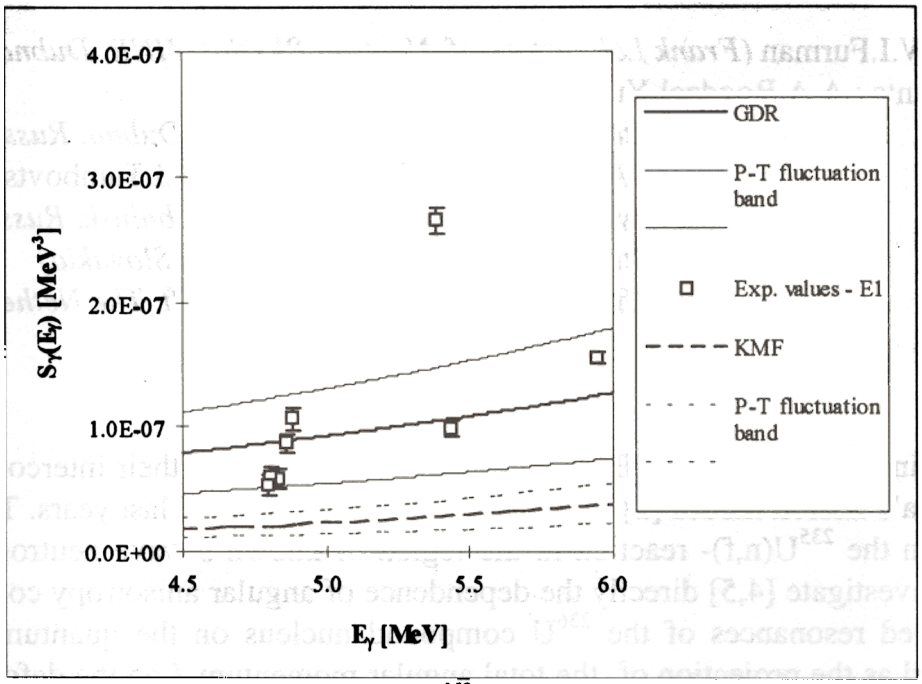

Fig. 1. Measured primary E1-strength for the ^{158}Gd(n, γ) reaction plotted versus E_γ energy. The calculated strength functions are plotted as solid (GDR - [10]) and dashed (KMF - [9]) curves. The predicted residual Porter-Thomas fluctuation bands are shown.

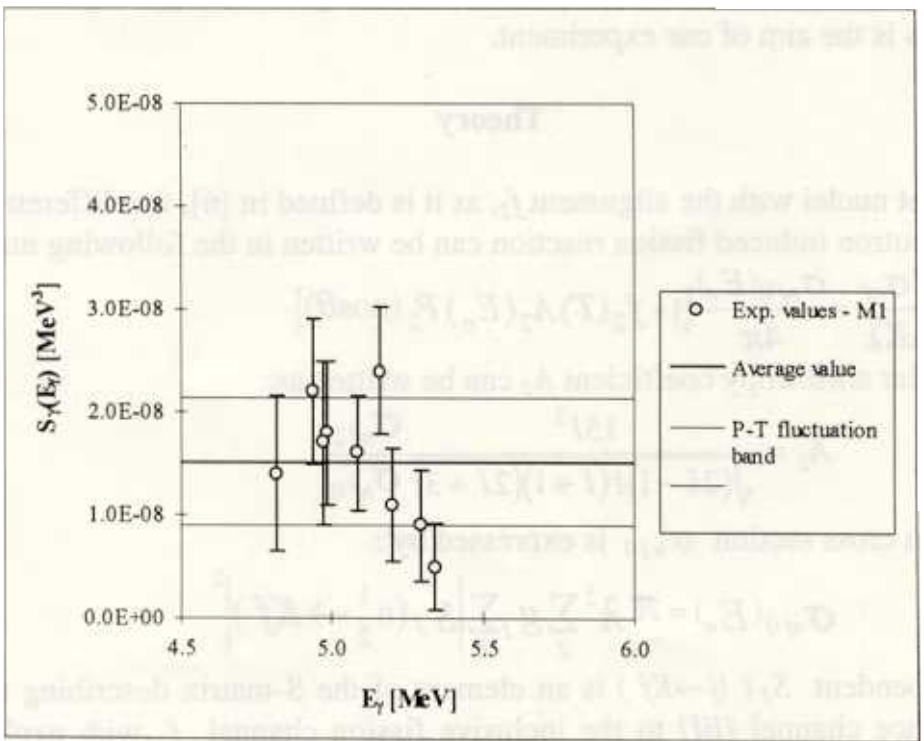

Fig. 2. Measured primary M1-strength for the ^{158}Gd(n, γ) reaction plotted versus E_γ energy

MEASUREMENT OF ENERGY DEPENDENCE OF FISSION FRAGMENT ANGULAR ANISOTROPY FOR RESONANCE NEUTRON INDUCED FISSION OF ^{235}U ALIGNED TARGET

Leader : W.I.Furman *(Frank Laboratory of Neutron Physics, JINR, Dubna, Russia)*
Participants : A.A.Bogdzel,Yu.N.Kopach, A.B.Popov,
(Frank Laboratory of Neutron Physics, JINR, Dubna, Russia)
N.N.Gonin, M.A. Guseinov, L.K.Kozlovsky, D.I.Tambovtsev
(Institute of Physics and Power Engineering, Obninsk, Russia)
J.Kliman *(Institute of Physics, SAS, Bratislava, Slovakia)*
H.Postma *(Delft University of Technology, Delft, The Netherlands.)*

Introduction

The origin and nature of the Bohr's fission channels [1] and their interconnection and relation to Brosa's fission modes [2] are the topic of discussions for last years. The use of an aligned target in the ^{235}U(n,f)- reaction in the region of known s-wave neutron resonances [3] allows to investigate [4,5] directly the dependence of angular anisotropy coefficients for a set of observed resonances of the ^{236}U compound nucleus on the quantum number K, which is defined as the projection of the total angular momentum J on the deformation axis of a fissioning nucleus. But new, more detailed investigation of epithermal neutron induced fission of oriented nuclei via largely isolated compound states, having a known spin J and parity π, may give a unique possibility to get new insight into the problem. So, more valuable information can be extracted from the study of energy dependence of this anisotropy. This is the aim of our experiment.

Theory

For target nuclei with the alignment f_2, as it is defined in [6], the differential cross-section of a neutron induced fission reaction can be written in the following manner [7] :

$$\frac{d\sigma_{nf}}{d\Omega} = \frac{\sigma_{nf0}(E_n)}{4\pi}\left[1 + f_2(T)A_2(E_n)P_2(\cos\theta)\right], \qquad (1)$$

where the angular anisotropy coefficient A_2 can be written as:

$$A_2 = \frac{15I^2}{\sqrt{(2I-1)I(I+1)(2I+3)}}\frac{\sigma_{nf2}}{\sigma_{nf0}} \qquad (2)$$

The total fission cross section σ_{nf0} is expressed by :

$$\sigma_{nf0}(E_n) = \pi \lambda^2 \sum_J g_J \sum_K \left| S_J(0\tfrac{1}{2} \rightarrow Kf) \right|^2 \qquad (3)$$

The energy dependent S_J ($lj \rightarrow Kf$) is an element of the S-matrix describing the transition from the entrance channel $\{ljI\}$ to the inclusive fission channel f with explicit quantum number JK. The energy dependent angular anisotropy part is expressed by :

$$\sigma_{nf2}(E_n)=\pi\lambda^2\sum_{JJ'}\sqrt{g_J g_{J'}}U(\tfrac{1}{2}IJ'2;JI)\sum_K C^{J'K}_{JK20}S^*_{J'}(0\tfrac{1}{2}\to Kf)S_J(0\tfrac{1}{2}\to Kf) \quad (4)$$

Here $g_J = (2J+1)/2(2I+1)$, $U(1/2\ IJ'2;JI)$ are Racah coefficients and $C^{J'K}_{JK20}$ are Clebsch-Gordan coefficients containing the K-dependence of the anisotropy part of the cross-section in a different way compared to the total cross-section (3). A new and important point predicted by formula (4) is the presence of interference between s-wave resonances of different spins.

Experiment

The experiment was performed at the beam of the IBR-30 pulsed booster source with a neutron pulse of about 4 μs and a burst frequency of 100 Hz using a flight path 29.4 m. At the sample position, the neutron beam parameters are: neutron flux $3\cdot10^4\cdot E^{-1}\ n/cm^2\cdot eV\cdot s$, energy resolution $3.8\cdot10^{-3}\cdot E^{1.5}\ eV$. A series of collimator in the flight tube reduced the beam size close to the cryostat to a diameter of 8cm.

As in the earlier experiments [4,5], the spins of ^{235}U target nuclei were aligned by electric hyperfine interaction of the quadrupole moment of ^{235}U with the strong electric field gradient at the ^{235}U nucleus within the uranyl group (UO_2) of crystals of the rubidium uranyl nitrate $RbUO_2(NO_3)_3$ (hereafter abbreviated to RUN), which were cooled to a low temperature. The bulk of these single crystals was grown using natural uranium with outside layers of about 1mg/cm^2 containing enriched ^{235}U. From these crystals slabs of about 3 mm thickness were cut and used to make two mosaic samples with a total area of 20 cm^2 and 24 cm^2. The ^{235}U layers had the following isotopic content (in %) : ^{234}U - $(4.2 \pm 0.1)\cdot10^{-3}$, ^{235}U - 99.42 ± 0.002, ^{236}U -$(1.5 \pm 0.1)\cdot10^{-3}$ and ^{238}U - $\leq 1.5\cdot10^{-4}$. The slabs were glued on to the opposite sides of a copper plate connected to the mixing chamber of the dilution refrigerator. The C-axes of all slabs were carefully oriented in the same direction.

The 3He-4He dilution refrigerator could keep a low temperature on the target during ~ 50 hours. The lowest temperatures 0.07 K without and 0.1 K under neutron irradistion were reached at the copper target plate using a 3He circulation rate of $7\cdot10^{-5}$ mole/s. In the same time it must be mentioned that deriving of the temperature of ^{235}U-containing layer is a difficult task. The presumably poor and unknown heat conductivity of the RUN crystals, high thermal resistance of glued contacts produce a significant temperature difference between the copper plate and ^{235}U-containing layer at the low temperatures. To solve this problem the α-emission anisotropy from the same samples was measured. For this purpose a small amount (< 0.1 %) of ^{233}U was added to the RUN solution from which the ^{235}U-containing layers were grown. The evaluation of the surface temperature under neutron irradiation from the angular anisotropy of α-particles gives T=(0.15 ± 0.02) K. Then using the estimated value of the electric hyperfine coupling constant P/k = (0.0154 ± 0.0027) K [3] the nuclear alignment parameter f_2 = - 0.15 ± 0.02 was calculated for ^{235}U.

The α-particles and fission fragments from each sample were detected by three silicon surface barrier semiconductor detectors of rectangular form (2x5 cm^2 active area each) mounted in the directions 0^0, 45^0 and 90^0 with respect to the C-axis of the RUN crystals which were oriented along the neutron beam. In comparison with [5] the detectors at 45^0 were added to improve the investigation of fission fragment angular distributions. For

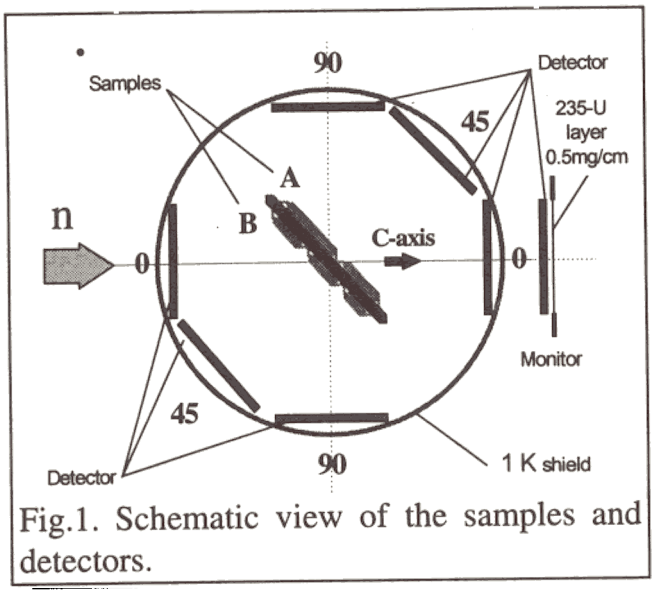

Fig.1. Schematic view of the samples and detectors.

monitoring of the neutron flux an additional layer of a non-oriented ^{235}U compound, about 0.5 mg/cm^2 thick, and a separate Si detector were placed in the neutron beam. With its qualitatively better alpha- and fission fragment spectra appeared also to be very useful for an independent control of the stability of the detectors inside the cryostat.

All detectors were kept at about 1K during the measurements. The positions of the samples and detectors are shown in Fig.1.

The data acquisition system (DAS) consisted of a set of analog, logical and digital CAMAC-blocks with a PC on-line. The DAS allowed to accumulate 7 separate energy spectra (1024 channel each) of α-particles and fission fragments and 7 time-of-flight spectra (4096 channel each) of fission fragments only. It had also automatic "controller of quality" of the input information and periodical saving of the accumulated data on the hard disk.

Results and discussion

The aim of this experiment is to obtain the energy dependence of the A_2 coefficients in the formula (1). To do this, several steps had to be taken :

- to evaluate and subtract the background properly;
- to measure the temperature of the samples and define the alignment parameters f_2, and finally
- to extract the A_2 values from the detectors counts as a function of neutron energy.

The background was measured separately at liquid nitrogen temperature using a set of thick beam filters: Co, W, Ag , Rh and Cd, which give "black resonances" and then approximated by the usual formula: $A / x + B + Cx$, where x is the channel number and A,B,C are fitting parameters. The background during the main runs was supposed to have the same behavior. Only Co and Cd filters were left in the beam for calibration.

After the background subtraction, the A_2 coefficients were calculated for a given TOF region from the system of equations:

$$\frac{N_{T_1}(\theta_i)}{N_{T_2}(\theta_i)} \Big/ \frac{M_{T_1}}{M_{T_2}} = \frac{(1 + A_2 \cdot f_2(T_1) \cdot \beta_2(\theta_i))}{(1 + A_2 \cdot f_2(T_2) \cdot \beta_2(\theta_i))}, \quad \theta_i = 0^0.45^0.90^0, \qquad (5)$$

where $N_T(\theta_i)$ are the counts of the detector at angle θ_i and temperature T; M_T are the counts of the monitor detector; $\beta_2(\theta_i) = \langle P_2(\cos\theta_i) \rangle$ are the averaged Legendre polynomials, calculated by the Monte-Carlo method. Since there is only one unknown, the χ^2 - method using FUMILI code of χ^2 minimization was used to obtain A_2.

Our energy resolution allowed us to obtain the energy dependence of A_2 with reasonable statistical errors in the neutron energy interval up to 20 eV.

The results of data processing for neutron energy 0.4 -20 eV of our first results [10] added with the data for new four-week measurements are presented in Fig. 2.

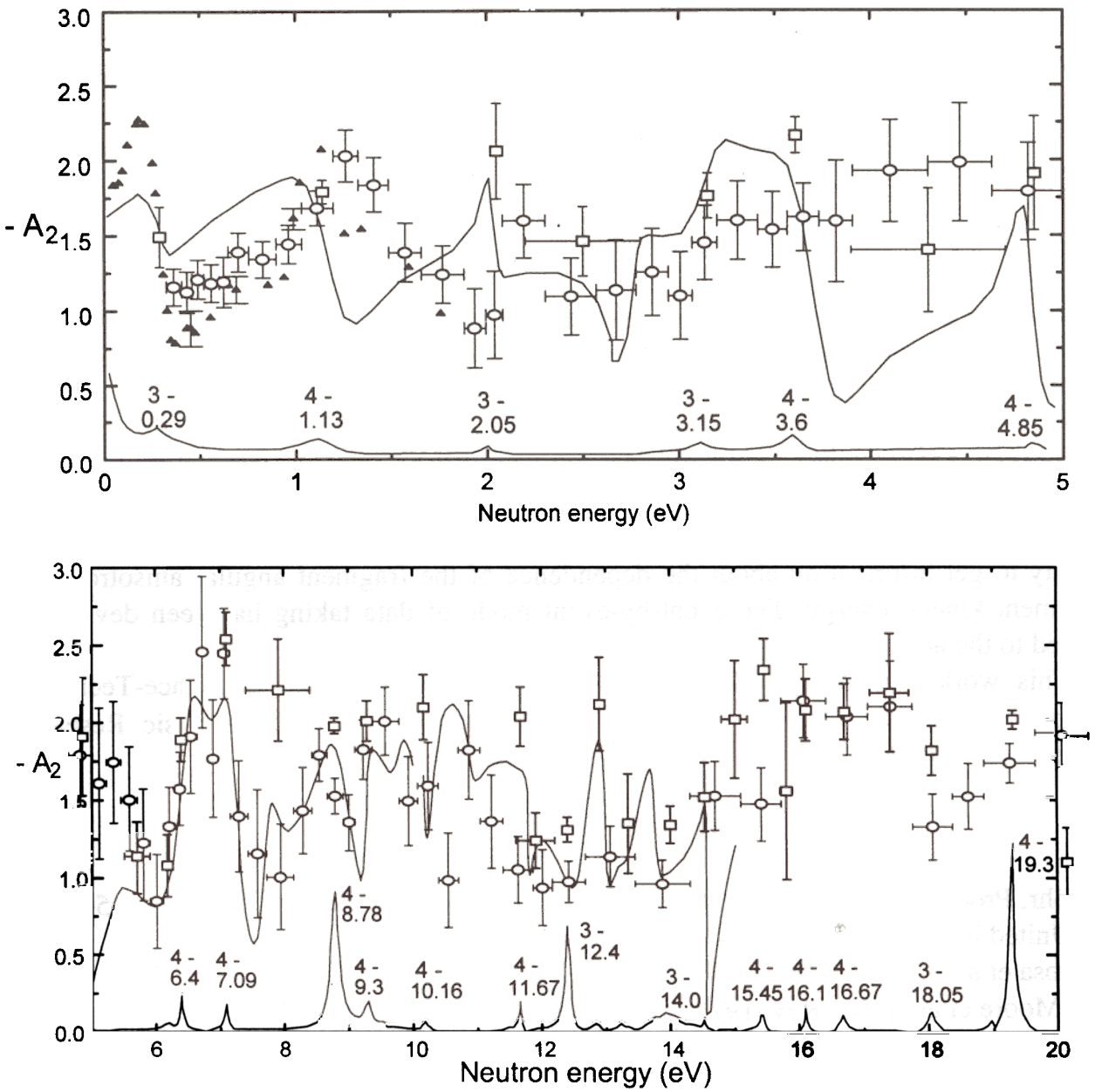

Fig.2. The energy dependence of fission fragment angular distribution coefficient A_2 from resonance neutron induced fission of ^{235}U aligned target : □ - [5], corrected for 10% misalignment of the crystals as mentioned in the original paper ; ▲ - [9]; ○ - present results. The solid is the result of an R-matrix multilevel two fission channel calculation [11]. The curve in the lower parts of the pictures is the fission cross section in arbitrary units.

Only statistical errors for A_2 are included in the fig. 2. The systematic errors due to uncertainty of the electric-hyperfine constant P/k and temperature are fairly large; they are estimated by us as ~ 20%. These uncertainties move the whole set of A_2 values, up or down, but don't change the energy dependence.

One can see that there is quite a good agreement of our data with the data of Pattenden and Postma, especially in the low energy region where our energy resolution was good enough, while the fitting curve, having been made by R-matrix multilevel two fission

channel calculation [11], does not seem to describe the energy dependence of A_2 properly.

The reason of this discrepancy, as we believe, is that this calculation was done without taking into account the interference between levels with different spins. A new approach developed by Barabanov and Furman [7] allows to include the 3^- - 4^- spin interference into the fitting program, and we hope that it will allow to obtain a new set of resonance parameters which will be in agreement with our data.

Conclusions

The experiment is continuing. A new modified 3He-4He dilution refrigerator which allows to keep a low temperature for a considerably longer time (one week or more) will be used during the next stage of the experiment. The refrigerator has been already installed at the IBR-30 neutron beam and has been tested. New (implanted) semiconductor detectors have also been manufactured, tested and selected.

A new mosaic sample with thinner (~ 0.3 mg/cm^2) ^{235}U-containing layer has been prepared and tested. The fission fragment amplitude spectrum from this sample gives us a possibility to get information about the dependence of the fragment angular anisotropy on the fragment kinetic energy. The event-by-event mode of data taking has been developed and added to the acquisition program to realize this aim.

This work was performed in the frame of the Russian State Science-Technical Program "Fundamental Nuclear Physics" under support of Russian Basic Research Foundation (project 93-02-16773) and the RFBR grant № 96-02-19162.

References

1. A.Bohr, Proc.1st. Intern. Confer. on Peaceful Uses of Atomic Energy, Geneva, 1956, United Nations, N.Y., 1956, v.2, p.151.
2. U.Brosa et al., Phys. Reports, 1990, v197, p. 167.
3. M.S.Moore et al., Phys. Rev. 1978, v.C18, p.1328.
4. J.W.T.Dabbs et al., Proc. 1st. IAEA Symposium on physics and Chemistry of Fission, Salzburg, 1965, v1, p.39.
5. N.J.Pattenden and H.Postma, Nucl.Phys. 1971, vA167, p.225.
6. H.A.Tolhoek and J.A.M.Cox, Physica,1953, v.19, p.101.
7. A.L.Barabanov and W.I.Furman, Proc. of Intern. Conf. on Nucl.Data for Science and Technology, Gatlinburg, Tennessee, USA, May 9-13, 1994, p.448.
8. M.A.Guseinov and L.K.Kozlovsky, Preprint IPPI-2356, Obninsk,1994.
9. H.Postma, Proc. Intern. Symp. on Neutron Capture, Gamma-ray Spectroscopy and Related Topics, Petten, 1974, p.619.
10. W.I.Furman, D.I.Tambovtsev et al., Proc. of Workshop on Nucl. Fiss. and Fussion-Product Spectroscopy, Seyssins, France, May 2-4, 1994, p.197.
11. M.S.Moore, Proc. IIId Intern. Seminar on Interaction of Neutrons with Nuclei, Dubna, april 26-28, 1995, to be published.

The Measurement of Independent Yields of Fragments from ^{239}Pu Fission Induced by Thermal Neutrons Using γ-Ray Spectroscopy

N.A.Gundorin, Yu.N.Kopach, Dao Ahn Minh, S.A.Telezhnikov, V.I.Furman

Fission fragments decay by emitting neutrons and γ-rays. The vast amount of information from spectrometry about decay schemes and level populations in residual nuclei allows one to use the high resolution γ-spectroscopy method for determining the independent yields of fission fragments. This method has an absolute resolution in the identification of mass A and charge Z for each isotope due to the individual sets of γ-rays from decay.

The spectrum of prompt γ-rays in fission is very complicated and the procedure of determining independent yields is somewhat ambiguous. Moreover, experiments on pulsed neutron sources have many difficulties connected with the high pulse rate of neutrons in resonances. That is why it was necessary to carry out an experiment in order to compare the results with data from other methods, and thus test the method and equipment. The measurement of γ-ray spectra of fragments from thermal neutron fission was done in this work.

Three methods of obtaining thermal neutrons were used. In the first method, fission neutrons from a highly intense source, ^{252}Cf, with a count rate of 2.3×10^7 n/sec were thermalized in a paraffin block sized 40×40×20 cm^3. There was a niche for the fission chamber in this block. The portion of thermal neutrons from such a moderator is about 20%. The Ge(Li)-detector was placed 28-30 cm from the source of neutrons and shielded by a boron polyethylene screen 10 cm thick to decrease radiation damage to the detector from fast neutrons. A lead collimator protected the detector from background γ-rays which entered from directions other than the fission chamber.

In the second method of obtaining thermal neutrons, fast neutrons from the IBR-30 reactor were used. The equipment was put 57 m from the reactor. The neutron beam with an 8 cm diameter fell on the paraffin moderator. The thermalized neutrons from the moderator entered the fission chamber, the axis of which was perpendicular to the beam. The distance between the beam axis and chamber centre was 30 cm. The detector was moved 9 cm away from the chamber and shielded by a paraffin plate 3 cm thick and a ^6Li metal screen, from fission neutrons which were produced in the chamber. A lead collimator 10 cm thick protected the detector from γ-rays exiting the moderator.

In the third method, thermal neutrons from the moderator of the pulsed reactor were used. Because of the fact that at a distance of 57 m from reactor, with a pulse frequency of 100 sec^{-1}, the energy of recycling neutrons is 0.17 eV, it is impossible to obtain thermal neutrons by the time of flight method. In all three methods, the "cadmium difference" procedure was used. Two measurements were made; in one, a cadmium filter was placed in the neutron beam. The anti-Compton spectrometer was used as a γ-ray detector in the third method of measurement. Three blocks of plastic scintillator 20×20×40 cm^3 and a NaI(Tl)-detector 15 cm in diameter and 10 cm thick surrounded the Ge(Li)-detector. The solid angle was 65-70% of 4π. The background suppression of this system was 2.6±0.2 for the γ-ray energy range from 170 to 370 keV.

The fission chamber had 19 layers of ^{239}Pu with a total weight of 1.6 g. Three series of measurements were fulfilled in which the three methods of obtaining thermal neutrons were used. Total time of measurement was 24 days. Total number of fissions was 2.2×10^9. In the measurements, three parameters of each fission event were registered: E_γ – γ-ray energy, T_n – the time interval between the start pulse of the reactor and the event in the chamber, and T_γ – the time interval between the fission event in the chamber and the

registration of the γ-ray in the Ge(Li)-detector. In the first measurement with the ^{252}Cf source, the start pulse of the reactor was imitated by the generator. Three γ-ray spectra for the three measurement configurations are shown in fig.1.

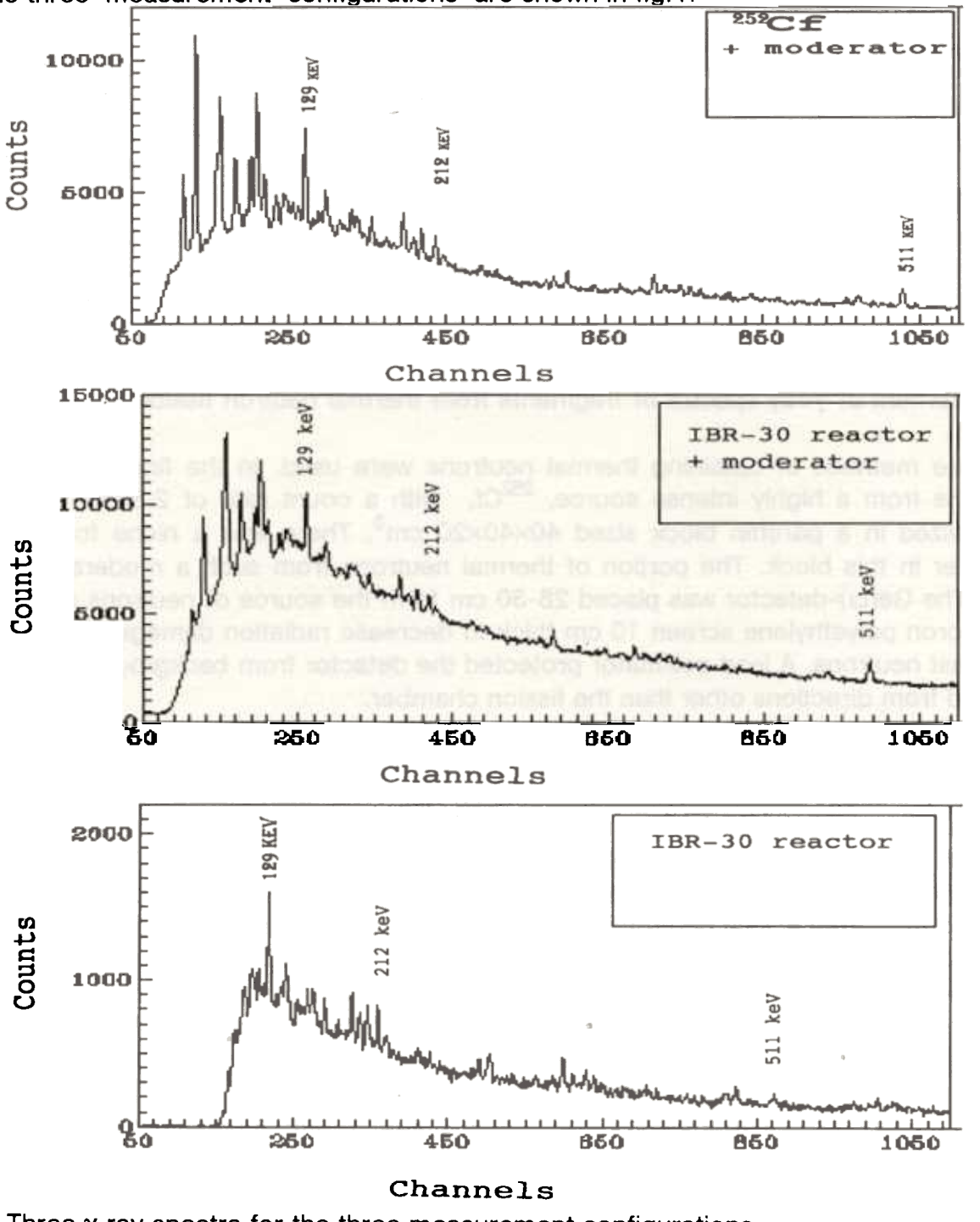

Fig.1. Three γ-ray spectra for the three measurement configurations

The spectrum of T_γ parameters has an interval in which only false coincidences take place. If we have the areas of ^{239}Pu peaks on the γ-ray spectrum from this interval of T_γ, we can calculate the value N_f^{eff} – the effective number of fissions – by the formula:

$$N_f^{eff} = \frac{N_\gamma^p}{N_\alpha \times k_\gamma^p \times \varepsilon_\gamma \times \Delta\tau} \times (1 - k_\alpha)$$

where N_γ^p is the area of the γ-ray peak of ^{239}Pu; N_α is the number of α-decays in the

chamber per second; k_γ^p is the intensity of γ-transitions in ^{239}Pu; ε_γ is the detector efficiency for γ-rays; $\Delta\tau$ is the time interval in the spectrum of T_γ in which all coincidences are false; k_α is the correction coefficient, which gives the sensitivity of the fission chamber to α-decays.

All γ-ray spectra were fitted two different ways: χ^2-minimizing method using FUMILI code, and background approximation by orthogonal polynomials.

The absolute yield of the γ-ray line can be calculated by the following expression:

$$Y_\gamma = \frac{N_\gamma \times (1+k_{ic})}{\varepsilon_\gamma \times N_f^{eff}}$$

where N_γ is the area of the γ-ray peak in the spectrum, k_{ic} is the internal conversion coefficient and ε_γ is the detector efficiency for this γ-ray.

For even-even isotopes, the intensity of the first γ-transition $2^+ \rightarrow 0^+$ is 100%. Therefore, the absolute yield of such isotopes is the same as the absolute yield of the first γ-transition $2^+ \rightarrow 0^+$. In this work, the absolute yields of 15 even-even isotopes were determined from the yields of corresponding first γ-transitions $2^+ \rightarrow 0^+$. The absolute yields $Y_{th}^{exp1,2,3}$ of even-even fission fragments which were determined by the three methods of obtaining thermal neutrons are given in Table I. In addition, the mean values of Y_{th}^{exp} and the recommended values of Y_{th}^{rec} from [1] are included

Table I. Independent yields of ^{239}Pu fission fragments induced by thermal neutrons.

$_zFr$	A	E_γ	Y_{th}^{exp1}	Y_{th}^{exp2}	Y_{th}^{exp3}	Y_{th}^{exp}	Y_{th}^{rec} [1]
		keV	%± Δ %	%± Δ %	%± Δ %	%± Δ %	%± Δ %
$_{36}Kr$	88	775	0.80±0.21		1.08±0.62	0.83±0.20	0.79±0.03
	90	707	1.10±0.19		1.71±0.69	1.14±0.18	1.18±0.05
$_{38}Sr$	94	837	2.92±0.32	2.92±0.82	2.31±0.57	2.79±0.26	3.12±0.16
	98	1223	2.75±0.28	3.57±0.89	3.15±0.84	2.85±0.25	2.85±0.14
$_{40}Zr$	100	212	4.50±0.23	4.85±0.39	4.99±0.28	4.72±0.16	4.76±0.24
	102	152	1.19±0.15		2.37±0.28	1.45±0.13	1.19±0.12
$_{42}Mo$	104	192	3.99±0.20	4.81±0.53	5.42±0.28	4.50±0.16	4.12±0.21
	106	171	1.80±0.20	2.28±0.16	2.10±0.27	2.09±0.11	2.05±0.10
$_{52}Te$	132	974	2.32±0.28	2.29±0.59	1.31±0.53	2.13±0.23	2.36±0.07
$_{54}Xe$	136	1313	2.86±0.30		0.88±0.80	2.62±0.28	3.02±0.36
	138	589	3.89±0.27	4.08±0.57	4.23±0.75	3.95±0.23	4.08±0.33
$_{56}Ba$	142	359	3.09±0.25	3.01±0.27	2.72±0.45	3.01±0.17	3.27±0.36
	144	199	2.39±0.14	2.42±0.36	2.59±0.26	2.43±0.12	2.09±0.23
$_{58}Ce$	146	259	0.79±0.13		1.27±0.29	0.87±0.12	0.95±0.11
	148	159	1.29±0.12		3.20±0.37	1.47±0.11	1.09±0.12

Mean square deviation $\chi^2/n = 1.07$

The experimental values of absolute yields were obtained at different count rates, background conditions, and qualities of γ-ray spectra and most agree with each other. The value χ^2/n for Y_{th}^{exp} and Y_{th}^{rec} is about 1. Hence, there are no systematic errors. This result proves the possibility of using γ-ray spectroscopy for measuring independent yields of fission fragments, the capacity of the equipment and the correctness of the fitting algorithms.

1. Wahl A.C. Atomic Data and Nuclear Data Tables, 1988, v.39, pp 118-121

3. PUBLICATIONS

CONDENSED MATTER PHYSICS

Diffraction

1. V.L.Aksenov. News form IBR-2. ICANS-XIII, Villigen, 10-13 October 1995. PSI Proc. 95-02, pp.56-62.
2. V.L.Aksenov, A.M.Balagurov, B.N.Savenko, V.P.Glazkov, I.N.Goncharenko, V.A.Somenkov, E.V.Antipov, S.N.Putilin, J.-J.Capponi. Neutron Diffraction Study of the High-T_c Superconductor $HgBa_2CaCu_2O_{6.3}$ under High Pressure. High Press. Res., 1995, v.14, pp.127-137.
3. V.L.Aksenov, A.M.Balagurov, G.D.Bokuchava, J.Schreiber, Yu.V.Taran. Estimation of Residual Stress in Cold Rolled Iron-Disks from Strain Measurements on the High Resolution Fourier Diffractometer. Communications of JINR, E14-95-37, Dubna, 1995.
4. V.L.Aksenov, A.M.Balagurov, S.L.Platonov, B.N.Savenko, V.P.Glazkov, I.V.Naumov, V.A.Somenkov, G.F.Syrykh. TOF Neutron Spectrometer for Microsamples Studies under High Pressure. High Press. Res., 1995, v.14, pp.181-191. PSI Proc. 95-02, pp.235-239.
5. V.L.Aksenov, A.M.Balagurov, V.A.Trounov, P.Hiismaki. Performance of the High Resolution Fourier Diffractometer at the IBR-2 Pulsed Reactor; Latest Results. ICANS-XIII, Villigen, 10-13 October 1995.
6. V.L.Aksenov, N.N.Isakov, R.M.A.Maayouf. The NSKAT Neutron Spectrometer for Quantitative Texture Analysis (NSKAT Project). Communications of JINR, E3-95-304, Dubna, 1995.
7. A.M.Balagurov, B.N.Savenko, A.V.Borman, V.P.Glazkov, I.N.Goncharenko, V.A.Somenkov, G.F.Syrykh. Experimental Study of the Vibrational Spectrum and Structure Variations in NH_4Cl under High Pressure. High Press. Res., 1995, v.14, pp.55-60.
8. A.M.Balagurov, J.Schreiber, Yu.V.Taran. Calibration of Residual Stress Measurements by Neutron Diffraction. Inter. Conf. *X*-Ray Powder Diffraction Analysis of Real Structure of Matter, Liptovsky Mikulas, Slovakia, 21-25 August 1995.
9. A.M.Balagurov, V.V.Sikolenko, V.G.Simkin, O.E.Parfionov, S.Sh.Shilshtein. Neutron Diffraction Study of $YBa_2Cu_{2.7}Zn_{0.3}O_{6+y}$ Isotope Enriched Samples. JINR, P14-95-465, Dubna, 1995 (in Russian). (Accepted for Physica C).
10. A.M.Balagurov. High-T_c Superconductor Studies by Means of High-Resolution and High-Intensity Neutron Diffraction at the IBR-2 Pulsed Reactor. EPDIC-IV, Chester, 10-15 July 1995.
11. A.M.Balagurov. Neutron Diffraction. Lecture at the VII School on Neutron Physics, Ratmino, September 1995, Dubna, v.1, p.257.
12. A.M.Balagurov. Peculiarities of Structural Studies by the Neutron Diffraction Method. Workshop on Synchrotron and Neutron Studies of Condensed Matter, Dubna, 22-24 August 1995.
13. A.I.Beskrovnyi, V.A.Sarin, E.E.Rider. Neutron Investigation of ZrO_2-Y_2O_3 Single Crystals. ECM-16, Lund, Sweden, 6-11 August 1995.
14. V.Yu.Bezzabotnov, V.V.Nietz, S.A.Oleynik. Nonliner Periodic Waves and Solitons in Uniaxial Antiferromagnets at Spin-Flop Transition. Communications of JINR, P17-95-87, Dubna, 1995 (in Russian).
15. G.D.Bokuchava, E.Schneider, J.Schreiber, Y.Taran, K.Herold, W.Theiner. On the Calibration of Magnetic and Ultrasonic Methods of Residual Stress Measurements in Cold Rolled Iron-Disks by Neutron Diffraction Technique. 7th Inter. Symp. on Nondestructive Characterization of Materials, Prague, Czech Republic, 19-22 June 1995.
16. S.A.Buyko, D.Georgiev, K.Krezhov, V.V.Nietz, G.Pasazhov. Induced Antiferromagnetism in $HoFeO_3$. Journal of Physics: Condensed Matter, 1995, v.7, pp.8099-8107.
17. E.V.Colla, E.Yu.Koroleva, Yu.A.Kunzerov, B.N.Savenko, S.B.Vakhrushev. Ferroelectrics Phase Transition in Materials Embedded in Porous Media. Ferroelectrics Letters (in press).

18. D.Georgiev, K.Krezhov, V.V.Nietz. Weak Antiferromagnetism in $YFeO_3$ and $HoFeO_3$. Solid State Communications, 1995, v.96, p.535.

19. D.Georgiev, V.V.Nietz, T.B.Petukhova, A.P.Sirotin, G.A.Varenik, A.A.Yakovlev. Spectrometer for Neutron Studies of Condensed Matter with a Pulsed Magnetic Field. (Submitted to Journal of Neutron Research).

20. D.Georgiev, V.V.Nietz. Observation of Hysteresis at Spin-Flop Transition Induced by a Pulsed Magnetic Field. Communications of JINR, P14-94-429, Dubna, 1994 (in Russian). (Submitted to Journal of Magnetism and Magnetic Materials).

21. J.Heinitz, A.S.Kirilov. A Software Complex for Neutron Time-of-Flight Measurements by Means of a VME Based Accumulation, Control and Supervising System. Communications of JINR, D13-95-462, Dubna, 1995.

22. T.I.Ivankina, A.N.Nikitin, K.Ullemeyer. The Reconstruction of the Geodynamic State of Rock in the Lithosphere by Means of Texture Analysis. Journal of Earthquake Prediction Research, 1995, v.4.

23. A.N.Ivanov, D.F.Litvin, B.N.Savenko, L.S.Smirnov, V.I.Voronin, A.E.Teplykh. High Pressure Cell for Neutron Diffraction Investigations. High Pressure Research, 1995, v.14, pp. 209-214.

24. A.N.Ivanov, N.A.Nikolaev, N.V.Pashkin, B.N.Savenko, L.S.Smirnov, Yu.V.Taran. Ceramic High Pressure Cell with Profiled Anvils for Neutron Diffraction Investigations (up to 7Gpa). High Pressure Research, 1995, v.14, pp.203-208.

25. G.Klose, A.Islamov, B.Koenig, V.Cherezov. Structure of Mixed Multilayers of Palmitoyolphosphatidylcholine and Oligooxyethelene Glycol Monododecyl Ether Determined by X-Ray and Neutron Diffraction. Langmuir, 1995 (in press).

26. G.Klose, St.Eisenblaetter, J.Galle, A.Islamov, U.Dietrich. Hydration and Structural Properties of a Homologous Series of Nonionic Alkyl Oligo (Ethelene Oxide) Surfactants. Langmuir, 1995, v.11, pp.2889-2892.

27. Yu.A.Kumzerov, A.A.Naberezhnov, B.N.Savenko, S.B.Vakhrushev. Freezing and Melting of Mercury in Porous Glass. Phys.Rev.B, 1995, v.52, pp.4772-4774.

28. I.S.Lyubutin, S.T.Lin, C.M.Lin, K.V.Frolov, T.V.Dmitrieva, A.M.Balagurov, F.Bouree, I.Mirebeau. Comparative Mossbauer Spectroscopy and Neutron Diffraction Analysis in $YBa_2(Cu_{1-x}Fe_x)_3O_y$. I. Structural Transitions. Physica C, 1995, v.248, pp.222-234.

29. I.S.Lyubutin, S.T.Lin, C.M.Lin, K.V.Frolov, T.V.Dmitrieva, A.M.Balagurov, F.Bouree, I.Mirebeau. Comparative Mossbauer Spectroscopy and Neutron Diffraction Analysis in $YBa_2(Cu_{1-x}Fe_x)_3O_y$. II Magnetic Transitions. Physica C, 1995, v.248, pp.235-246.

30. G.M.Mironova, A.M.Balagurov, H.Fuess. Time-Resolved Neutron Scattering Study of Copper Oxidation. ECM-16, Lund, Sweden, 6-11 August 1995.

31. G.M.Mironova. Phase Transition Shifting in HTSC by Thermal Shock. 3rd French-Russian Seminar, Col de Porte, Grenoble, 23-28 March 1995.

32. V.V.Nietz, S.A.Oleynik. Nonliner Periodic Waves and Solitons - Equilibrium Germs of a New Phase in Ferromagnets at the First Order Phase Transition. Communications of JINR, P17-95-88, Dubna, 1995 (in Russian).

33. V.V.Nietz. Supercritical Point on Hematite Phase Diagram in External Magnetic Field. (Submitted to Journal of Magnetism and Magnetic Materials).

34. A.N.Nikitin, T.I.Ivankina. On the Possible Mechanisms of the Formation of Piezoelectric Active Rocks with Crystallographic Textures. Textures and Microstructures, 1995, v.6, pp.1-11.

35. A.N.Nikitin, W.A.Sukhoparov, J.Heinitz, K.Walther. Investigation of Texture Formation in Geomaterials by Neutron Diffraction with High Pressure Chambers. High Pressure Research, 1995, v.14, pp.155-162.

36. F.Prokert, B.N.Savenko, A.M.Balagurov. Neutron Diffraction Study of Phase Transitions in Mixed Crystal $Sr_{0.7}Ba_{0.3}Nb_2O_6$ between 20 and 300 K. Ferroelectrics (in press).

37. F.Prokert, B.N.Savenko, A.M.Balagurov. Thermal Diffuse Scattering in Time-of-Flight Neutron Studies on SBN and TSCC Single Crystals. Acta Cryst., 1995, v.A51, pp.124-129.

38. S.Siegesmund, K.Ullemeyer, M.Dahms. Control of Magnetic Rock Fabrics by Mica Preferred Orientation: a Quantitative Approach. J.Struct.Geol., 1995, v.17, pp.1601-1614.

39. G.A.Sobolev, S.M.Kireenkova, G.A.Efimova, A.N.Nikitin, N.G.Panajotova. Study of Geomaterials Structure for Substantiation of Earthquake Physics. High Pressure Research, 1995, v.14, pp.163-173.

40. Yu.V.Taran, J.Schreiber, P.Mikula, P.Lukas, M.Vrana, G.D.Bokuchava, H.Kockelmann. Neutron Diffraction Measurements of Residual Stresses in an Austenitic Steel Tube with a Welded Ferritic Cover. Inter. Workshop Neutron Scattering Applications, Prague, Czech Republic, 4-6 October 1995.

41. S.B.Vakhrushev, A.A.Naberezhnov, N.M.Okuneva, B.N.Savenko. Determination of Polarisation Vectors in PMN. FTT, 1995, v.37, pp.65-73.

42. K.Walther, J.Heinitz, K.Ullemeyer, M.Betzl, H.-R.Wenk. Time of Flight Texture Analysis of Limeston Standard: Dubna Results. J.Appl.Cryst., 1995, v.28, pp.503-507.

Small-Angle Scattering

1. L.A.Bulavin, V.M.Garamus, T.V.Karmazina, S.P.Shtanko. Micellar Solutions of Triton X-100. Small-Angle Neutron Scattering Data. Colloid J. Russ.Acad.Sci.-Engl., 1995, v.57, pp.902-905.

2. L.A.Bulavin, V.M.Garamus, Yu.M.Ostanevich. Study of Micellar Solutions of Ethoxylated Diisononylphenol by Small-Angle Neutron Scattering. Colloids and Surfaces, 1995, v.94, pp.53-57.

3. V.I.Gordeliy, M.A.Kiselev. The Definition of Lipid Membranes Structural Parameters from Neutronographic Experiments with the Help of Strip Function Model. Biophys. J., 1995, v.69, pp.1424-1428.

4. V.I.Gordeliy, V.Cherezov, A.D.Tugan-Baranovskaya, L.S.Yagujinskiy. Investigation of the Structure of Thylakoid Membranes (Spinach) by Means of Small-Angle Neutron Scattering (accepted in Biochemistry and Molecular Biology International). (Accepted for Biological Membranes).

5. V.I.Gordeliy, V.G.Cherezov, A.V.Anikin, M.V.Anikin, V.V.Chupin, J.Teixeira. Evidence of Entropic Contribution to "Hydration" Forces between Membranes. 1. The Forces between Polymeric Lipid Membranes. (Submitted to Progress in Colloid and Polymer Science).

6. V.I.Gordeliy, V.G.Cherezov, J.Teixeira. Evidence of Entropic Contribution to "Hydration" Forces between Membranes. II. Temperature Dependence of "Hydration" Force. A Small Angle Neutron Scattering Study. (Accepted for J. of Molecular Structure).

7. N.Gorski, J.Kalus, A.I.Kuklin, L.S.Smirnov. SANS-Investigation of the Micelle System *TDMAO-D_2O* at High Hydrostatic Pressure. Deutsche Neutronenstreutagung'95, Reinstorf/Luhenberg, 18-21 September 1995, p.86.

8. N.I.Gorski, A.N.Ivanov, A.I.Kuklin, L.S.Smirnov. Small-Angle Neutron Scattering Setup for High Pressure Measurements at IBR-2. High Press.Res., 1995, v.14, pp.215-220.

9. A.Islamov, V.Cherezov, S.S.Funari, G.Klose, F.Frisius, G.Lantzsch. Small-Angle Neutron Scattering Studies of Lipid/Nonionic Surfactant Mixtures. (Submitted to Langmuir, 1995).

10. I.N.Serdyuk. Small-Angle Neutron Instrument YuMO (JINR, Dubna): Some New Results and Perspectives. Physica B, Condensed Matter, 1995, v.212-213, pp.892-984.

11. I.Serdyuk. Novel Tendencies in Developing Small-Angle Neutron Scattering Methods for Studying the Structure of Biological Macromolecules. ICANS-XIII, Villigen, 10-13 October 1995. PSI Proc. 95-02, pp.118-122.

Inelastic Neutron Scattering

1. N.D.Afanasiev, V.G.Gavriliuk, S.P.Efimenko, V.V.Sumin. Investigation of Nitrogen and Carbon Effect Lattice Dynamics in Austenic Steels. Mat. Sci. and Engineering, 1995, v.31, pp.145-150.

2. R.Baddour-Hadjean, F.Fillaux, S.Belushkin, I.Natkaniec, L.Desgranges, D.Grebille. Inelastic Neutron Scattering Study of Proton Dynamics in *$Ca(OH)_2$* at 20 K. Chemical Physics, 1995, v.197, pp.81-90.

3. O.A.Bannjuch, K.B.Povarova, V.V.Sumin, N.K.Kazanskaja, N.V.Fadeeva, M.D.Bespalova. Neutron Diffraction Studies of Atomic Ordering in *NiAl-FeAl* and *NiAl-CoAl* Quasi-Binary Systems. Izvestiya Russ.Acad. of Sci. "Metally", 1995, No.3, pp.81-85 (in Russian).

4. N.B.Blagoveshchenskii, I.V.Bogoyavlenskii, L.V.Karnatsevish, Z.A.Kozlov, V.G.Kolobrodov, V.B.Priezzhev, A.V.Puchkov, A.N.Skomorokhov, V.S.Yarunin. Structure of Liquid *He-4* Excitation Spectrum. Phys.Rev.B, 1994, v.50, p.16550.

5. L.Bobrowicz, K.Holderna-Natkaniec, M.Mroz, I.Natkaniec, W.Nawrocik. Neutron Scattering Studies of Phase Transitions in Protonated and Deuterated Ammonium Hydrogen Sulphate. Ferroelectrics, 1995, v.167, pp.125-128.

6. L.Bobrowicz, I.Natkaniec, T.Sarga, S.I.Bragin. Neutron Scattering Studies of Pressure Induced Phase Transitionsin NH_4HSO_4. High Pressure Research, 1995, v.14, pp.61-65.

7. L.Bobrowicz, K.Holderna-Natkaniec, M.Mroz, I.Natkaniec, W.Nawrocik. Structural Phase Transitions and Molecular Dynamics in NH_4HSO_4. X Polish Conference of "Molecular Crystals '95", Poznan, Poland, 3-6 September 1995.

8. C.Cachet, A.Belushkin, I.Natkaniec, A.Lecerf, F.Fillaux, L.T.Yu. Characterization with Inelastic Neutron Scattering of Various Protonic Species in Manganese Dioxides. Physica B, 1995, v.213&214, pp.827-829.

9. M.Dorr, J.Kalus, M.Monkenbush, I.Natkaniec, U.Schmelzer. The Lattice Dynamics of a Polar Disordered Crystal of 2,3-Dimethylanthracene. Phonons 95, Sapporo, Japan, 24-28 July 1995.

10. V.G.Gavriliuk, S.P.Efimenko, S.A.Danilkin, V.P.Minaev, V.V.Sumin. Study of the Influence of Nitrogen, Carbon and Metal Components on the Interatomic Interactions in Austenite by Inelastic Neutron Scattering. Izvestiya Russ.Acad. of Sci. "Metally", 1995, No.3, pp.200-204 (in Russian).

11. V.G.Gavriluk, S.A.Danilkin, S.P.Efimenko, G.G.Lishkevich, V.P.Minaev, V.M.Nadutov, V.V.Sumin. Study of Effect of Nitrogen, Carbon and Metallic Components on Atomic Interaction in Steels Using Inelastic Neutron Scattering. Izvestiya Russ.Acad. of Sci. "Metally", 1995, No.5, pp.51-54 (in Russian).

12. K.Holderna-Natkaniec, I.Natkaniec, S.Habrylo. Hydrostatic Pressure and Temperature Dependence Study of d-Camphor and dl-Borneol by Neutron Scattering. High Pressure Research, 1995, v.14, pp.73-80.

13. K.Holderna-Natkaniec, I.Natkaniec, J.Wasicki. Structural Phase Transition and Molecular Structure in Bornyl Chloride. Journal of Molecular Structure, 1996, v.374 (special issue), p.155.

14. J.Kalus, M.Monkenbusch, I.Natkaniec, M.Prager, J.Wolfrum, F.Worlen. Neutron and Raman Scattering Studies of the Lattice and Methyl-Group Dynamics in Solid *p*-Xylene. Mol.Cryst.Liq.Cryst., 1995, v.268, pp.1-20.

15. V.Yu.Kazimirov, A.V.Belushkin. Inelastic Neutron Scattering Spectrometer for the IN-06 Neutron Source at the Moscow Meson Factory. Proc. ICANS-XIII, Villigen Oct.11-14, 1995, vol.I, pp.155-163.

16. A.I.Kolesnikov, V.E.Antonov, A.M.Balagurov, S.Bennington, M.Prager, J.Tomkinson. Neutron Scattering Studies of Ordered *PdCuH* and *PdAgH* Prepared under High Hydrogen Pressure. High Press. Res., 1995, v.14, pp.81-89.

17. A.I.Kolesnikov, V.V.Sinitsyn, O.I.Barkalov, E.G.Ponyatovskii, V.K.Fedotov, A.M.Balagurov, G.M.Mironova, I.Natkaniec, L.S.Smirnov. Neutron Scattering Studies of Structural Transformations and Vibrational Spectra of Ice after High Pressure Treatment. High Press. Res., 1995, v.14, pp.101-109.

18. A.I.Kolesnikov, V.V.Sinitsyn, E.G.Ponyatovsky, I.Natkaniec, L.S.Smirnov. Similarity of Vibrational Spectra of High-Density Amorphous Ice and High-Pressure Phase Ice VI. Physica B, 1995, v.213&214, pp.474-476.

19. A.Yu.Muzychka. Contribution of Mixing Interaction to Crystal Field in $RE\text{-}TR_2Sr_2$ Compounds. 3rd French-Russian Electronic Systems, Grenoble, Col de Port, March 23-28 1995, XIII Meeting on Using Neutrons in Solid States Physics, Zelenogorsk, 20-22 June, 1995.

20. I.Natkaniec, A.V.Belushkin, L.S.Smirnov, A.I.Solov'ev. The Study of Ammonium Dynamics in the Orthorhombic Phase of $K_{1-x}(NH_4)_xSCN$ at $x<0.15$. XIV Russian Conference on Physics of Ferroelectrics, Ivanovo, Russia, 1995.

21. I.Natkaniec, L.S.Smirnov, S.I.Bragin, A.I.Solov'ev. Ammonium Dynamics in the $K_{1-x}(NH_4)_xI$ Solid Solutions. XIII Workshop on Neutron Application in Solid State Physics, Zelenogorsk, Russia, 1995.

22. I.Natkniec, L.S.Smirnov, A.I.Kolesnikov, A.I.Ivanov. Neutron Spectroscopy of Ice III. High Pressure Science and Technology, Warszawa, 1995.

23. I.Natkaniec, L.S.Smirnov, A.I.Solov'ev. Ammonium Dynamics in the Ordered and Disordered Phases of $K_{1-x}(NH_4)_xSCN$ Solid Solutions. Physica B, 1995, v.213&214, pp.667-668.

24. I.Natkaniec, A.V.Puchkov. Neutron Spectrometry at the IBR-2 Pulsed Reactor. Proc. 2nd International Seminar PANS-II, JINR, Dubna, 1995, pp.31-43.

25. A.Pawlukojc, L.Bobrowicz, I.Natkaniec, J.Leciejewicz. The IINS Spectroscopy of Amino Acids: l- and dl-Valine. Spectrochimica Acta, 1995, v.51A, pp.303-308.

26. S.N.Rapeanu, I.Padureanu, Zh.A.Kozlov, V.A.SemenovA.G.Novikov, Gh.Rotarescu. Structure and Dynamics in Solid and Liquids by Neutron Scattering. Rom.Journ.Phys., 1994, v.39, pp.695-721.

27. L.S.Smirnov, I.Natkaniec, Yu.A.Shadrin, A.I.Solov'ev. Neutron Diffraction Studies of Lattice Parameters and the Phase Diagram of $K_{1-x}(NH_4)_xSCN$ Solid Solution. Acta Physica Hungarica, 1994, v.75, pp.275-278.

28. V.V.Sumin. Inelastic Neutron Scattering Study of Interstitial Atoms in Titanium. Eighth World Conference on Titanium, Birmingham, UK, 1995, p.P2/9.

Reflectometry, Polarized Neutrons

1. V.L.Aksenov, E.B.Dokukin, V.K.Ignatovich, S.V.Kozhevnikov, E.I.Kornilov, Yu.V.Nikitenko, A.V.Petrenko, Yu.V.Bugoslavskij, A.A.Minakov. Anamalous Dependence of Neutron Depolarization on Magnetic Field in $YBa_2Cu_3O_{6.9}$ Ceramics Near T_c. Pis'ma v ZhETF, 1995, v.61, N4, pp.294-298 (in Russian).

2. V.L.Aksenov, E.B.Dokukin, Yu.V.Nikitenko. Neutron Depolarization Investigation of High-Temperature Superconductors in the Mixed State. Physica B, Condensed Matter, 1995, v.213&214, pp.100-106.

3. V.L.Aksenov, E.B.Dokukin, S.V.Kozhevnikov, Yu.V.Nikitenko, A.V.Petrenko. The Behavior of a Type-II Superconductor *Nb* in a Magnetic Field as Investigated in Polarized-Neutron Transmission Experiments. Physica B, 1995, v.213&214, pp.134-135.

4. V.L.Aksenov, Yu.V.Nikitenko. Time Collimation for Elastic Neutron Scattering at a Pulsed Sourse. ICANS XIII-Meeting, 11-14 October 1995. PSI Proc. 95-02, 165-174.

5. V.I.Bodnarchuk, L.S.Davtyan, D.A.Korneev. The Effects of Geometric Phase in Neutron Optics. Communications of JINR, P3-95-164, Dubna, 1995 (in Russian).

6. D.A.Korneev. Fourier Analysis of Space-Periodic Magnetic Configuration Using Resonance Depolarization of Polarized Neutron. Physica B, 1995, v.213&214, pp.996-998.

7 D.A.Korneev, V.I.Bodnarchuk, L.S.Davtyan. Observation of Nonadiabatic Geometrical Effects in Time-of-Flight Experiment with Polarized Neutrons. Physica B, 1995, v.213&214, pp.993-995.

8 D.A.Korneev, N.V.Chernenko, L.P.Chernenko. Computer Simulation of Neutron Depolarization Process. Physica B, 1995, v.213&214, pp.999-1001.

9. D.Korneev, Y.Lvov, G.Decher, J.Schmitt, S.Yaradaikin. Neutron Reflectivity Analysis of Self-Assembled Film Superlattices with Alternate Layers of Deuterated and Hydrogenated Polysterensulfonate and Polyallylamine. Physica B, 1995, v.213&214, pp.954-956.

Accelerated Ions

1 A.D.Bozhko, A.P.Kobzev, D.A.Korneev, L.P.Chernenko, D.M.Shirokov. Full Depth Profiling of Diamond-Like Films. XXV International Conference on Physics of Interaction between Charged Particles and Crystals, Moscow, 29-31 May 1995 (in Russian).

2 T.Czyzewski, L.Glowacka, M.Jaskola, J.Braziewicz, M.Pajek, J.Semaniak, M.Haller, R.Karschnick, W.Kretschmer, A.P.Kobzev, D.Trautmann. M-Shell. *X*-Ray Production by *C*, *N* and *O* Ions. 7th International Conference on Particle-Induced *X*-Ray Emission and its Analytical Applications (PIXE-7), Padua, Italy, 26-30 May 1995, Nuclear Instruments and Methods in Physics Research B.

3. K.Frolich, J.Souc, D.Machajdik, A.P.Kobzev, F.Weiss, J.P.Senateur, K.H.Dahmen. Properties of thin Epitaxial Aerosol MOCVD CeO_2 Films Grown on (1102) Sapphire. Journal de Physique IV, 1995, v.5, pp.533-540.
4. L.Hrubcin, J.Huran, R.Sandrik. A.P.Kobzev, D.M.Shirokov. Application of the ERD Method for Hydrogen Determination in Silicon (Oxy)Nitride Thin Films Prepared by ECR Plasma Deposition. Nuclear Instruments and Methods in Physics Research B, 1994, v.85, pp.60-62.
5. D.Machajdik, K.Frolich, A.P.Kobzev, F.Weiss. *X*-Ray and RBS Study of the Thin $SrTiO_3$ Film Deposited on *(100) MgO* Monocrystal Substrate. Size-Strain '95 International Conference, Liptovsky Mikulas, Slovakia, 21-25 August 1995.
6. D.Machajdik, K.Frolich, F.Weiss, A.P.Kobzev. Texture Analysis of the *YBCO* Thin Films Reveals Twinning in the *YBCO* Crystallites. EPDIC IV, Chester, England, 10-14 July 1995.
7. J.Semaniak, J.Braziewicz, T.Czyzewski, L.Glowacka, M.Haller, M.Jaskola, R.Karschnick, A.P.Kobzev, M.Pajek, W.Kretschmer, D.Traytmann. *L*-Subshell Ionization by ^{14}N Ions. Nuclear Instruments and Methods in Physics Research B86, 1994, pp.185-189.

Theory

1. V.L.Aksenov, Yu.A.Ossipyan, V.S.Shakhmatov. Phase Transition in AC_{60} *(A=K,Rb)* Fulleride Crystals. Pis'ma v ZhETF, 1995, v.62, N5, pp.417-421 (in Russian).
2. A.S.Alexandrov, V.V.Kabanov. Excitonic Polaron in the Photoemission Spectra of C_{60}^- and the Origin of High-T_c Superconductivity of Doped Fullerenes. Pis'ma v ZhETF, 1995, v.62, N12, p.920 (in Russian).
3. B.Chesca. On the Theory of the RF Pumped Double SQUID. Physica C, 1995, v.241, pp.123-136.
4. B.Chesca. A Thermal Activation Model for Intrinsic Noise in RF Pumped Double SQUIDs. (Accepted for Physica C).
5. V.V.Kabanov and D.K.Ray. Temperature Dependence of Optical Conductivity in High-T_c Oxides. Phys.Rev.B, 1995, v.52, pp.13021-13024.
6. A.A.Skoblin. Resonance Phenomenon as a Transmutation of the Quasienergy Spectrum. JINR Communications, 1994, E4-94-426.
7. A.A.Skoblin, Neutron Scattering by a Film Containing a Rotating Magnetic Field. JINR Communications, 1994, E14-94-470.
8. A.A.Skoblin. Non-Resonant Precession of the Neutron Magnetic Moment in Antiferromagnets. Communications of JINR, 1995, E4-95-534.

NEUTRON NUCLEAR PHYSICS

Experiment

1. A.Aleaksejevs, S.Barkanova, J.Tambergs, W.Waschkowski, G.S.Samosvat. Evaluation of Neutron Fundamental Parameters from Total Cross Section Data in the Framework of Optical Model. ISINN-3: Neutron Spectroscopy, Nuclear Structure, Related Topics, JINR, E3-95-307, Dubna, 1995, p.252.
2. M.A.Ali, E.V.Vasilieva, A.V.Voinov, O.D.Kestarova, A.M.Sukhovoj, V.A.Khitrov, Yu.V.Kholnov. Cascade γ-Decay of the ^{196}Pt Compound State Excited Following Thermal Neutron Capture in ^{195}Pt. Izv. RAN, ser.fiz., 58 (11) 1994, 152 (in Russian).
3. M.A.Ali, V.A.Khitrov, Yu.V.Kholnov, A.M.Sukhovoj, A.V.Vojnov. Properties of the *Gd-158* Compound State Gamma-Decay Cascades. J. Phys. G: Nucl. Part. Phys., 20 (1994) 1943.
4. V.P.Alfimenkov, A.N.Chernikov, L.Lason, Yu.D.Mareev, V.V.Novitsky, L.B.Pikelner, V.R.Skoy and M.I.Tsulaya, Parity Nonconservation Study with Polarized *La* Target., Preprint JINR, E3-95-244, Dubna, 1995.
5. V.P.Alfimenkov, GB.Valsky, A.M.Gagarsky, P.Geltenbort, I.S.Guseva, I.Last, G.A.Petrov, A.K.Petukhov, L.B.Pikelner, Yu.S.Pleva, V.E.Sokolov, W.I.Furman, K.Schrekenbach, O.A.Shcherbakov. Interference Effects in Angular Distributions of Fission Fragments from the Resonance and Thermal Neutron Induced Fission of Heavy Nuclei. Yad.Fiz., 58 (5), 1995, 799-807 (in Russian).

6. H.Beer, P.V.Sedyshev, Yu.P.Popov, H.Oberhummer, W.Balogh, H.Herndl. Cross Sections of $^{36}S(n,\gamma)^{37}S$. IK-TUW-Preprint 9510401, Wien, 1995.
7. H.Beer, F.Käppeler, J.Meißner, M.Wiescher, H.M.Schatz, P.V.Sedyshev, Yu.P.Popov. Measurement of Neutron Capture Cross Section by Fust Cyclic Activation Technique. In: Proc. Int. Conf. on Nucl. Data for Science and Technology, Gaithlinburg, TN, 1994, ed. J.K.Dickens, (American Nuclear Society 700205), v.2, p.1052.
8. A.A.Bogdzel, W.I.Furman, Yu.N.Kopach, A.B.Popov, N.N.Gonin, M.A.Guseinov, L.K.Kozlovsky, D.I.Tambovzev, J.Kliman, H.Postma. Measurement of Energy Dependence of Fission Fragment Angle Anisotropy for Resonance Neutron Induced Fission of ^{235}U Aligned Target. Proc. of XIII Meeting on Physics of Nuclear Fission in the Memory of Prof. Smirenkin, Obninsk, 3-6 October, 1995.
9. S.T.Boneva, V.A.Khitrov, A.M.Sukhovoj, A.V.Vojnov. Excitation Study of High-Lying States of Differently Shaped Heavy Nuclei by the Method of Two-Step Cascades. Nucl. Phys., A589 (1995) 293.
10. V.A.Bondarenko, I.L.Kuvaga, P.T.Prokofjev, A.M.Sukhovoj, V.A.Khitrov, Yu.P.Popov, S.Brant, V.Paar, Levels of ^{137}Ba Studied with Neutron Induced Reactions. Nucl. Phys., A582 (1995) 1.
11. V.A.Bondarenko, I.L.Kuvaga, P.T.Prokofjev, A.M.Sukhovoj, V.A.Khitrov, Yu.P.Popov, S.Brant, V.Paar, Lj. Simicic, Particle-Hole States in ^{138}Ba. Nucl. Phys., A584 (1995) 279.
12. S.B.Borzakov, E.Dermendjiev, Yu.S.Zamyatnin, S.S.Pavlov, B.M.Nazarov, A.D.Rogov, I.Ruskov. The Instrument for Investigating Delay Neutrons and the Preliminary Results of the Determination of the β_{eff} Value for ^{233}U Relative to ^{235}U. Atomn.Energ., 1995, v.79, issue 3, p. 231 (in Russian).
13. S.B. Borzakov, E.Dermendjiev, V.Yu.Konovalov, Tz.Panteleev, I.Ruskov, Yu.S.Zamyatnin. Yields of Delayed Neutrons for the Thermal and Cold Neutron Induced Fission of the ^{233}U, ^{235}U, ^{239}Pu. XIII Meeting on Physics of Nuclear Fission in the Memory of Prof. G.N. Smirenkin, Obninsk, 3-6 October, 1995.
14. S.B. Borzakov, E.Dermendjiev, A.A.Goverdovsky, V.Yu.Konovalov, I.Ruskov, Yu.S.Zamyatnin. Fission γ-Ray Emission at Subthreshold Fission of ^{237}Np and Search for the $(n,\gamma f)$-process, XIII Meeting on Physics of Nuclear Fission in the Memory of Prof. G.N. Smirenkin, Obninsk, 3-6 October, 1995.
15. J.D.Bowman, L.Y.Lowie, G.E.Mitchell, E.I.Sharapov. Extraction of Parity Violating Matrix Elements from Data on Neutron Resonances. ISINN-3: Neutron Spectroscopy, Nuclear Structure, Related Topics, 1995, JINR, E3-95-307, Dubna 1995, p.57.
16. J.D.Bowman, C.M.Frankle, A.A.Green, J.N.Knudson, S.I.Penttila, S.J.Seestrom, Yi-Fen Yen, V.W.Yuan, B.E.Crawford, N.R.Roberson, C.R.Gould, D.G.Haase, L.Y.Lowie, G.E.Mitchell, S.I.Stephenson, P.P.J.Delheij, E.I. Sharapov, H.Postma, Y.Masuda, H.M.Shimizu, M.Iinuma, A.Masaike, Y.Matsuda, K.Fukuda. Parity Violation in Nuclear Compound States. Chinese Journal of Physics, 32, 989 (1995).
D. Budnik A, G.A. Ososkov, Yu. N. Pokotilovski, A.D. Rogov. Monte Carlo Calculation of Slow Neutron Background in the n-n Scattering Experiment at the Pulse Reactor BIGR. JINR Comm., E3-95-351, Dubna, 1995.
18. G.G.Bunatyan. "Nucleon and Meson Properties in Hot and Dense Hadronic Matter". In: Proc. INPC'95 (Inter. Nucl. Phys. Conf.), 21-26 Aug. 1995, Beijing,. Book of Abstr., p. 2-32.
19. G.F.Gareeva, Al.Yu.Muzychka, Yu.N.Pokotilovski. Monte Carlo Simulation of Nonstationary Transport and Storage of UCN in Horizontal Neutron Guides and the Storage of UCN. JINR Preprint, E3-95-106, Dubna, 1995.
20. R.Georgii, P. von Neunan-Cosel, T.von Egidy, M.Grinberg, V.A.Khitrov, J.Ott, P.Prokofjevs, A.Richter, W.Schauer, C.Schlegel, R.Schulz, L.J.Simonova, Ch. Stoyanov, A.M.Sukhovoj, A.V.Vojnov. Unusual Neutron-Capture Gamma-Rays Cascade in ^{124}Te: A Fingerprint of Octupole-Coupled Multiphonon States. Phys. Lett., B351 (1995) 82.
21 R.Georgii, T. von Egidy, J. Klora, H. Lindner, U. Mayerhofer, J. Ott, W. Schauer, P. von Neuman-Cosel, A.Richter, C. Schlegel, R. Schulz, V.A.Khitrov, A.M.Sukhovoj, A.V.Vojnov, J.Berzins, V.Bondarenko, P.Prokofjevs, L.J.Simonova, M.Grinberg, Ch.Stoyanov. Complete Level Scheme of ^{124}Te up to 3 MeV. Nucl. Phys., A592 (1995) 307.
22. Yu.M.Gledenov, V.I.Salatski, P.V.Sedyshev, M.V.Sedysheva, P.E.Koehler, V.A.Vesna, I.S.Okunev. Recent Results of Measurements of the $^{14}N(n,p)^{14}C$, $^{35}Cl(n,p)^{35}S$, $^{36}Cl(n,p)^{36}S$ and $^{36}Cl(n,\alpha)^{33}S$ Reaction Cross Sections. In: Nuclei in the Cosmos III, AIP Conf.Proc. 327, Italy 1994, ed. M.Busso, R.Gallino, C.M.Raiteri, AIP Press, New York, 1995, p.173.
23 Yu.M.Gledenov, G.Khuukhenkhuu, M.V.Sedysheva, Bao Shanglian, Tang Guoyou, Cao Wentian, Qu Decheng, Chen Zemin, Chen Yingtang, Qi Huiquan. Investigation of the Fast Neutron Induced (n,α) Reaction (Experimental Techniques). JINR Communications, E3-95-445, Dubna, 1995.

24. Yu.M.Gledenov, G.Khuukhenkhuu, M.V.Sedysheva, Tang Guoyou, Bao Shanglian, Qu Decheng, Bai Xinhua, Shi Zaomin, Chen Jinxiang, Fan Jihong, Chen Yingtang, Qi Huiquan. Study of the Fast Neutron Induced (n, α) Reactions for ^{40}Ca, ^{58}Ni and ^{64}Zn. In: Neutron Spectroscopy, Nuclear Structure, Related Topics. III-Int. Seminar on Inter. of Neutron with Nuclei. JINR, E3-95-307, 1995, Dubna, p.92.
25. A.A.Goverdovsky, E.Dermendjiev, Yu.S.Zamyatnin, I.Ruskov. The Cross Section of the ^{237}Np Fission Induced by Neutrons with the Energy $En \leq 500$ эВ. Yad. Fiz., 1995, v.58, No 1, p. 27-29 (in Russian).
26. G.P.Georgiev Yu.V.Grigoriev, N.A.Gundorin, N.B.Janeva, H.Stanczyk. "Neutron Resonances in ^{113}In, ^{115}In Investigations ", International Seminar on the Interaction of Neutrons with Nuclei, 26-28 April 1995, JINR, E3-95-307, Dubna, 1995, p.170-177.
27. Yu.V.Grigoriev, G.P.Georgiev, K.Faikov-Stanczyk, G.V.Muradyan, N.B.Janeva. Neutron Resonance Parameters of ^{117}Sn. Preprint PHEI, 2445, Obninsk, 1995 (in Russian).
28. G.P.Georgiev, T.A.Madjarski, N.B.Janeva. "Statistical Analysis of Gamma Multiplicity Experimental Data". International Seminar on the Interaction of Neutrons with Nuclei, 26-28 April 1995, Dubna, Russia. JINR, E3-95-307, Dubna, 1995, p.101-108.
Yu.V.Grigoriev, V.V.Sinitsa, G.P.Georgiev, N.A.Gundorin. "Investigation of Resonance Structure and Temperature Dependence of the Cross Sections for ^{239}Pu", XIII Meeting on Physics of Nuclear Fission in memory of Prof. G.N.Smirenkin, 3-6 October, 1995, Obninsk, Russia.
Yu.V.Grigoryev, V.Sinitsa, G.P.Georgiev, N.A.Gundorin "Investigation of Resonance Structure and Doppler-Effect of Cross-Sections for ^{232}Th, ^{235}U and ^{239}Pu". International Seminar on the Interaction of Neutrons with Nuclei, 26-28 April 1995, Dubna, Russia. JINR, E3-95-307, Dubna, 1995, p.324-329.
31. Yu.V.Grigoriev, V.V.Sinitsa, G.P.Georgiev. Measuring and Calculation of the Doppler Effect in the Transmission and Cross-Sections of ^{232}Th, ^{235}U, *and* ^{239}Pu. Preprint PHEI-2422, Obninsk, 1995 (in Russian).
32. Yu.V.Grigoriev, G.P.Georgiev, N.A.Gundorin, H.Faikow-Stanczyk, N.B.Janeva. Gamma-Radiation in Neutron Resonance of ^{113}In, ^{115}In. Topics in Atomic Science and Technology, Issue 1, Ser. Nuclear Constants, 1995 (in Russian).
33. Yu.V.Grigoriev, G.P.Georgiev, G.V.Muradyan, H.Faikow-Stanczyk, N.B.Janeva. Investigations of Gamma-Multiplicity Spectra for the Neutron Radiative Capture by the Nuclei ^{113}In, ^{115}In". Preprint PHEI-242b, Obninsk, 1995; Topics in Atomic Science and, Issue 1., Ser. Nuclear Constants, 1995 (in Russian).
34. E.Dermendjiev, S.B.Borzakov, V.Yu.Konovalov, I.Ruskov, Yu.S.Zamyatnin. Fluctuation of γ-Ray Yields in ^{237}Np Low Energy Fission Resonances. III International Seminar on Interaction of Neutrons with Nuclei, Dubna, April 26-28, 1995. JINR, E3-95-307, Dubna, 1995, p.63.
35. E.Dermendjiev. The (n,γ f)-Process in the 2nd Minimum of the Two-Bump Fission Barrier for ^{237}Np. JINR Comm., P3-95-469, Dubna, 1995 (in Russian).
36. T.L.Enik, L.V.Mitsyna, V.G.Nikolenko, A.B.Popov, G.S.Samosvat, P.Prokofjevs, A.V.Murzin, W.Waschkowski. Precize Measurements of σ_{tot} for ^{208}Pb. ISINN-3: Neutron Spectroscopy, Nuclear Structure, Related Topics, JINR, E3-95-307, Dubna, 1995, p.238.
37. V.A.Ermakov, P.V.Sedyshev, M.V.Sedysheva, V.G.Tishin, Yu.M.Gledenov. The Multi-Parameter Measurement and Acquisition Module for the Two-Grid Ionization Chamber. JINR Comm., P10-95-438, Dubna, 1995 (in Russian).
38. V.K.Ignatovich. The Optical Potential of Interaction of Neutrons with Condensed Matter. VII International School on Neutron Physics, Book of Lectures, V. 1, P. 156, JINR, Dubna, 1995 (in Russian).
39. V.K.Ignatovich. The Possible Explanation of UCN Anomaly and the Consequences. JINR, P4-95-196, Dubna, 1995 (in Russian).
40. V.K.Ignatovich. The Additional Result on the Neutron Life-Time Extracted from Experiments of UCN Storage. JINR, P3-95-194, Dubna, 1995; JETP Letters, 62, 1, 3, 1995 (in Russian).
41. M.V.Kazarnovski, O.A.Langer, G.K.Matushko, V.I.Matushko, Yu.P.Popov. The New Method for Generation of the Maxwellian Neutron Spectra with Stellar Temperatures. In: Neutron Spectroscopy, Nuclear Structure, Related Topics. III-Int. Seminar on Inter. of Neutron with Nuclei. JINR, E3-95-307, 1995, Dubna, p.199.
42. V.A.Khitrov, A.M.Sukhovoj, The Peculiarities of Transforming the "Order" of Low-Lying Levels to the "Chaos" of Neutron Resonances. In: Measurement, Calculation and Evaluation of Photon Production Data, Bologna, Italy, November 1994 NEA/NSC/DOC(95)1, Ed. C.Coceva, 1995, 69.
43. V.A.Khitrov, Yu.V.Kholnov, A.M.Sukhovoj, A.V.Vojnov, The Possibilities of Experimental Discovery of Multiplets of Low-Lying Levels, ibid., 303.
44. G.Khuukhenkhuu, Yu.M.Gledenov, M.V.Sedysheva, G.Unenbat. The Isotopic Effect in the (n,α) Reaction Induced by Fast Neutrons. In: Neutron Spectroscopy, Nuclear Structure, Related Topics. III-Int. Seminar on Inter. of Neutron with Nuclei. JINR, E3-95-307, 1995, Dubna, p.90.

45. J.N.Knudson, J.D.Bowman, B.E.Crawford, P.P.J.Delheij, C.M.Frankle, C.R.Gould, D.G.Haase, M.Iinuma, L.Y.Lowie, A.Masaike, Y.Masuda, Y.Matsuda, G.E.Mitchell, S.I.Penttila, H.Postma, N.R.Roberson, S.J.Seestrom, E.I.Sharapov, H.M.Shimizu, S.L.Stephenson, Yi-Fen Yen, V.W.Yuan. A High-Rate Detection System to Study Parity Violation with Polarized Epithermal Neutrons at LANSCE. Proceedings of the Workshop "New Tools for Neutron Instrumentaions", Les Houches, France, 6-9 June, 1995; LANL Report LA-UR-95-1865, Los Alamos, 1995.
46. L.Koester, W.Waschkowski, L.V.Mitsyna, G.S.Samosvat, P.Prokofjevs, J.Tambergs. Neutron-Electron Scattering Length and Electric Polarizability of the Neutron Derived from Cross Section of Bismuth and of Lead and Its Isotopes. Phys.Rev.C, 1995, v.51, N6, p.3363-71.
47. S.K.Lamoreaux, V.K.Ignatovich. Tidal Pressure Induced Neutrino Emission as an Energy Dissipation Mechanism in Binary Pulsar Systems. JINR, E3-95-195, Dubna, 1995.
48. Al.Yu. Muzychka, Yu. N. Pokotilovski. Monte Carlo Simulation of Spectral Filters for UCN. JINR Comm., E3-95-282, Dubna, 1995.
49. V.G. Nikolenko, A.B.Popov, G.S.Samosvat, T.Yu.Tretyakova. The Problem of Neutron Charge Radius and Proposals of New Experiments to Estimate the n,e-Amplitude. III Int. Seminar on Interaction of Neutrons with Nuclei. - ISINN-3, Dubna, April 26-28, 1995. JINR, E3-95-307, Dubna, 1995, p.217.
50. A.B.Popov. The Subject and Methods of Neutron Spectroscopy. Proceedings of the VII International School on Neutron Physics, Ratmino, September 3-22, 1995, JINR, Dubna, 1995, p. 59 (in Russian).
51. Yu.P.Popov. Neutron Spectroscopy: Reactions Followed by Charged Particles., ibid., p.77-85.
52. Yu.P.Popov. The Spectrometry of Neutrons by the Slowing-Down Time in Lead. From the "Spectrometer for Poor" (E. Wigner) to Record Fluxes. Particle and Nuclei, 26 (b), 1995, 1503-1523 (in Russian).
53. Yu.P.Popov. Neutron Resonances and Chaos in the, In: Modern Problems of Nuclear Physics (To the 7-th Anniversary of V.G.Soloviev), JINR, D4-95-308, Dubna, 1995, p.204-212 (in Russian).
54. V.A.Pshenichnyi, Yu.M.Gledenov. Proton Decay Probabilities of the Compound Nucleus ^{51}V. JINR Comm., P4-95-309, Dubna, 1995 (in Russian).
55. Yu. N. Pokotilovski - Production and Storage of Ultracold Neutrons at Pulse Neutron Sources with Low Repetition Rates. Nucl. Instr. & Meth. A356 (1995) p. 412-414.
56. G.S.Samosvat. Investigations of p-Wave Neutron Scattering by Nuclei. Phys.Elem.Chastits.At.Yadra, 1995, v.26, N6, p.1567 (in Russian).
57. G.S.Samosvat. Electric Charge Radius and Polarizability of Neutron. VII School on Neutron Physics, Ratmino, 3-22 September 1995. Lectures, v.1, JINR, E3,14-95-323, Dubna 1995, p.49 (in Russian).
58. E.I.Sharapov, J.D.Bowman, B.E.Crawford, P.P.J.Delheij, C.M.Frankle, K.Fukuda, C.R.Gould, A.A.Green, D.G.Haase, M.Iinuma, J.N.Knudson, L.Y.Lowie, A.Masaike, Y.Masuda, Y.Matsuda, G.E.Mitchell, S.I.Penttila, Yu.P.Popov, H.Postma, N.R.Roberson, S.J.Seestrom, H.M.Shimizu, S.L.Stephenson, Yi-Fen Yen, V.W.Yuan. Parity Violation in the Compound Nucleus. ISINN-3: Neutron Spectroscopy, Nuclear Structure, Related Topics, 1995, JINR, E3-95-307, Dubna, 1995, p.27.
59. E.I.Sharapov, J.D.Bowman, B.E.Crawford, P.P.J.Delheij, C.M.Frankle, K.Fukuda, C.R.Gould, A.A.Green, D.G.Haase, M.Iinuma, J.N.Knudson, L.Y.Lowie, A.Masaike, Y.Masuda, Y.Matsuda, G.E.Mitchell, S.I.Penttila, Yu.P.Popov, H.Postma, N.R.Roberson, S.J.Seestrom, H.M.Shimizu, S.L.Stephenson, Yi-Fen Yen, V.W.Yuan. Parity Violation in Neutron Resonances: the TRIPLE Collaboration Recent Results. LEND-95: Low Energy Nuclear Dynamics, April 18-22, 1995, St.Petersburg, to be published by World Scientific, Singapore.

E.I.Sharapov, C.M.Frankle. Neutron Depolarization in Aligned Holmium and Tests of Time-Reversal Invariance. Phys. Rev., B51, 5875 (1995).

61 A.M.Sukhovoj. Cascade Gamma-Decay of Neutron Resonances: Hypotheses and Experiment. In: VII School on Neutron Physics, Ratmino, September 1995, Dubna 1995, v. 1, 88.

62. A.M.Sukhovoj. From the "Order" of the Low-Lying Levels to the "Chaos" of Neutron Resonances: Experiment. In: Proc. of the IV Inter. Conf. on Selected Topics in Nuclear Structure, Dubna, July 1994, Ed. V.G.Soloviev, JINR, E4-94-371, Dubna, 1994, p.329.

V.N.Shvetsov. Gas Neutron Detectors. VII International School on Neutron Physics, Book of Lectures, V. p. 120, Dubna, JINR, 1995 (in Russian).

64 V.N.Shvetsov. Ultracold Neutrons and Fundamental Physics Problems. VII International School on Neutron Physics, Book of Lectures, V.1, p. 216, Dubna, JINR, 1995 (in Russian).

65. E.V.Vasilieva, A.V.Voinov, A.M.Sukhovoj, V.A.Khitrov, Yu.V.Kholnov. Two-Quantum Decay Cascades of the ^{192}Ir Compound Nucleus Excited on Thermal Neutron Capture. Izv. RAN, Ser.Fiz., 59 (11) (1995) 99.
66. E.V.Vasilieva, A.V.Voinov, A.M.Sukhovoj, V.A.Khitrov, Yu.V.Kholnov. Investigations of the Scheme of the γ-Decay $^{146}Eu \rightarrow ^{146}Sm$ by the Method of γ-γ Coincidences and Summing of Coinciding Pulse Amplitudes.

Izv. RAN, Ser. Fiz., 59 (11) (1995) 21 (In Russian).
67. E.V.Vasilieva, A.V.Voinov, A.M.Sukhovoj, V.A.Khitrov, Yu.V.Kholnov. The Cascade γ-Decay of the Compound State ^{160}Tb. Izv. RAN, Ser. Fiz., 59 (11) (1995) 11 (in Russian).
E.V.Vasilieva, A.V.Voinov, O.D.Kestarova, Yu.P.Popov, A.M.Sukhovoj, V.A.Khitrov, Yu.V.Kholnov. The Cascade γ-Decay of the ^{124}Te Compound State Excited by Thermal Neutron. Izv. RAN, ser.fiz., (11) (1994) 160 (in Russian).
69. A.V.Voinov. On Possible Equidistance of Some Groups of Levels in Deformed Nuclei at Excitation Energies up to 5 MeV. In: Perspectives for the Interacting Boson Model on the Occasion of its 20th Aniversary, Padova, Italy, 13-17 June, 1994, Ed. R.F.Casten et al, World Scientific, 1994.

Theory

70. A.L.Barabanov, W.I.Furman. Theory of the Resonance Neutron Induced Fission. General Formalism for Differential Fission Cross Section. In XIII Meeting on Physics of Nuclear Fission in the Memory of Prof. G.N. Smirenkin, Obninsk, 3-6 October, 1995.
71. V.B.Belyaev, M.Decker, H.Fiedeldey, S.A.Rakityansky, W.Sandhas, S.A.Sofianos, Muonic Molecules of Charge $Z \geq 3$: Coulombic Properties and Nuclear Transitions. Nucleonica, 40(2), 1995, pp. 3-24.
72. V.B.Belyaev, S.A.Rakityansky, S.A.Sofianos, M.Braun, W.Sandhas, Interaction of Eta-Meson with Light Nuclei. Few Body Systems Suppl., 8, 1995, p.312.
73. V.K.Ignatovich. Enigmatic Neutrons. Some Trends in the Development of Quantum Mechanics. Proceedings of the Workshop: Present Status of Quantum Theory of Light. 27-30 August 1995. York University, Toronto, Canada.
74. V.K.Ignatovich. The Optical Potential of Interaction of Neutrons and Condensed Matter. VII International School on Neutron Physics, Book of Lectures, V.1 P. 156, Dubna, JINR, 1995 (in Russian).
75. V.K.Ignatovich. The Theory of Dynamic Diffraction on Monocrystals. VII International School on Neutron Physics. Book of Lectures, V.1, P. 167, Dubna, JINR, 1995 (in Russian).
76. D.E. Lanskoy, T.Yu.Tretyakova. Structure of Λ-Hypernuclei with Neutron Halo. Proc. of the XXIII Int. Symposium on Nuclear and Particle Physics with Meson Beams in the 1 GeV/c Region. Universal Academy Press, Inc., Tokyo, Japan, 1995, p.209.
77. I.G.Nosov, A.I.Frank. The Matrix of Density and the Slow Neutron Beam Transformation. JINR Preprint, P4-94-441, Dubna, 1994 (in Russian).
78. I.G.Nosov, A.I.Frank. The Dispersion Law for Long Wave Neutrons and the Possibility of Its Precision Verification. Yad. Fiz., 1995, v.58, No. 6, p.353-360 (in Russian).
79. A.I.Frank, V.G.Nosov Diffraction in Time and New Type Interferometry with Nonseparated Beams. In: Fundamental Problems in Qantum Theory: A Conference Held in Honor of Professor John A.Wheeller. (Eds by D.M.Greenberger and A.Zeilinger). Annals of the New York Academy of Sciences, 1995, v. 755, p.293-302.
80. A.I.Frank, D.B.Amandzholova. Neutron Multiray Reflection. In: Fundamental Problems in Quantum Theory: A Conference Held in Honor of Professor John A.Wheeller. (Eds by D.M.Greenberger and A.Zeilinger. Annals of the New York Academy of Sciences, 1995, v. 755, p.858.
81. S.A.Rakityansky, S.A.Sofianos, W.Sandhas, V.B.Belyaev. Threshold Scattering of the Eta-Meson of Light Nuclei. Phys. Lett., B359, 1995, p.33.

APPLIED RESEARCH

1. I.V. Alekseev. Calculation of Spectral Distributions of the Sensitivity of a Nonlinear Gamma-Detector, submitted to the Russian journal Physics and Technology of Superconductors (in Russian).
2. V.P.Chinaeva, M.V.Frontasyeva, S.F.Gundorina, N.V.Lukina, V.M.Nazarov, V.V.Nikonov, S.S.Pavlov, V.F.Peresedov, T.M.Ostrovnaya. Epithermal Neutron Activation Analysis for Monitoring Northern Ground Ecosystems. Book of Abstracts of the Russian Conference "Anthropogenic Soil Changes over North Industrial Regions" (July 25-27, 1995, Apatity, Russia), p. 75 (in Russian).
3. V.P.Chinaeva, M.V.Frontasyeva, S.F.Gundorina, N.V.Loukina, V.M.Nazarov, V.V.Nikonov, S.S.Pavlov, V.F.Peresedov T.M.Ostrovnaya. Epithermal Neutron Activation Analysis for Monitoring Northern Terrestrial Ecosystems. Book of Abstracts 3rd International Meeting "Nuclear Physics for Protection of the Environment" (May 23-28, 1995, Dubna), p. 66.
4. M.V.Frontasyeva, F.Grass, V.M.Nazarov, E.Steinnes. Intercomparison of Moss Reference Material by

Different Multi-Element Techniques. J. Radioanal. and Nucl. Chem., vol. 192, No. 2 (1995) 371-379.

5. M.V.Frontasyeva, E.Steinnes. Epithermal Neutron Activation Analysis of Mosses Used to Monitor Heavy Metal Deposition around an Iron Smelter Complex. The Analyst, vol. 120, No. 5 (1995) 1437-1440.
6. M.V.Frontasyeva, V.M.Nazarov, V.P.Chinaeva, E.Steinnes, K.A.Rahn. Study of Trace elements in Annual Segments of Moss Biomonitors Using Epithermal Neutron Activation Analysis. Link with Atmospheric Aerosols. Book of Abstracts "9th Int.Conf. Modern Trends in Activation Analysis MTAA 9" (24030 September, Seoul, South Korea), submitted to the J. of Radioanalytical and Nuclear Chemistry.
7. A.V.Gorbunov, T.L.Onischenko, M.V.Frontasyeva. Estimates of Background Changes in the Microelement Composition of Biological Objects. Book of Abstracts 3rd International Meeting "Nuclear Physics for Protection of the Environment" (May 23-28, 1995, Dubna), p.123.
8. V.M.Nazarov, M.V.Frontasyeva, V.F.Peresedov, V.P.Chinaeva, T.M.Ostrovnaya, S.F.Gundorina, V.V.Nikonov. Resonance Neutrons for Determination of Elemental Content of Moss, Lichens and Pine Needles in Atmospheric Deposition Monitoring. JINR Rapid Communications, Dubna, No. 3[71]-95, p.25-34; J.Radoanal. and Nucl. Chem., vol. 192, No. 2 (1995) 229-238.
9. V.M.Nazarov, V.F.Peresedov. Recent Developments of Radioanalytical Methods at the IBR-2 Pulsed Fast Reactor. J.Radioanalytical and Nucl. Chem., vol. 192, No. 1 (1995) 17-28.
10. V.M.Nazarov, S.S.Pavlov, V.F.Peresedov, I.L.Sashin, M.V.Frontasyeva The Fast Activation System for Neutron Activation Analysis. Proceedings of the Third Int. Workshop on Short Time Activation Analysis, High Rate Gamma Spectroscopy and X-Ray Techniques (3-7 April, 1995, Vienna, Austria) (in print).
11 F.I.Tyutyunova, Ye.M.Grachevskaya, M.V.Frontasyeva, S.F.Gundorina. Optimization of the Early Diagnostics on Bioindication of Urban Territory Contamination. Book of Abstracts 3rd International Meeting "Nuclear Physics for Protection of the Environment" (May 23-28, 1995, Dubna), p.123.
12. F.I.Tyutyunova, Ye.M.Grachevskaya, V.M.Nazarov, V.P.Chinaeva, M.V.Frontasyeva, S.F.Gundorina, T.M.Ostrovnaya. Pollution of Aquatic Landscapes: Criteria for Assessment. Book of Abstracts 3rd International Meeting "Nuclear Physics for Protection of the Environment" (May 23-28, 1995, Dubna), p.45.

NEUTRON SOURCES

V.L.Aksenov. Reactor Neutron Sources in Large Facilities in Physics, Ed. M.Jacob and H.Schopper. World Scientific, 1995, p.273-291.

2. V.D.Ananiev, A.V.Vinogradov. The IBR-2 Pulsed Research Reactor: Status Report. International Seminar on Advanced Pulsed Neutron Sourses PANS-II. June 14-17, 1994 Dubna, Russia.
3. V.D.Ananiev, A.V.Vinogradov, I.M.Baranov, V.D.Syzarev, A.I.Menyalov. Problems of Nuclear Power Facility Vibroacoustic Diagnostics. Topical Seminar on Management of Ageing of Research Reactors. Geesthach/Hamburg, Germany 8-12 May 1995.
4. A.A.Belyakov, V.G.Ermilov, V.V.Melikhov, E.P.Shabalin. Solid Methane Moderator. Proceedings of the Second Institute Seminar PANS-II. June 14-17 1994, Dubna, Russia, PANS-II, pp. 217-234, 1995.
5. V.L.Lomidze. The Effective Gradient Method in the Fuel Bowing Problem, JINR Preprint, E3-95-509, Dubna, 1995.
6. Yu.N.Pepyolyshev, S.V.Chuklyaev, A.B.Tulaev, V.F.Bobrakov. The Dynamic Method for Time-of-Flight Measurements of Thermal Neutron Spectra from Pulsed Sources. Nuclear Instruments & Methods, A364, (1995) 501-506.
7. Yu.N.Pepyolyshev, W.Dzwinel, P.Jirsa, J.Rejchrt. Comparison of the Noise Diagnostics System Based on Pattern Recognition Discriminant Method. Ann. Nuclear Energy, vol.22, No.8, (1995), 543-551.
8. Yu.N.Pepyolyshev, W.Dzwinel, J.Dlugopolski. Feed-Forward Neutral Nets Application for Prediction of Nuclear Reactor Operation. "10th Summer School on Computing Techniques in Physics", September 5-14, 1995. Skalsky Dvur, Czech Republic.
9. Yu.N.Pepyolyshev, W.Dzwinel. Pattern Recognition, Neutral Networks, Genetic Algorithms and High Performance Computing in Nuclear Reactor Diagnostics - Results and Perspectives. "Seventh Symposium on Nuclear Reactor Surveillance and Diagnostics, SMORN VII", Avignon, France, 19-23 June, 1995.

10. Yu.N.Pepyolyshev, A.B.Tulaev. The Main Results of the Investigation of the Spectrum of Leakage Neutrons from the Surface of the Cryogenic Moderator of the IBR-2 Reactor. "Int. Seminar on Advanced Pulsed Neutron Sources, PANS-II", JINR, D3-95-169, Dubna, 1995.

11 A.K.Popov. The IBR-2 Reactor Pulse Transfer Factor. JINR Communications, P3-95-463, Dubna, 1995 (in Russian).

12. A.K.Popov. Simple Nonlinear Model of the IBR-2 Reactor Power Feddback. JINR Communications, P13-95-464, Dubna, 1995 (in Russian).

MEASUREMENT AND COMPUTATION COMPLEX

Yu.A.Astakhov, A.Bogdzel, F.L.Levchanovsky, B.Michaelis, V.E.Novozhilov, A.I.Ostrovnoy, V.I.Prikhodko, V.E.Rezaev, A.P.Sirotin, G.A.Sukhomlinov, Yu.A.Volkov. Development of the FLNP Measurement and Computation Complex. Proc. of the Conference "13th Meeting Advanced Neutron Sources", Villigen, Switzerland, October 11-14, 1995 (to be published).

2. Yu.A.Astakhov, A.I.Ostrovnoy, V.I.Prikhodko, G.A.Sukhomlinov. The Development of the FLNP Network Infrastructure and the SUN-Cluster. JINR, P10-95-490, Dubna, 1995 (in Russian).

3. V.F.Bobrakov, A.B.Tulaev. The Automated System for the Analysis of Vibrations of the IBR-2 Movable Reflector. JINR Communication, P10-95-18, Dubna, 1995 (in Russian).

4. A.A.Bogdzel, W.I.Furman, P.Gelfenbort, N.N.Gorin, J.Kliman, Yu.N.Kopach, L.K.Kozlovski, A.B.Popov, H.Postma, N.S.Rabotnov. Measurement of Energy Dependence of Fission Angular Anisotropy for Resonance Neutron Induced Fission of ^{235}U Aligned Target. Proc. of the XIII Meeting on Physics of Nuclear Fission in the Memory of Prof. Smirenkin, Obninsk, October 3-6, 1995 (to be published).

5 V.A.Butenko, V.A.Drozdov, A.S.Kirilov, V.E.Novozhilov, A.I.Ostrovnoy, V.E.Rezaev, V.I.Prikhodko. The DSP-Based RTOF-Correlator for High Resolution Fourier Diffractometers. Proc. of the XVI International Symposium on Nuclear Electronics. (Varna, September 12-18, 1994), pp.107-112, Dubna, 1995.

6. V.A.Butenko, V.A.Drozdov, A.S.Kirilov, V.E.Novozhilov, A.I.Ostrovnoy, V.E.Rezaev, V.I.Prikhodko. DSP-System for Real-Time Correlation Spectrometry at the IBR-2 Pulsed Neutron Source. Proc. of the Conference "ESCONE Real-Time Data-95" (Warsaw, September 27-29, 1995), pp.87-93.

7. O.I.Elizarov. Commutator-Power Amplifier for Step Motors. JINR Communication, P13-95-245, Dubna, 1995 (in Russian).

8. V.A.Ermakov, Yu.M.Gledenov, P.V.Sedyshev, M.V.Sedyshev, V.G.Tishin. The Measuring-Accumulating Module for the Ionization Chamber with Two Grids. JINR Communication, P10-95-438, Dubna, 1995 (in Russian).

9 V.A.Ermakov, T.B.Petukhova, L.N.Sedlakova. The Development of the Measurement and Computational Module of the DIFRAN Spectrometer at the IBR-2 Reactor. JINR, P13-95-215, Dubna, 1995 (in Russian).

10. J.Heinitz, A.S.Kirilov. A Software Complex for Neutron Time-of-Flight Measurements by Means of a VME Based Accumulation, Control and Supervising System. JINR D13-95-462, Dubna, 1995.

11 D.A.Korneev, E.I.Litvinenko, D.I.Lyapin, V.V.Zhuravlev. Measuring and Accumulating Module of the SPN-1 Polarized Neutron Spectrometer. JINR, P3-95-140, Dubna, 1995 (in Russian).

12. V.E.Rezaev. Spectrometric VME-Based Storage Device. Proc. of the XVI International Symposium on Nuclear Electronics. (Varna, September 12-18, 1994), pp.107-112, Dubna, 1995.

13. A.P.Sirotin. The Hardware for Designing Systems to Automatize Neutron Spectrometric Measurements. Abstract to the Dissertation Thesis. JINR 13-94-85, Dubna, 1994 (in Russian).

14 V.G.Tishin. On the Conceptions of the Development of Multi-Dimensional Measuring Systems at the FLNP Installations. Proc. of the XVI International Symposium on Nuclear Electronics. (Varna, September 12-18, 1994), pp.73-78, Dubna, 1995.

15 A.B.Tulaev. The Dynamic Method for Time-of-Flight Measurement of Thermal Neutron Spectra from Pulsed Sources. Nuclear Instruments and Methods in Physics Research A368 (1995), pp.501-506.

16. A.B.Tulaev. Hardware and Software for Designing and Constructing Automated Diagnostic and Research Systems at the IBR-2 Reactor. Abstract to the Dissertation Thesis. JINR, 13-95-85, Dubna, 1995 (in Russian).

4. PRIZES

Frank Prize:

P.Ageron (ILL, Grenoble, France), A.Steyerl (University of Rhode Island, USA), A.V.Strelkov (FLNP) for "Pioneer Researches in the Field of UCN Production and Investigation of Their Properties"

JINR Prizes:

For Applied Research:

First Prize:

V.M.Nazarov, M.V.Frontasyeva, V.F.Peresedov, S.S.Pavlov, S.F.Gundorina, V.P.Chinaeva, T.M.Ostrovnaya. "Neutron Activation Analysis at the IBR-2 in Environmental Protection Problems"

Encouraging Prize:

A.M.Balagurov, I.S.Lyubutin. "Atomic and Magnetic Structure of $YBa_2(Cu_{1-x}{}^{57}Fe_x)_3O_{6+y}$ Studied on Enriched Samples"

FLNP Prizes:

In Nuclear Physics:

First Prize:

Yu.P.Popov, A.M.Suhovoj, V.A.Khitrov. "The Main Singularity of Cascade Gamma-Decomposition of Compound-Conditions and Modern Nuclear Spectroscopy"

Second Prize:

A.A.Bogdzel, N.A.Gundorin, Yu.N.Kopach, A.B.Popov, S.A.Telezhnikov, V.I.Furman. "Spectroscopy of the Instantaneous Gamma-Emission in Pu-240 Fission"

Third Prize:

E.V.Vasilyeva, Yu.N.Kholnov. "Investigation of Eu-146 - Sm-146 Decomposition"

In Condensed Matter Physics:

First Prize:

V.L.Aksenov, E.B.Dokukin, V.K.Ignatovich, D.A.Korneev, E.I.Kornilov, S.V.Kozhevnikov, Yu.V.Nikitenko, A.V.Petrenko. "Investigation of the High-Temperature Superconductors by Polarized Neutrons"

Second Prize:

A.M.Balagurov, V.V.Sikolenko, V.G.Simkin, O.E.Parfenov, S.Sh.Shilshtein. "Neutron Diffraction Study of the $YBa_2Cu_{2.7}Zn_{0.3}O_{6+y}$ Structure"

Third Prize:

A.N.Nikitin, T.I.Ivankina, K.Walther. "Development of the Theory of Texture Formation in Inhomogenious Materials on the Base of New Data of Neutron Scattering Texture Analysis"

In Applied Physics:

First Prize:

V.L.Aksenov, A.M.Balagurov, B.N.Savenko, S.L.Platonov. "Diffractometer for Investigation of Microsamples at the High Pressure"

Second Prize:

V.F.Bobrakov, A.B.Tulaev. "Automatic System for IBR-2 Movable Reflector Vibration Analysis"

Third Prize:

Yu.A.Astakhov, V.I.Prikhodko, A.I.Ostrovnoy, G.A.Sukhomlinov. "Development of the Computing Network of FLNP SUN-Cluster"

5. NEUTRON SOURCES

5.1. THE IBR-2 REACTOR

On the 27th of March, 1995 the IBR-2 reactor began regular operations with the new PO-2R movable reflector (MR), which is the third in a series of movable reflectors at IBR-2 since the reactor startup. The structure of the new movable reflector repeats the structure of the previous one but has a more developed system for reactor state diagnostics and parameter control. The movable reactor enables the pulsed mode of reactor operation with reactivity modulation frequencies of 5 and 25 Hz. The rotation speed of the main movable reflector (MMR) rotor is 1500 rot/min and of the auxiliary movable reflector (AMR) rotor—300 rot/min.

The data on the MR operation time for 1995 are given in Table 1 (the same inclusive of the on-site test operation time - in Table 2.) No MR operation failures were registered in the reported period.

The radiation fluence at the center of the PO-2R blade is $7.64 \cdot 10^{20}$ n/cm^2 (for $E_n > 0.1$ MeV).

In 1995, reactor operations for physical experiments on 12 extracted neutron beams were conducted. As of December 1, 1995 seven measuring cycles had been performed. The reactor operation is detailed in Table 1, the evidence of steady reactor operation and a low number of emergency shutdowns.

For comparison, data on the specific frequency of emergency shutdowns per year are given below:

1991 - 2.3/cycle

1992 - 3.2/cycle

1993 - 3.7/cycle

1994 - 1.7/cycle

1995 - 2/cycle

On August 16, a leakage of sodium occurred as a result of a depressurization of the air heat transfer (AHT) coil pipe in loop *A* of Contour II. As soon as the leakage was detected, sodium from loop *A* of Contour II was drained into the drain tank of loop *A* of Contour II. Helium density and color defectoscopy tests of the AHT were conducted, revealing micro-cracks in two AHT coil pipes.

In September-October 1995, the malfunctioning AHT units Contour II were fixed. Repairs and necessary tests were conducted by specialists of NIKIMT (Scientific Research and Designing Institute of Assembly Technologies). Following the repair work and sodium refill, the technical reliability of the equipment and pipes of loop *A* of Contour II were conducted together with representatives of GOSATOMNADZOR (Atomic Inspection Committee of Russia).

In 1995, work to estimate the residual resources of the reactor jacket, TVELs (fuel elements), and the fuel system of the core was completed. The decision was made to continue operation of the reactor control and safety system (RCSS) until December 31, 1996 allowing the possibility of a further extension of its operation period.

Table 1

IBR-2 reactor operation characteristics for 1995 (7 cycles)

Cycle №	Start and completion dates of cycles	Operation time for physical experiments, $T_{ph.e.}$	MR operation time, T_{MR}	Number of emergency, N_{ES}	Causes of emergency shutdowns (malfunction classification according to RD-04-10-94)				Number of operating beams
					Voltage drops (MR8)	Equipment breakdowns (MR7)	Electronic equipment breakdowns (MR7)	Personnel malfunctioning (MR5)	
1	27.03—08.04	206	274	6	2		4		12
2	17.04—28.04	247	261	2		1		1	12
3	15.05—26.05	265	271	1			1		12
4	05.06—15.06	217	245	2			2		12
5	26.06—07.07	264	274	0					12
6	17.07—28.07	265	276	0					12
7	20.11—01.12	220	273	3			3		12
Total:		1684	1874	14	2	1	10	1	

Table 2

The state of the reactor (as of Dec. 1, 1995)

№	Parameter (from the start of reactor operations)	Value
1	Total operation time for physical experiments, hrs.	28440
2	Total generated energy, MW/hrs.	53723
3	PO-2R total operation time, hrs. (inclusive of operation time during tests)	2116
4	Maximum fluence on the reactor jacket in the center of the active core: (10^{22} n/cm^2)	
	for $E_n > 0.8$ MeV	0.97
	for $E_n > 0.1$ MeV	2.24
5	Maximum fuel burning, (%)	4.48
6	Total number of emergency shutdowns	337

The above calculations shows that operation with the reactor jacket and active core at rated parameters will be possible through the year 2001 and then, in the period from 2002 to 2004, the reactor jacket, fuel load, stationary reflectors, RCSS mechanisms, and water moderators, will have to be replaced.

The concept of IBR-2 modernization in the period from 1995 to 2005 was elaborated. The main directions of IBR-2 development and upgrading are:

- improve the main parameters of the reactor
- increase the reliability and safety of reactor
- modernize the main equipment of the reactor.

The main stages of the modernization project are:

- design and manufacture of new main equipment 1996—1998
- assembly and tests of the equipment 1999—2001
- replacement of the equipment and fuel reloading,
- physical startup, power startup 2002—2004
- IBR-2 startup for physical experiments 2005

The following proposals for changes in the reactor structure are planned to be realized:

- manufacture a compact active core (without the central channel) with 67 fuel cassettes instead of 78 cassettes (Fig. 1). This will increase the average thermal neutron flux in a number of beams at the same IBR-2 mean power of 2 MW (see Table 3).
- Use of pellet TVELs in all fuel cassettes to ensure deeper burning of the fuel (8.2% instead of 6.5%).
- Use a lower rotation speed for the heterogenic type movable reflector for reactivity.

Table 3

Ratio of thermal neutron fluxes on a sample in the 10 m flight path for the new and old configurations of the IBR-2 active core

Beam No.	1	2	3	4	5	6	7	8	9	10
Gain factor	0.57	1.41	1.46	0.93	0.93	0.93	1.79	1.72	0.65	1.48

In 1995, work to create a cryogenic moderator (CM) for the IBR-2 continued. In the first half of the year, technical drawings for the CM were completed, contracts with NIKIET and other organizations for manufacturing the CM were concluded, and investigations of the strain and stress fields for the standard CM configuration, as well as of the metrological equipment for the CM, were conducted. Unfortunately, the work tempo was reduced by delays in financing.

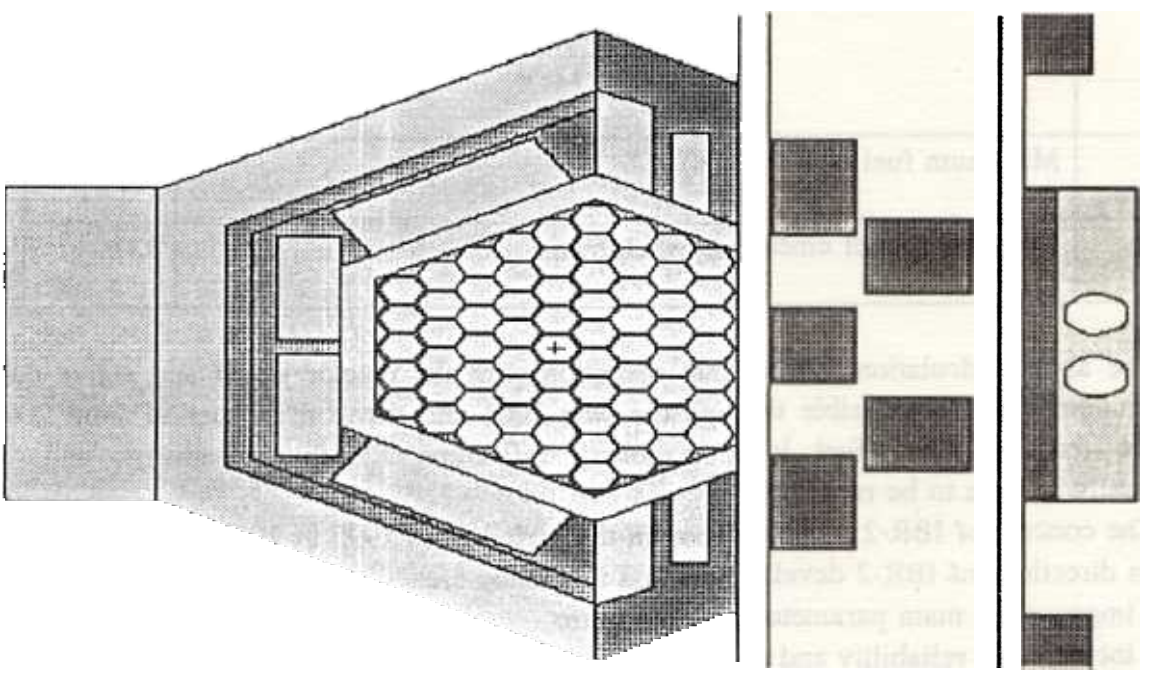

Fig. The calculated scheme of the IBR-2 reactor (69 cassettes).

5.2. THE IBR-30 BOOSTER

In 1995, the LUE-40+IBR-30 complex operated for 1980 hours. Seven neutron beams and the IBR-30 reactor were used to realize the scientific program on neutron nuclear physics, and to test IREN units and systems as well as to conduct irradiation experiments in the framework of the ATLAS project. After completion of the tests at IBR-30, the new design electron-neutron converter was installed, thus making it possible to lower the temperature of the converter considerably.

5.3. THE IREN PROJECT

Following the recommendations of the 77th session of the JINR Scientific Council, the JINR Directorate adopted the detailed work schedule for the IREN project for 1995. The financing schedule for the work on the project carried out by the JINR laboratories was established by special order. Because of the budget deficit and irregular receipt of dues from JINR member-states, the work was not financed according to the adopted schedule. As a result, the IREN completion date was shifted to the end of 1998.

Nevertheless, in 1995, under the agreement with INP SB RAS, Novosibirsk, we managed to start working on the creation of the acceleration sections, the buncher and a system to double the HF power. RMIR (St. Petersburg) completed the work on the redesign of the M-250 "OLIVIN" modulators into M-350's for the 5045-type clystrons which have been accepted as standard for the IREN accelerator. The first set of equipment for the OLIVIN stations has been shipped from Yerevan to Dubna. In FLNP, assembly of the stand for the M-350 modulator was begun in Building 118. In cooperation with the ISTOK industrial enterprise (Fryazino), MEPI (Moscow) completed the construction of elements for the HF feeder. Cold tests of the feeder are being carried out. In LNP, JINR, the design and modelling of the magnetic focusing system of the accelerator were completed. The LNP-LHE-LPP collaboration together with INP, SB RAS elaborated the technical specifications for the electron source and a number of units for the HF power supply were constructed. In collaboration with GSPI (Moscow), specifications for the general design of the electron accelerator (in Building 43) were worked out. NIKIET (Moscow), in cooperation with JINR, completed the specifications for the multiplying target with improved characteristics of the neutron pulse. The MAYAK industrial enterprise in Chelyabinsk-65 started manufacture of the fuel elements (TVELs) based on metal plutonium. According to the project of VNIINM (Moscow), the manufacture of the TVEL components—special thin-walled tubes of stainless steel and tantalum, and other construction elements—was started. At the LUE-40+IBR-30 complex, a number of variants of a radically new electron converter designed for IREN were successfully tested. The results permit us to begin constructing the regular converter for IREN. NIKIMT (Obninsk) prepared the specifications for dismantling IBR-30.

6. MEASUREMENT AND COMPUTATION COMPLEX

Work performed in 1995 was focused on two main activities:

- design of electronics and software for the spectrometer measurement and control systems at the IBR-2 and IBR-30 reactors;
- development of the FLNP measurement and computational infrastructure.

A distinguishing characteristic of this year is that, in addition to current work on the modernization and operation of the measuring modules of the spectrometers based on CAMAC equipment and personal computers, a number of electronic blocks and software packages for the new generation of systems for experiment automation were developed on the basis of VME equipment and workstations integrated into the local computational network. These systems, compared with those already in operation, should exhibit qualitatively new measuring (in particular, for the IREN installation) and operational parameters and will ensure parallel (including remote) control over data acquisition and accumulation, information processing and visualization as well as for varying the conditions at the sample.

Methodical questions, including analysis of the current state and the development of systems for acquiring, accumulating and processing data coming from the spectrometers and information service of FLNP, and assessments of the required resources as well as specific technical solutions, are considered in the relevant project which is scheduled for realization in 1996-98.

An essentially new requirement voiced by physicist users is the creation of a unified set of hardware and software for the entire complex of Laboratory spectrometers, centralized archives of experimental data, and unified means for analyzing and graphically presenting data. Implementation of this requirement will simplify the operation of the spectrometers and essentially facilitate the transition to the user policy at the experimental setups.

In 1995, a large amount of preparatory work in all lines of activity considered in the above-mentioned project was completed.

Detector electronics. The main tasks in the field of detector electronics are the improvement of the parameters of preamplifiers, shaping amplifiers, discriminators, ADC and other spectrometric devices, and the change-over to up-to-date components.

In 1995, the detector track electronic units for the new detector system of the NERA-PR spectrometer (fifty SNM-65 rectangular helium neutron counters), were designed and constructed. The detectors, along with their electronics, were tested and the basic parameters were measured. Analogous systems were also developed for the NSVR spectrometer. At present, construction of the units is under way.

A considerable amount of work was carried out at HRFD: adjustment and startup of the electronics for two multi-section scintillation detectors; measurement of the Li-glass parameters; study of the character of noises and pickups, and working out the methods to reduce them.

The prototype of the charge-sensitive preamplifier for the Si-detectors of the spectrometer with oriented nuclei was designed and constructed. The unified spectrometric amplifier and high-speed analog-digital converter are in the development stage. Computer simulation and calculations of the basic parameters of the detector electronics for the position-sensitive gas detectors were made.

Unfortunately, for a number of reasons, mainly because of mismanagement, tests of the position-sensitive annular detector of the YUMO spectrometer were not completed. This work

needs to be completed in the shortest possible time and the decision made whether to replace the detector or to design new electronics.

Systems of data acquisition and accumulation. The initial stage of the project to develop a unified VME-based data acquisition and accumulation equipment for the FLNP spectrometers has been accomplished. The module based on the high performance TMS320C40 signal processor has been proposed as a basic module, which would provide a universal standard for the construction of data acquisition systems for any spectrometer. At the present time, the functional potentials of the module are being considered and technical details are being revised and verified. The development of a number of unified blocks for data acquisition systems is also in progress.

In 1995, a set of electronic blocks in VME standard (TDC-6 time-to-number converter, histogram memory with a capacity of 2 Mbytes and a memory address conversion block, and detector number encoder with 16 inputs) was built for the acquisition and accumulation of low resolution spectra at HRFD. The blocks were regulated and adjusted both jointly and separately. The basic blocks for the VME-systems of the NERA-PR spectrometers have also been constructed. The VME-module processor, based on the T800 transputer, was designed and constructed for the DN-12 spectrometer, and a set of micro-programs for data acquisition and accumulation was written.

The development stage is complete and engineering specifications were prepared for constructing the following VME blocks:

- digital rate meter;
- encoder of the 128 units point detector number;
- RTOF-analyzer based on the TMS320C51 digital signal processor;
- block for controlling experiments;
- block for registering ultrasonic signals.

For the DN-12 and DIN-2 spectrometers, the detector number encoders with 32 inputs (CAMAC) were made and adjusted.

Multi-dimensional measuring and accumulation systems for the ROMASHKA, KASKAD and PARKS spectrometers and the UCN gravitational spectrometer were updated and put into operation.

Control systems of the equipment for the spectrometers. The main tasks on which the specialists from the department for electronics, computers and networks focused their efforts, were unification of the control systems for executive mechanisms (step motors for goniometers, neutron scanners, rotating platforms, *etc.*) and the standardization of temperature regulators. The Euroterm temperature regulators which had been previously ordered were received and, at the moment, they are being brought into service at NSVR, HRFD, *etc.*

The control system for the step motors on the basis of the VD-OUT32 VME-units has been designed, and at present, work is proceeding on the installation of the system at the NERA-PR spectrometer. A stand for testing the software for these systems has been made.

At the REFLEX spectrometer, the CAMAC-based control system for executive mechanisms was put into service. The system is based on the employment of a commutator-power amplifier for alternate control of the step motors. An analogous module in VME standard has been constructed for NSVR. The 16-channel input/output register with a comparator to control the shutter and phase of the beam chopper has been integrated into the VME equipment at the NERA-PR and NSVR spectrometers.

At NERA-PR and DN-2, the equipment for controlling the LTC and DRC refrigerators has been modernized. At HRFD, the neutron scanner was connected to the control system. A number of analog electronic blocks have been designed for the high-pressure chamber (NSVR) and the REFLEX setup (current sources, switches, preamplifiers, *etc.*). Work to upgrade the control systems of the neutron beam choppers has been started.

A considerable amount of work on the development of the systems for correlation analysis of the power pulses of the IBR-2 reactor, and for measuring the movable reflector vibrations was completed.

Software for data accumulation and control systems of the spectrometers. Work is now under way on designing unified software for the data accumulation and control systems on the basis of VME-standard equipment. The testing software for the VME units (interface for controlling step motors, time encoder with the memory for accumulating spectra, register for controlling the setup) has been developed. In addition to the previous methodical developments, the specification for designing the control and interface modules was worked out, as well as the basic principles for design and realization of unified software for the automation systems, which will be used in the new generation systems being realized at the NERA-PR and HRFD spectrometers. When designing the software for the entire system, an object-oriented approach will be employed.

The software for the spectrometer measuring and control systems in service today were also improved.

The software of the SPN-1 and REFLEX spectrometers was complemented by new possibilities for the analysis of accumulated data. In particular, the software for processing intensity profiles in graphic mode and of spectra by formulas, for auto-saving, editing, and processing the parameters which characterize the essential spectrometric information, were enhanced. Furthermore, additional modes for data analysis were realized and the means for keeping a protocol of users' jobs were developed. For the UGRA spectrometer, the program for processing experimental data and calculating cross-sections, with the possibility of correcting for hydrogen, was written.

Work to create the software for the DIFRAN spectrometer was completed. The resulting program for controlling the spectrometer maintains the operation of two accumulation channels, provides remote control over the mechanical parts of the spectrometer via a special communication line (the computer is placed at a distance of about 500 m from the spectrometer) and utilizes automatic modes to accumulate spectra for different relative positions of the sample and the detector. The program also monitors the level of neutron beam intensity, and stops accumulating data if the intensity drops below the allowable limit. In this case, the user can continue measurements by using a special command.

The MAK program used at the DIN-2 and IZOMER spectrometers was significantly improved. Additional subroutines made it possible to install this program for conducting measurements at the NERA-PR and KDSOG spectrometers. The software for the NSVR spectrometer was also developed.

Development of the SUN-cluster and network infrastructure. Throughout the reported year, work on the development of the FLNP local computational network and SUN-cluster software was in progress.

In 1995, five new workstations (one SPARCstation 5 and four SPARCstation 20's), four X-terminals, and four black and white and two color network printers housed in the Laboratory's main buildings, were connected to the network. Work to optimize the local network was

conducted. One central segment, including the main servers and workstations with general access software, and two segments for SD CMP and SD NP oriented to serve those computers whose functions are to control experiments, data acquisition and processing from the spectrometers at the IBR-2 and IBR-30 reactors, were formed.

The software of the FLNP computers was modified and adapted to use the network printers and was complemented by additional functions which enable one to control the users' access to the mentioned devices (in particular, to the color printers) and the number of sheets printed by each of the users. It also allows the users to print via NFS from their PCs.

The SUN-workstation cluster was equipped with a FAX-server and three modems enabling access to computers via telephone lines. The JukeBox laser disk archive system with a total capacity of 40 Gbytes was also connected and the appropriate software was provided. The PV-Wave program package for analysis and graphical representation of data was installed on two powerful workstations. Programs for converting the data formats used at currently operating spectrometers into PV-Wave compatible formats were created. In addition, the Open GENIE program package for spectra processing and viewing developed at RAL was adapted for SUN computers. The Viewlogic and ALTERA program packages for computer-aided electronics design were purchased and installed.

In the reported year new versions of free software used intensively by the FLNP users were installed as well. In particular, these are the ELM, XRN, FWVM, Netscape, and EMACS program packages with the integrated Ispell spellcheck system.

In addition, new versions of ANSI C, C++, F77, GCC translators and the CERN LIB library (v.94b) were installed. In the near future, the XNTP time synchronization system will be loaded on the SUN-workstation cluster.

Seventeen papers were published and two dissertation theses were defended in 1995.

7.1. STRUCTURE OF LABORATORY AND SCIENTIFIC DEPARTMENTS

Directorate:
Director:
V.L.Aksenov
Deputy Directors:
A.V.Belushkin
W.I.Furman
Scientific Secretary:
V.V.Sikolenko

Reactor and Technical Departments
Chief engineer: V.D.Ananiev
IBR-2 reactor
Chief engineer: A.V.Vinogradov
IBR-30 booster + LUE-40
Head: S.A.Kvasnikov
Nuclear physics and pulsed neutron sources sector
Head: V.L.Lomidze
Mechanical maintenance division
Head: A.A.Belyakov
Electrical engineering department
Head: V.P.Popov
Design office
Head: V.I.Konstantinov
Construction
Head: A.N.Kuznetsov

Scientific Departments and Sectors
Condensed matter department
Head: A.M.Balagurov
Nuclear physics department
Head: V.N.Shvetsov
Department of electronics, computers and networks
Head: V.I.Prikhodko
Department of IREN
Head: A.K.Krasnykh
Activation analysis and radiation research sector
Head: V.A.Sarin
Applied research sector
Head: V.I.Luschikov

Administrative Services
Deputy Director: S.V.Kozenkov
Secretariat
Finances
Personnel

Scientific Secretary Group
Translation
Graphics
Photography
Artwork

THE CONDENSED MATTER DEPARTMENT

Sub-Division	Title	Head
Group No.1	HRFD	A.M.Balagurov
Group No.2	DN-2	A.I.Beskrovnyi
Group No.3	DN-12	B.N.Savenko
Group No.4	HRNS	K.Ullemeyer
Group No.5	SNIM-2	V.W.Nietz
Group No.6	YUMO	M.A.Kiselev
Group No.7	Biomolecular neutron diffraction	I.N.Serdyuk
Group No.8	SPN-1	Yu.V.Nikitenko
Group No.9	REFLEX	D.A.Korneev
Group No.10	NERA-PR	I.Natkaniec
Group No.11	KDSOG	A.Yu.Muzychka
Group No.12	DIN-2	Zh.A.Kozlov
Group No.13	EG-5	A.P.Kobzev
Group No.14	Theoretical condensed matter physics	E.I.Kornilov
Group No.15	Technical support	V.V.Zhuravlev

THE NUCLEAR PHYSICS DEPARTMENT

Sub-Division	Title	Head
Group No.1	Polarized neutrons and nuclei	V.P.Alfimenkov
Group No.1	Neutron spectroscopy	A.B.Popov
Group No.3	Nuclear reactions	Yu.S.Zamyatnin
Group No.4	Properties of the neutron	Yu.A.Alexandrov
Group No.5	Proton and α-decay	Yu.M.Gledenov
Group No.6	Properties of γ-quanta	A.M.Sukhovoy
Group No.7	Radiation capture of neutrons	G.P. Georgiev
Group No.8	Ultra-cold neutrons	V.N.Shvetsov
Group No.9	Neutron structure	G.S.Samosvat
Group No.10	Rare reactions	Yu.N.Pokotilovsky

7.2. USER POLICY

The IBR-2 reactor usually operates 10 cycles a year (2500 hrs. total) to serve the experimental programme. A cycle is established as of 2 weeks of operation for users, followed by a one week period for maintenance and machine development. There is a long shut-down period between the end of June and the middle of October.

All experimental facilities of IBR-2 are open to the general scientific community. The User Guide for neutron experimental facilities at FLNP is available by request from the Laboratory's Scientific Secretary.

Condensed matter studies at the IBR-2 facility have undergone some changes in accordance with the experience gained during the last two years. It was found to be necessary to establish specialized selection committees formed of independent experts in their corresponding fields of scientific activities. The following four committees were organized:

1. Diffraction
   - V.A.Somenkov - Russia - Chairman
   - V.A.Trounov - Russia
   - L.Rosta - Hungary
   - J.Shveitser - France
   - J.B.Forsyth - United Kingdom
   - A.Z.Menshikov - Russia
2. Inelastic scattering
   - J.Janik - Poland - Chairman
   - W.Gotze - Germany
   - V.Dimic - Slovenia
   - L.Bata - Hungary
   - A.V.Chalyi - Ukraine
3. Neutron optics
   - A.I.Okorokov - Russia - Chairman
   - S.V.Maleyev - Russia
   - T.Rekveldt - The Netherlands
   - H.Lauter - France - Germany
4. Small angle scattering
   - L.Cser - Hungary - Chairman
   - J.Plestil - Czech Republic
   - J.Teixeira - France
   - G.Zaccai - France
   - H.Stuhrmann - Germany
   - H.Fuess - Germany

Scientific Secretary of FLNP, Dr. Vadim V. Sikolenko, is responsible for user policy. Dr. Gizo D. Bokuchava has been appinted as the scientific coordinator of user policy at FLNP. There are two deadlines for proposal submission: for the experimental period from October through February, the deadline is May 16; and for the period from February through June, the deadline is November 16.

The scientific coordinator is responsible for organizing all necessary work for:

- distribution of "Application for Beam Time" forms to potential users
- reception and registration of proposals

- proposal review by instrument scientists to estimate the technical feasibility of proposals

- sending feasible proposals to members of the selection committees and receiption of the comments and recommendations.

The IBR-2 beam schedules are drawn up by the head of the Condensed Matter Department, together with the persons responsible for individual instruments, on the basis of the experts' recommendations. Schedules as adopted by the FLNP Director or the Deputy Director for condensed matter physics are sent to the chairmen of the selection committees. After the completion of an experiment, an "Experimental Report" form is filled out by the experimenter(s), which is then submitted to the scientific coordinator of user policy.

The first call for proposals in 1995 resulted in 76 applications requesting 406 experimental days on 7 of the 12 IBR-2 spectrometers. The average overload factor for these instruments is 1.16, the largest being for the NERA-PR high resolution inelastic scattering spectrometer (2.4) and the MURN small-angle scattering spectrometer (2.1).

Contact address:
Dr. V.Sikolenko or Dr. G.Bokuchava
Frank Laboratory of Neutron Physics
Joint Institute for Nuclear Research
141980 Dubna, Moscow region
Russia
Tel.: (+7)-095-926-22-53, (+7)-09621-65096
Fax: (+7)-09621-65882
E-mail: sikolen@nf.jinr.dubna.su
gizo@nf.jinr.dubna.su

7.3. MEETINGS AND CONFERENCES

In 1995, the following meetings were organized:

1.	Workshop on Mathematical Methods of Texture Analysis	March 21-24	Dubna
2.	Russian-French Seminar "Strongly Correlated Electronic Systems"	March 23-28	Grenoble
3.	3rd International Seminar on the Interaction of Neutrons with Nuclei (ISINN-3)	April 26-28	Dubna
4.	3rd International Meeting "Nuclear Physics for Protection of the Environment"	May 23-28	Dubna
5.	Meeting on Synchrotron and Neutron Investigations	August 21-25	Dubna
6.	VII International School on Neutron Physics	September 3-22	Dubna

In 1996, the following meeting will be organized:

1.	4th International Seminar on the Interaction of Neutrons with Nuclei (ISINN-4)	April 27-30	Dubna
2.	International Seminar on Relaxor Ferroelectrics	May 21-23	Dubna
3.	International Seminar "Polarized Neutrons in Condensed Matter Investigations"	June 18-20	Dubna
4.	Russian-French Seminar on the Application of Neutron and Synchrotron Radiation for Condensed Matter Investigations	June 25-July 3	Novosibirsk-Irkutsk

7.4. COOPERATION

List of Visitors from Non-Member States of JINR in 1995

Name	Organization	Country	Dates
H.-J.Lauter	ILL, Grenoble	France	13/01-20/01
A.El-Shafey	AEA, Cairo	Egypt	17/01-19/01
I.El-Sayed	AEA, Cairo	Egypt	17/01-19/01
Y.El-Shaer	AEA, Cairo	Egypt	17/01-19/01
B.N.Figgis	Univ. of Western Australia	Australia	22/01-24/01
E.Steinnes	Trondheim University	Norway	16/02-19/02
K.Walther	FZ Rossendorf	Germany	13/03-07/04
E.Niederschlag	In-t Mineralogie, Aachen	Germany	13/03-07/04
K.Helming	GKSS, Geesthacht	Germany	20/03-31/03
W.H.Urbanus	FOM-Institute	The Netherlands	22/03-26/03
A.B.Sterk	FOM-Institute	The Netherlands	22/03-26/03
R.Maayouf	AEA, Cairo	Egypt	26/03-05/04
P.Reichel	FZ Rossendorf	Germany	27/03-07/04
W.Boede	FZ Rossendorf	Germany	27/03-07/04
M.Betzl	FZ Rossendorf	Germany	27/03-07/04
M.Rudalics	Linz University	Austria	29/03-29/04
V.Lauter	ILL, Grenoble	France	30/03-12/04
H.J.Lauter	ILL, Grenoble	France	06/04-12/04
S.Ahmad	Plevsound Ltd., London	United Kingdom	12/04-13/04
A.Pyzalla-Schieck	Ruhr Univ., Bochum	Germany	18/04-01/05
J.Schreiber	Inst. f. zerstoer. Pruefver., Dresden	Germany	18/04-29/04
W.Ulbricht	Univ. Bayreuth	Germany	20/04-27/04
S.Biriukov	Beer-Sheva Inst.	Israel	24/04-28/04
Heiweng Wang	Uhan University	China	23/05-28/05
S.Loureiro	ILL, Grenoble	France	24/05-24/05
K.Walther	FZ Rossendorf	Germany	24/05-16/06

B.Leiss	Univ. Gottingen	Germany	26/05-30/05
K.Pahn	Inst. of Oceanography	USA	01/06-01/06
T.Reinert	TU Clausthal	Germany	05/06-14/06
S.Loureiro	ILL, Grenoble	France	08/06-08/06
S.Loureiro	ILL, Grenoble	France	16/06-16/06
T.Koeble	Frauenhofer In-t Eiskirchen	Germany	26/06-02/07
H.-G.Priesmeyer	GKSS Geesthacht	Germany	26/06-02/07
J.Schreiber	Inst. f. zerstoer. Pruefver., Dresden	Germany	26/06-09/07
V.Zagrebnov	CPT, Marseille	France	04/07-02/08
V.Lauter	ILL, Grenoble	France	12/07-28/07
H.J.Lauter	ILL, Grenoble	France	12/07-28/07
He Jian	IAE, Beijing	China	22/07-29/07
Yang Tonghua	IAE, Beijing	China	22/07-29/07
J.Schreiber	Inst. f. zerstoer. Pruefver., Dresden	Germany	27/07-28/07
M.Ono	Kyoto University	Japan	06/08-25/08
J.W.Lynn	NIST, Washington	USA	19/09-20/09
D.M.Kilany	NRC-AEA, Cairo	Egypt	22/09-28/09
H.I.Hassan	NRC-AEA, Cairo	Egypt	02/10-01/01
P.Reichel	FZ Rossendorf	Germany	13/11-24/11
W.Boede	FZ Rossendorf	Germany	13/11-24/11
K.Walther	FZ Rossendorf	Germany	13/11-01/12
T.Gutberlet	Univ. Leipzig	Germany	10/12-24/12
J.Schreiber	Inst. f. zerstoer. Pruefver., Dresden	Germany	12/12-20/12
M.Russina	HMI, Berlin	Germany	15/12-20/12

7.5. EDUCATION

The University Centre (UC) affiliated with the Joint Institute for Nuclear Research and based on the faculties of the Moscow State University and Moscow Engineering Physics Institute admits, for continuation studies, undergraduate students of the last two years of study in higher education institutions who have attended introductory specialized courses or lectures in the following topics: particle physics, nuclear physics, investigation of condensed matter at nuclear reactors and accelerators, radiation biology. The second and third specializations are in line with research performed at FLNP, which has at its disposal a good experimental base for both sectors comprising the the IBR-2 reactor and the IBR-30 booster pulsed neutron sources.

The education courses and practical training for the students affiliated with FLNP have been organized, to a large extent, to prepare specialists in neutron physics for both the Laboratory and for other Russian neutron centres.

As an example illustrating this aim, we present the list of courses taught by lecturers of the Condensed Matter Physics Chair of the UC (Head: Prof.V.L.Aksenov):

- theoretical methods in condensed matter physics

- methods of investigation of condensed matter at nuclear reactors and accelerators
- fundamentals of neutron physics and neutron sources
- methods for structure analysis of ideal and real crystals
- synchrotron radiation spectroscopy of solid matter
- influence of radiation on solid-state properties
- methods of experimental data processing.

A number of leading FLNP scientists take part in delivering these courses. Each student is allowed access to the Laboratory's computer network. An obligatory condition for successful completion of the 4th year is the capability to use modern personal computers. Earlier, students were included in the research groups led by their instructors, which made it possible for undergraduate students working on their theses to take part in preparing or performing experiments.

In 1995, the teaching process at UC continued successfully. Ten students who had their UC training course at FLNP were employed by JINR or other scientific centers in Russia.

The Condensed Matter Physics Chair gave graduation certificates to its third group of students in the reported year. This group had 7 students, making the total number of students who have graduated from the Chair, 30. Nine of them have been employed by FLNP and who have renewed the staff of the FLNP Scientific Department of Condensed Matter Physics to a noticeable degree. A somewhat smaller influx of graduates (3) came from the Nuclear Physics Chair of the UC.

7.6. PERSONNEL

Table 4

Personnel of the Directorate as of 31.12.95

Country	People
Armenia	1
Bulgaria	1
Germany	3
Georgia	2
Egypt	1
KPDR	4
Kazakhstan	1
Moldavia	1
Mongolia	2
Poland	8
Romania	5
Russia	16
Slovakia	1
Ukraine	1
United States	1
Vietnam	1

Table 5

Distribution of the Main Staff Personnel per Department as of 31.12.95

Departments	Permanent personnel			Contracts		
	S.	E. & T.	St.	S.	E. & T	St.
Nuclear Physics Department	2	1	0.5	29.5	6.5	5.5
Personnel of the Directorate				13	3	
Condensed Matter Physics Department	1	2	-	43	7	6
Personnel of the Directorate				26	5	
Physical and Technical Research Sector	5	2	1	2	6	3
Activation Analysis Sector	2	5	-		3	
Personnel of the Directorate				1	1	
Department of Electronics, Computers and Networks				17	28	9
Personnel of the Directorate				1		
IREN Department				7	5	2
Personnel of the Directorate				1	1	
Nuclear Safety Sector				6	1	1
IBR-30 Department					17	3
IBR-2 Department					40	7
Technical services:						
Mechanical and Technical Department					13	47
Electric and Technical Department		3	1		9	23
Personnel of the Directorate					1	
Central Experimental Workshops, Design Bureau, Tool and Cleaning Services			12		19	45
Management Services	1	2	-	3	17	3
Personnel of the Directorate					1	
	40.5 (7.69%)			486.5 (92.31%)		
Total	**527 (100%)**					

Comment: S. - Scientists, E. & T. - Engineers & Technicians, St. - Staff.

7.7. FINANCE

Table 6

Financing of the FLNP Scientific Research Plan in 1995

No.	Theme	Financing plan, $ th	Expenditures for 12 months, $ th	In % of JINR budget	
				Plan	Actual
I	**Condensed matter physics**	**3192.3**	**2615.5**	**14.6**	**13.8**
	1. Investigations of high temperature superconductivity	470.4	91.6		
	2. Neutron scattering investigations of condensed matter	1517.6	1835.5		
	3. Development and modernization of the IBR-2 complex	869.1	426.3		
	4. Development of the FLNP measurement and computation complex	251.4	184.6		
	5. Activation andlysis and radiation investigations at IBR-2	83.8	77.5		
II	**Nuclear physics**	**924.9**	**816.2**	**4.24**	**4.3**
	1. Realization of the IREN project	623.2	395.4		
	2. Study of the fundamental properties of neutrons and nuclei	301.7	420.8		
III	Elementary particle physics (under the auspices of the ATLAS project)	**5.1**	**6.5**		
IV	**Total:**	**4122.3**	**3438.2**	**19.0**	**18.2**

Table 7

The part of the JINR budget assigned to FLNP (%)

Year	Plan	Fact
1992	21.70	13.30
1993	16.70	14.70
1994	16.80	13.00
1995	19.01	18.20